

Studies on the expression of recombinant Chimeric Chitin Deacetylase

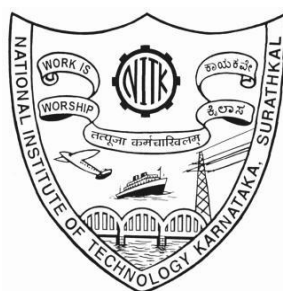
Thesis

Submitted in partial fulfilment of the requirements
for the degree of

DOCTOR OF PHILOSOPHY

By

Priyanka Bhat
Reg. No. 165142CH16F04



**DEPARTMENT OF CHEMICAL ENGINEERING
NATIONAL INSTITUTE OF TECHNOLOGY KARNATAKA,
SURATHKAL, MANGALORE - 575 025
December 2021**

DECLARATION

I at this moment *declare* that the Research Thesis entitled “**Studies on expression of recombinant Chimeric Chitin Deacetylase**”, which is being submitted to the **National Institute of Technology Karnataka, Surathkal**, in partial fulfilment of the requirements for the award of the Degree of **Doctor of Philosophy** in the Department of Chemical Engineering is a *bonafide report of the research work carried out by me*. The material contained in this Research Thesis has not been submitted to any University or Institution for the award of any degree.



Name: Priyanka Bhat

Place: NITK Surathkal

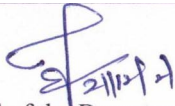
Date: 23-12-2021

Registration No.

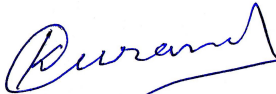
165142Ch16F04

CERTIFICATE

This is to certify that the Research Thesis entitled “**Studies on expression of recombinant Chimeric Chitin Deacetylase**” submitted by **Mrs. Priyanka Bhat (Register Number: 165142Ch16F04)** as the record of the research work carried out by him, is *accepted as the Research Thesis submission* in partial fulfilment of the requirements for the award of degree of **Doctor of Philosophy**.



Head of the Department
CHAIRMAN - DRPC



Research Guide

Dr. Keyur Raval
Associate Professor
Dept. of Chemical
Engineering
NITK, Surathkal

**DEDICATED TO MY
GRANDFATHER**

ACKNOWLEDGEMENT

Pursuing the path of a doctorate has been a core part of the journey of my life. This research thesis is successfully been compiled with the support and motivation of many people. Through this platform, I want to thank each and every one who made this research journey an outstanding experience by providing their precious support.

First and foremost, I want to express my gratefulness to my research guide **Dr. Keyur Raval**, for his encouraging guidance and gracious support during this whole journey. He relentlessly guided me to stay motivated on achieving my goal. His opinions and comments have always given me the right direction and to move forward with this research in depth.

I am sincerely thankful to the RPAC committee members **Dr. Jagannathan T.K** for his valuable comments which have enabled me to practice several ideas for this thesis and **Dr. Soumen Mandal** for his valuable direction at different stages of my research, which were inspirational and helped me to work intelligibly. I am highly grateful to Dr. Ritu Raval for her constant guide and friendly support during this research journey.

I am thankful to the Department of Science & Technology (**DST**), Government of India and also the Ministry of Human Resource Development (**MHRD**), Government of India, for the funding received towards my work.

My respectful gratitude to the **Director, NITK** and the present Head of the Department of Chemical Engineering, NITK, Surathkal **Dr. P.E JagadeeshBabu**, the former heads of the department, **Dr. Raj Mohan B, Dr. Hari Mahalingam and Dr. Prasanna B D** for providing me all the facilities in order to pursue my research work.

I am grateful to all the faculty members of the Department of Chemical Engineering for providing an efficient research ambience and their support during my research. My sincere thanks to **Mr. Sadashiva, Mrs. Thrithila Shetty, Mrs. Shashikala Mohan, Mrs. Bhavya, Mrs. Sandya, Mr. Mahadeva, Mr. Harish Shetty, Mr. Suresh and Mr. Ramesh** and all other non-teaching staff members of the Department of Chemical Engineering for their well-timed assistance in official documentation works and their help with handling different types of equipment.

I am gratifying all my former and current research colleagues for providing a fun-filled and work environment during my stay in NITK.

I specifically thank my dear friends **Mrs. Diksha Sharma**, who has been a constant companion for the past few years, **Mrs. Vrushali Kadam and Mr. Rohit Kalnake**, for their support during this research work.

My highest gratitude to my family for being with me and provin immense support and encouragement throughout this journey. I wish to thank my parents, **Mr. Tej Krishan Bhat** and **Mrs. Bimla Bhat** and my brother **Mr. Sandeep Bhat**. I am also grateful to my Husband, **Mr. Akshay Pandita** and my in-laws **Mr. Sushil Pandita & Mrs. Sudesha Pandita** and **Mr. Sanjeev Pandita & Mrs. Anjali Pandita** supporting me to finish my work successfully. I also want to thank my Brothers-in-law, **Mr. Abhishek Pandita and Mr. Aditya Pandita** for their Love and support. Other members of the **Bhat and Pandita** family and all other relatives and friends of mine for their constant support, love and motivation in this life journey.

Last but not least would like to thank **God** and **Guru Maharaj** for all the grace bestowed upon me.

Priyanka Bhat

Table of contents

Table of contents.....	xii
LIST OF FIGURES	xviii
LIST OF TABLES	xxi
LIST OF ABBREVIATIONS.....	xxv
CHAPTER 1	1
1 INTRODUCTION	3
1.1 History of Chitin	5
1.2 Physical Structure of Chitin	6
1.3 Commercial Sources of Chitin and Chitosan.....	8
1.4 Production of Chitin.....	9
1.5 Chitin production from Chitinous waste.....	9
1.6 Steps in the Isolation of Chitin.....	10
1.6.1 Deproteinization.....	10
1.6.2 Demineralization.....	11
1.6.3 Decolourization.....	11
1.6.4 Deacetylation of Chitin	12
1.7 Physical Structure of Chitosan.....	14
1.8 Biomedical applications of Chitosan	16
1.8.1 Antibacterial Activity.....	16
1.8.2 Antifungal activity	16

1.9 Influence of the Preparation Methods on the Physicochemical Characteristics	18
2. LITERATURE REVIEW	23
2.1 carbohydrate-active enzymes	23
2.3 Sources of deacetylases.....	25
2.3.1 Insect chitin deacetylase	25
2.3.2 Fungal chitin deacetylase	25
2.3.3 Bacterial chitin deacetylase.....	26
2.4 Biochemical studies	26
2.5 Molecular studies of chitin deacetylase	27
2.6 Recombinant CDA.....	28
2.7 Molecular weight of CDA from various sources	29
2.8 Glycerol based media for fermentation.....	29
2.9 Characterization of CDA	30
2.10 Current limitations	33
2.11 Exploring novel CDAs and biological roles	34
2.12 Biological roles of novel CDA	35
2.13 Catalytic mechanism of Novel CDA	36
2.13.1 Multiple attack mechanism	36
2.13.2 Multiple chain mechanism.....	37
2.14 Dealing with the crystalline chitin	38
2.16 Sources.....	40
2.16.2 Carbohydrate-Binding Module from <i>Clostridium thermocellum</i>	41
2.16.3 Chitin Binding Protein from <i>Serratia proteamaculans</i>	41

2.16.4 Amplification and cloning of Chitin Binding Protein from <i>S. proteamaculans</i> 568.....	41
2.16.5 Chitin Binding Protein from <i>Serratia marcescens</i>	42
2.17 CBPs increase substrate accessibility and efficiency of chitinases	42
2.18 Antifungal activity of CBPs.....	43
2.19 CBPs are oxido-hydrolytic.....	43
2.20 Mode of action of CBP	45
2.21 Synthesis of fusion protein.....	46
3. MATERIAL AND METHOD	51
Chemicals used	51
Materials Used	51
3.1 Cloning of BI-CDA gene in pET22b and its expression in <i>E. coli</i> Rosetta pLysS cells. 51	
3.1.1 Cloning of BI-CDA gene.	51
3.1.2 Vector Transformation in <i>E. coli</i> Rosetta pLysS cells. (Heat Shock Transformation method)	55
3.1.2.1 Competent Cell Preparation: CaCl ₂ Method	55
3.1.3. Study of cell biomass and growth curve studies.....	57
3.1.3.1. Plasmid Extraction	57
3.1.3.2. Growth curve studies	58
3.1.4 Expression of CDA in <i>E. coli</i> Rosetta pLysS cells.....	58
3.1.5 Study of enzyme (CDA) activity.	59
3.1.6 Optimization of processing parameters	60
3.1.6.1 Effect of the rotational speed	60
3.1.6.2 Effect of medium filling volume on biomass growth and CDA production....	60

3.1.6.3 Study of the CDA production in different media.....	61
3.1.6.4 Study of the effect of different nitrogen sources on CDA production.....	61
3.1.7 Optimization of Glycerol Based Media	61
3.1.7 Purification of CDA protein by Ni-NTA chromatography.....	61
3.1.7.1 SDS PAGE.....	63
3.1.8 Characterization of enzymatic reaction catalysed by BI-CDA.....	63
3.1.8.1 Effect of co-factors on CDA activity	63
3.1.8.2 Effect of concentration of Co ion on CDA activity	64
3.1.8.3 Effect of pH on CDA activity	64
3.1.8.4 Effect of temperature on CDA activity	64
3.1.9 Estimation of production cost	64
3.2 Identification of CBP from suitable microorganism.....	65
3.2.1 Genomic DNA extraction	65
3.2.2 Designing of primer pair	66
3.2.3 Polymerase Chain Reaction	67
3.2.3.1 PCR optimization.....	67
3.2.4 Optimized PCR	68
3.2.5 PCR product purification	71
3.2.6 Gel elution.....	71
3.2.7 Sanger sequencing	72
3.3 Fusion of CDA gene with CBP gene	72
3.3.1 Restriction digestion and ligation method	72
3.3.2 Optimization of PCR parameters	73
3.3.3 Optimizing Ligation of CBP gene into pET22b CDA plasmid	77

3.3.4 Designing Primers for CDA-CBP fused gene.	78
3.17 Specifications of the fused Primer pair.	78
3.4 Expression and purification of the recombinant fused protein	78
3.4.1 Fused protein purification.	78
3.5 Efficiency of recombinant fused protein on Soluble and Insoluble chitin substrates.	79
3.5.1 Activity time profile of the fused protein	79
3.5.2 Characterization of the enzymatic reaction catalysed by CDA-CBP fused protein.	80
3.5.2.1 Effect of cofactors	80
3.5.2.2 Effect of concentration of Ca ²⁺ ions.	80
3.5.2.3 Effect of pH.	80
3.5.2.4 Effect of Temperature.	80
CHAPTER 4	81
Results and Discussion	81
4. Results and Discussion	83
4.1 Cloning of Blcda in pET22b and its expression in E. coli Rosetta pLysS.....	83
4.2 Vector transformation in E. coli Rosetta pLysS	84
4.3 Effect of operating condition on CDA production	85
4.4 Study of cell biomass and enzyme activity	89
4.5 Purification of CDA	90
4.6 Characterization of enzymatic reaction catalysed by Bl-cda.....	91
4.6.1 Effect of co-factors on CDA activity.....	91
4.6.2 Effect of concentration of Co ion on CDA activity.	92

4.6.3 Effect of pH on CDA activity.	92
4.6.4 Effect of temperature on CDA activity.	92
4.7 Identification of CBP	94
4.7.1 Design of primer pairs	94
4.7.2 Gene amplification and sequencing	97
4.8 In-silico studies of CDA-CBP fusion	97
4.8.1 Restriction digestion and ligation method	97
4.8.2 Fusion primer pair	99
4.8.3 Fusion Product	100
4.9 In-Vitro study of CDA-CBP fusion.	100
4.9.1 Fusion PCR I.....	100
4.9.2 Optimized Fusion PCR I.....	101
4.10 Cloning of Sm CBP gene in pET22b_CDA_ His6 plasmid	102
4.11 Vector transformation in <i>E. coli</i> BL21	104
4.12 Expression and Purification of the fused protein.....	104
4.13 Catalytic efficiency of recombinant fused protein on soluble and insoluble chitin substrates.....	106
4.14 Activity time profile of the fused protein	108
4.15 Characterization of the enzymatic reaction catalyzed by the fusion chimera (CDA-CBP).....	108
5. Summary and Conclusion	113
5.2 Future Scope	115
REFERENCES	119
APPENDICES	139

Research Publications	145
BIO-DATA	147

LIST OF FIGURES

Figure 1.1 Structure of Chitin and Chitosan.....	4
Figure 1.3 Chitin structure and organization. (a) Chemical structure of chitin showing β -1,4 linked <i>N</i> -acetylglucosamine units. (b) The different polymorphic forms of chitin. (c) Example of how chitin is packed in the exoskeleton of the lobster <i>Homarus americanus</i>	7
Fig. 1.4 Traditional method of Production of Biopolymers, Chitin and Chitosan	13
Figure 1.5 Chemical structure of chitosan.....	14
Figure 1.6. Alkaline conversion of chitin to chitosan (Carvalho, C et al. 2012).....	18
Figure 2.1. Mechanism of action of Chitin Deacetylase.....	32
Figure 2.2 The pathway of (GlcNAc) ₄ deacetylation by an exo-type chitin deacetylase from <i>M. rouxii</i> (A) and an endo-type chitin deacetylase from <i>C. lindemuthianum</i> (B).....	37
Figure 2.3 Details of the <i>CICDA</i> active site.....	38
Figure 4.1. (a) The amplified product of CDA gene. (b) The vector map of the pET 22b (+) with the chitin deacetylase gene cloned.....	83
Figure 4.2. Gel picture showing the double digested vector to ensure the size of the gene.....	84
Figure 4.3. Transformed colonies of <i>E. coli</i> Rosetta cells on LB agar plates	85
Figure 4.4 Effect of rotational speed (solid line - (◆) 120, (■) 200, (□) 250 rpm) and medium volume (dashed line - (+) 40 ml, (X)12 ml)) on recombinant <i>E. coli</i> growth in LB medium.....	86
Figure 4.5 Effect of different growth media on CDA activity.....	87

Figure 4.6 (A) Effect of different nitrogen sources (LB: Luria-Bertani, YE: Yeast Extract, BE: Beef Extract, Pep: Peptone, Try: Tryptone), (B) Effect of different glycerol concentrations (0.5 – 2%) on CDA activity.....	88
Figure 4.7. Study of the enzyme activity in LB media (250 ml flask, 5% inoculum, 80 ml medium volume, 120 rpm).....	89
Figure 4.8. Biomass growth and CDA activity in control conditions and under optimized conditions (250 ml flask, 2% glycerol, 5% inoculum, 12 ml medium volume and 250 rpm).....	89
Figure 4.9. SDS PAGE of CDA purification stages. Here, “M” represents molecular weight marker, Lanes 1: flow through, 2: wash, 4: 250 mM imidazole buffer, 5: 500 mM imidazole buffer.....	90
Figure 4.10. Effect of (A) Cofactors, (B) Cobalt concentration, (C) pH and (D) temperature on the purified CDA activity.....	91
Figure 4.11 The Michaelis-Menten plot for the enzymatic deacetylation of glycol chitin.....	92
Figure 4.12 <i>Serratia marcescens</i> CBP 21 precursor.....	95
Figure 4.13 Agarose gel displaying CBP gene.....	95
Figure 4.14 Alignment scores in BLAST.....	96
Figure 4.15 Schematic diagram showing fusion of Bl-CDA and Sm-CBP genes.....	98
Figure 4.16 Fusion primer pair with restriction sites.....	99
Figure 4.17 SmCBP 21 gene fused with CDA in pET22b vector.....	100
Figure 4.18. Gradient PCR for CBP gene. L1, L2, L3, L4, L5 and L6 shows the amplified gene at annealing temperatures 76, 78, 80, 82, 84 and 86 resp.	101
Figure 4.19 Agarose gel displaying desired band.....	102

Figure 4.20. Agarose gel showing double digested fused plasmid. L1 shows the CDA gene (752 bp) and L2 shows the double digested fused plasmid with SalI and NdeI enzymes.....	103
Figure 4.21. Agarose gel showing amplified fused CDA-CBP gene.....	103
Figure 4.22. Transformed colonies of <i>E. coli</i> BL21 cells on LB agar plates	104
Figure 4.23. Indole test showing positive result for <i>E. coli</i>	105
Figure 4.24. SDS PAGE of the purified fused protein. MM represents the molecular marker, S1, S2, S3 and S4 are the purified samples collected in four different tubes.....	105
Figure 4.25 Effect of fusion chimera on different Chitin substrates.....	107
Figure 4.26 Activity time profile of the fusion chimera.....	107
Figure 4.27 Effect of (A) Temperature (B) pH (C) Cofactors (D) Ca ²⁺ ion concentration on the Fusion chimera activity.....	109

LIST OF TABLES

Table 1.1 Sources of chitin in nature.....	8
Table 1.2 Main applications of chitosan in pharmaceutical and biomedical domains (Younes and Rinaudo 2015).	17
Table 2.1 Biochemical Characteristics of reported Chitin Deacetylases.....	31
Table 2.2 Details of bacterial CBPs and their binding preferences (Purushotham et al. 2012).....	44
Table 3.1 Specific primers designed for BI-CDA gene.....	52
Table 3.2. PCR components.....	52
Table 3.3. Thermo-cycling conditions for routine PCR.....	53
Table 3.4 Optimized PCR components.....	54
Table 3.5 Optimized Thermo-cycling conditions for routine PCR.....	54
Table 3.6 Buffer preparation for protein purification.....	63
Table 3.7 Primer specifications.....	67
Table 3.8. Optimized PCR.....	70
Table 3.9 Optimized PCR cycling conditions.....	70
Table 3.10 Modified CBP Primers designed for fusion.....	73
Table 3.11 Components for Fusion PCR-I.....	74
Table 3.12 Optimizing parameters for the Fusion PCR-I.....	74
Table 3.13 Optimized Fusion PCR-I.....	76
Table 3.14 Optimized Fusion PCR-I parameters.....	76
Table 3.15 Optimized Ligation components. (CBP gene in pET22b CDA plasmid)...	77
Table 3.16 Optimized Ligation Parameters. (CBP gene in pET22b CDA plasmid)...	77

Table 4.1 The below calculations are based on 100mg purified protein obtained from 5L of culture broth as per the method given in Biochemical Engineering Fundamentals by Bailey and Ollis, McGraw Hill.....93

LIST OF ABBREVIATIONS

DD	Degree of deacetylation
KOH	Potassium hydroxide
HCl	Hydrochloric acid
CDA	Chitin deacetylase
CBP	Chitin Binding Protein
GH	Glycosyl Hydrolase
CBM	Carbohydrate Binding Module
DP	Degree of Polymerization
kDa	Kilo Daltons
NaCl	Sodium Chloride
CaCl ₂	Calcium Chloride
MgCl ₂	Magnesium Chloride
CoCl ₂	Cobalt Chloride
ZnCl ₂	Zinc Chloride
PCR	Polymerase Chain Reaction
μl	Micro Litre
μM	Micro Molar
mM	Mili Molar
M	Molar
rpm	Rotations per minute
ml	Mili Litre

mg	Mili gram
g	Gram
F. P	Forward Primer
R. P	Reverse Primer
dNTPs	Deoxyribo Nucleotide Tri Phosphates
U	Units
w/v	Weight/ Volume
w/w	Weight/ Weight
T _m	Melting Temperature
bp	Base Pair

CHAPTER 1

INTRODUCTION

1 INTRODUCTION

The natural polymers which are used for innumerable applications in the field of life sciences have numerous advantages, such as biodegradability and biocompatibility, which leads to the possibility of generating chemically or enzymatically modified variabilities for ecological safety and specific end uses. The shrimp species which are used commercially usually give a profit of about 50 billion dollars every year. It is mentioned in the literature that 7 million tons were the total shrimp production in the year 2010 (ITP Business Publishing Ltd 2013). The USA, Japan and Singapore are the major markets for frozen shrimps (Department of Business and Economics, 1999). Approximately 45-55% of the weight of raw shrimp is generated by the industries as a biowaste during shrimp processing. The head and skin materials of the shrimp has calcium, protein content and chitin 10-20 %, 30-65%, 8- 10% respectively on a dry basis and are considered low in terms of economic value and are either sold to animal feed industries or treated as bio-waste (Rojsitthisak and Stevens 2014). Cellulose, pectin and starch are derived from the former and chitin and chitosan are derived from the latter. After cellulose, chitin is the most abundant biopolymer on the earth and over 10 gigatons of the polymer are available every year. Chitin is most commonly segregated in the exoskeleton or cuticle of many invertebrates and the cell wall of fungi and most algae (Harish Prashanth and Tharanathan 2007). Polysaccharides are the class of natural macromolecules tha have the propensity of being tremendously bioactive and are by and large the derivative of agricultural feedstock and crustacean shell wastes (Tsigos et al. 2000). Agricultural feedstock derivatives are generally cellulose, starch, pectin etc. but chitin and chitosan are derived from the crustacean shells (Figure 1.1).

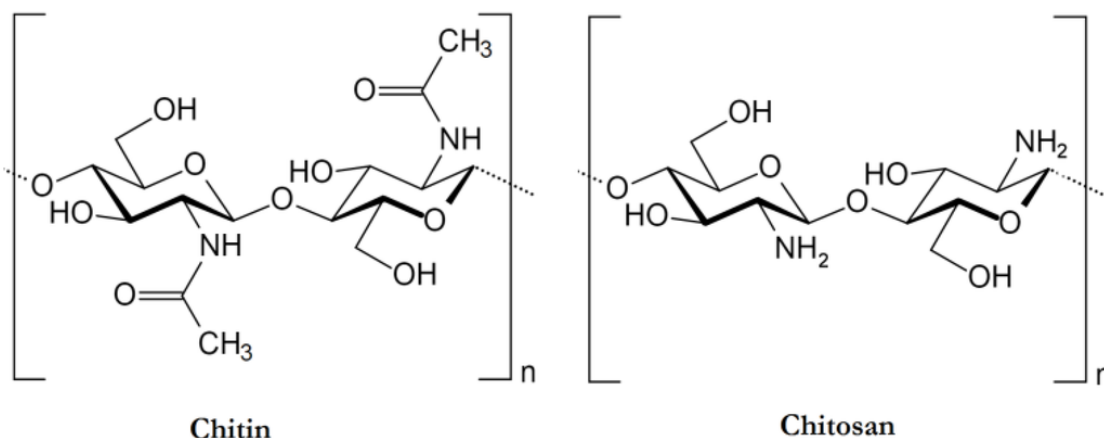


Figure 1.1 Structure of Chitin and Chitosan (Younes and Rinaudo 2015).

Chitin is the second-largest biopolymer on the earth after cellulose, accessible to the degree of more than ten gigatons yearly. It is generally located in the fungi cell wall, exoskeletons, or cuticles of many invertebrates and most algae. It is the most biocompatible biopolymer and is available in large quantities. But chitin being highly crystalline and insoluble in different aqueous and natural solvents has immensely been exploited by various major industries (Aam et al. 2010). It is the copolymer of N-acetyl-D-glucosamine (GlcNAc) units linked with β -(1-4) glycosidic bonds. Despite its abundance, chitin is such a natural resource that remained unused for the long term because it is highly crystalline in nature and insoluble in various aqueous and organic solvents. (Aam et al. 2010). Chitosan, the major derivative of chitin belongs to the family in which the compounds have varying degrees of deacetylation. This deacetylated form contains β -(1-4) linked glucosamine units. The polymers showing the different degrees of deacetylation depicts their varying behaviour and also their physiochemical properties. The behaviour and the physicochemical properties of the polymer completely depends on the degree of deacetylation, such as its solubility (Supe et al. 2000), (Sannan et al. 1975), biological activity (Muzzareui 1993) (Zhao et al.

2010), and reactivity (Hjerde et al. 1997). The acid-solubility of the material increases as the Degree of deacetylation increase to 50% and the material is called 14 chitosan (polycationic polymer) (Percot et al., 2003). The natural widespread of chitin is more than that of chitosan however, its occurrence is discovered in some fungi (Chemistry and Fungp 1968).

1.1 History of Chitin

Braconnot, in 1811 was the first to isolate the chitin during the warm dilute alkali treatment of some mushrooms and especially *Agaricus violaceus* (Society 2014). Chitin name for the very first time was recommended by Odier in 1823, who then isolated chitin from cockchafer beetle by repeated hot KOH treatments (Hamed et al. 2016). He discovered chitin as the primary material in the exoskeletons of all insects. In 1895 Rouget described and recognized chitosan and reported that chitin on being treated with a concentrated alkali like KOH, yielded a 'modified chitin' which shows the solubility in organic acids (Dhillon 2008). In 1894 authors while heating the crustacean shells in concentrated alkali (KOH at 180 °C) yielded a readily soluble product in mildly acidic solutions. Later the name chitosan was proposed by the author for the product (Dhillon 2008).

There was a huge misperception between cellulose, chitin, and Chitosan till nineteenth century. Recently the structures of chitin and Chitosan were given and broadly accepted that chitin, of animal and fungal origin, mainly poly[P-(1-4)-2-acetamido-2-deoxy-D-glucopyranose]. D-glucosamine residues can also be found in molecular fractions whose distribution depends on the chitin source.

1.2 Physical Structure of Chitin

Chitin with the property of being a largely crystalline substance of high tensile strength and low solubility. Results of chitin by the X-ray studies showed that chitin chains are associated with hydrogen bonds to form highly crystalline structures (Webster et al. 2006) (Gooday 1990). Chitin has three polymorphic crystalline regions that differ in the packing and polarization of chains (Jang et al., 2004). There is antiparallel and parallel arrangement of chains in α -chitin and β -chitin respectively. In γ -chitin, there are two 'up' chains for each 'down' chain, as shown in figure 1.2 (Jang et al. 2004), (Gooday and Occurrence 1990).

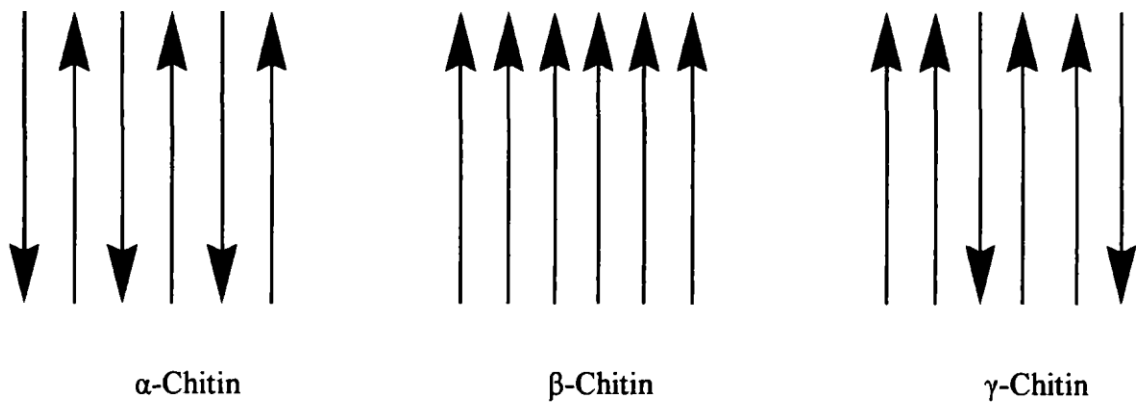


Figure 1.2 Arrangement of the chitin chains found in the three polymorphic forms

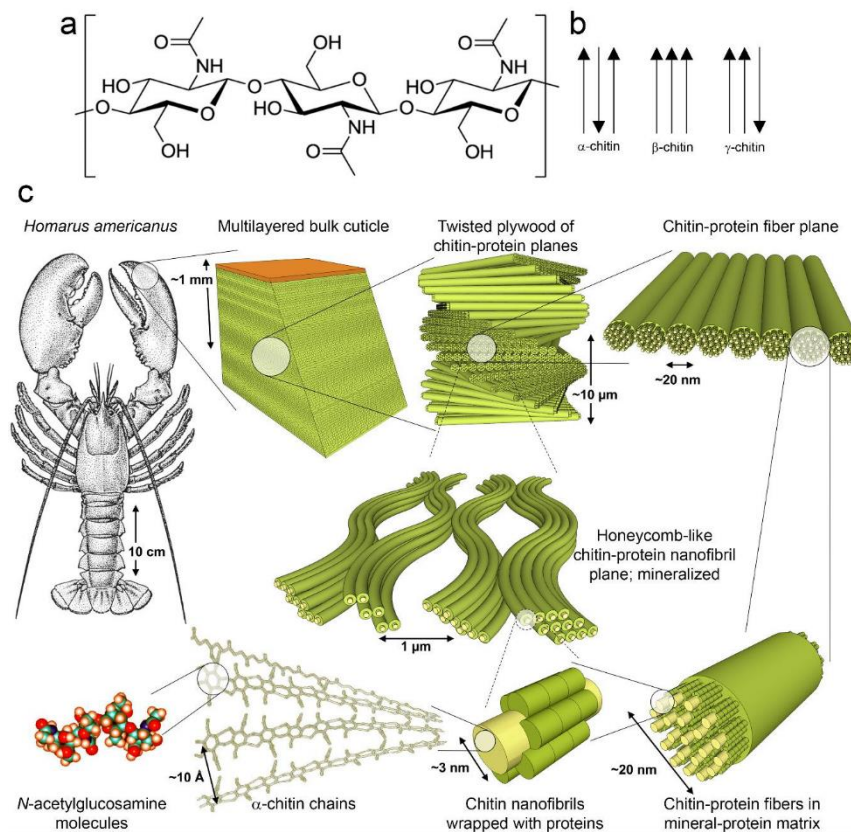


Figure 1.3 Chitin structure and organization. (a) Chemical structure of chitin showing β -1,4 linked *N*-acetylglucosamine units. (b) The different polymorphic forms of chitin. (c) Example of how chitin is packed in the exoskeleton of the lobster *Homarus americanus*.

The main three characteristics of chitin were determined by its chain composition, its toughness, solubility and reactivity as shown in figure 1.3. α -chitin consists of a more rigid hydrogen bond network and as a result, is the most crystalline and compressible form being found in areas that require extreme rigidity, for example in the cell walls and shells of fungi and crustaceans respectively. The framework of β and γ chitin is less rigid. These are found in the parts of the body that require flexibility, mobility and durability for example squid pens contain more β -chitin and γ -chitin in beetles cocoon fibres and squid gastric mucosa. β -chitin has a lower degree of intermolecular crosslinking and has been shown to be a highly soluble substance that gives it the ability

to swell. Now the (3D) 3-dimensional structure of chitin is elucidated which has increased our acceptance of its function in nature and enabled us to tune its physics. The most abundant polymorphic form is α -chitin. It is the most stable form than both β and γ chitin as by destroying the crystal, the β and γ chitin can again be converted into the α -form.

1.3 Commercial Sources of Chitin and Chitosan

Crustaceans and molluscs such as prawns, crabs and squids are attractive sources of chitin. These amount to millions of tons annually (No and Meyers 1989). The alternative source of chitin for industrial purposes is the biowaste from the marine and fish processing industries. The thermal behaviour and the chemical composition of shrimp, crab and lobster cephalothoraxes also constitute important sources of both α and β polymers. There is advancement in the study of chitin science yet a large volume of chitin remains inaccessible.

Table 1.1 Sources of chitin in nature

Source	Chitin amount
Worms	In between 20-30%
Squids/octopus	Upto 20%
Scorpions	Mostly 30%
Spiders	Approximately 38%
Water beetle	Approximately 37%
Shrimps	About 40%

Hermit crab	Upto 60%
Edible crab	Upto 70%

The chitin isolated from different sources are over 80% similar in all cases but the polymer characteristics change according to the raw material (Supe et al. 2000).

1.4 Production of Chitin

No and Meyers demonstrated that the astaxanthin-rich lobster shell waste acts as a valuable natural resource for food additives (colorant). It also serves as a major renewable resource for the two biopolymers. Therefore, chitin and Chitosan represent a full use of crawfish shell waste as a source of astaxanthin (No and Meyers 1995).

1.5 Chitin production from Chitinous waste

Shellfish processing industries all over the planet turn out a substantial quantity of head and shell as industrial waste. This waste must be removed quickly from the premises without permitting spoiling to prevent contamination of the processing environment, and it must be discarded in a way that is not favourable for the receiving environment. The scale of the waste management issue in the fishing industry depends on the volume of waste, its pollutant load, rejection rate and assimilation limit in the receiving environment. The shellfish waste disposed from the industries poses severe environmental problems. The only available ways to dispose the industrial waste include ocean dumping, incineration or disposal of landfill sites (Ferrer and Goajira 1996). The annual global production of crustacean shells is estimated at about 1000 million metric tons and approximately 1.25 lakh tons of shrimp processing residues are estimated in India which is a single large fishery waste of the country. A very small

portion of this finds application as an ingredient in shrimp/poultry feed mix and the waste from these industries contains mainly protein, minerals, and chitin. The shrimp shell waste causes serious environmental problems and over the years, serious efforts has been made to develop techniques for the utilization of chitin and its derivative from these wastes. In controls environmental pollution and in addition to that it saves the expenditure incurred by the industry to dispose the waste and generates more employment and the economy. The preparation of chitin from crustacean shells using chemicals to demineralize and deproteinize the source material leads to a formation product with varying qualities and properties.

1.6 Steps in the Isolation of Chitin

Following are the four steps involved for isolation of chitin from shell (Fig. 1.4):

Deproteinization

Demineralization

Decolourization

Deacetylation

1.6.1 Deproteinization

Chitin naturally occurs as chitin protein which consists of covalent bonds through either aspartyl and histidyl residues, or both, and forms the stable complex such as glycoprotein (Margaret and Zola 1967). Crustacean shell is usually crushed and treated with the solution of sodium hydroxide at a high temperature (65-100°C) for 0.5 to 12

hours which leads to depolymerisation. Relatively high ratios of solid to the alkaline solution are recommended to standardize the reaction (No and Meyers, 1995).

1.6.2 Demineralization

Conventionally HCl is used as the most common chemical in the process to harm the physiochemical properties of chitin. The process is very costly and can cause serious environmental problems by producing harmful effluent wastewater (Percot et al. 2003). It is mentioned in the literature that the concentrated acids which are used for the chitin demineralization process have a harmful effect on both the molecular weight and degree of acetylation of the polymer. This will adversely affect the fundamental properties of the crystalline chitin. In order to lessen the chitin breakdown and reduce impurities to an adequate level, the authors explained the importance of optimizing process parameters such as pH, time, temperature and solids/ acidic ratio. Therefore, a less harmful and cheaper demineralization process is needed.

1.6.3 Decolourization

The above process of demineralisation obtains a coloured chitin product which has to be decolourized for commercial acceptability. The pigment produced thus forms a complex with chitin, and the level of association is variable from one species to the other among crustaceans. The stronger is the bond, the more intense the treatment for the white-coloured chitin preparation. The colour of the chitin products generally ranges from creamy white to intermediate pink (No et al. 1989).

1.6.4 Deacetylation of Chitin

In this process the Acetamido groups in N-acetyl glucosamine units were removed by treatment with concentrated NaOH or KOH solutions. The process results in obtaining the major product called Chitosan through harsh alkaline treatment (No and Meyers, 1989). The Alkaline concentration, temperature, reaction time and even the particle size of chitin material are the main factors affecting the degree of deacetylation. (Sannan et al. 1975) investigated the controlled process of N-deacetylation of chitin with aqueous alkali and the resultant chitin material was soluble in water with an acetylation degree of 50%.

Generally, there are two most important methods through which Chitosan can be prepared from chitin with varying degrees of acetylation.

The heterogeneous deacetylation of solid chitin

The homogeneous deacetylation of pre-swollen chitin

In Heterogeneous deacetylation, the reaction which occurs in the polymer mostly in the amorphous regions is responsible for keeping the novel crystalline regions almost intact.

in the native chitin. It is most preferable in industrial treatment. Alternatively, in a homogeneous modification, (13% w/w) a medium-concentration alkali on pre-treated chitin is used to enhance the reaction. The reaction was incubated at 25-40 °C for 12-24 hours. Under both heterogeneous and homogeneous conditions concentrated alkaline solutions are used in the reaction and a long reaction time varies according to

the two conditions from approximately 1 to 80 hours. The major factors that have a great effect on the chitin deacetylation process include the density of chitin, particle size, previous treatments and the alkali concentration. On average 75-85% is the maximum degree of deacetylation that can be achieved in one alkaline treatment (Sannan et al. 1975).

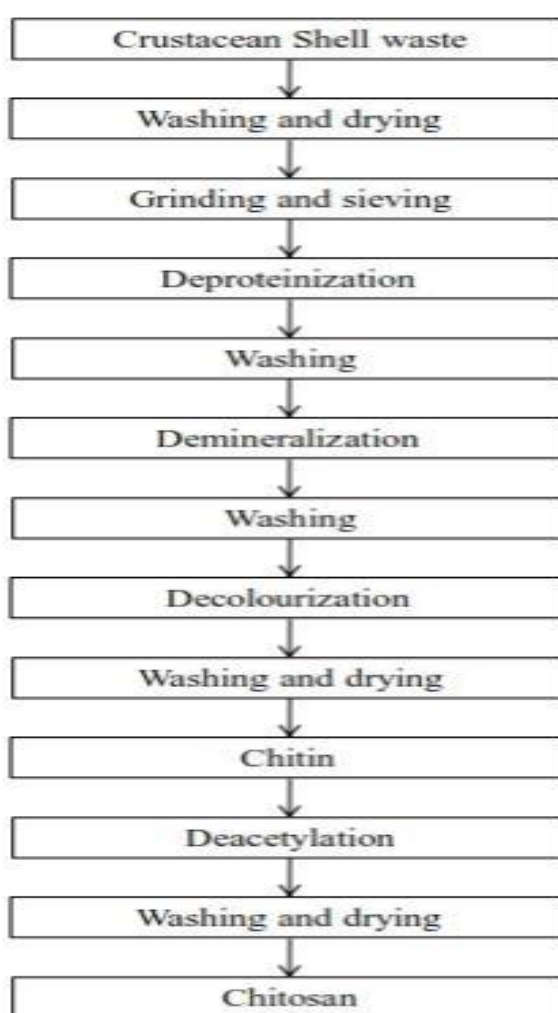


Fig. 1.4 Traditional method of Production of Biopolymers, Chitin and Chitosan

1.7 Physical Structure of Chitosan

Chitosan as a growing polymer in different industrial applications has developed a good interest in the area. However, hardly any literature is available for the structure of Chitosan. It is not less than a hurdle to studying the structure of Chitosan because of the different routes of preparation and starting material used. Among the three polymorphs of chitin, the α -chitin form is the utmost prevailing polymorphic form of chitin than β or γ chitin (Batista and Roberts 1990).

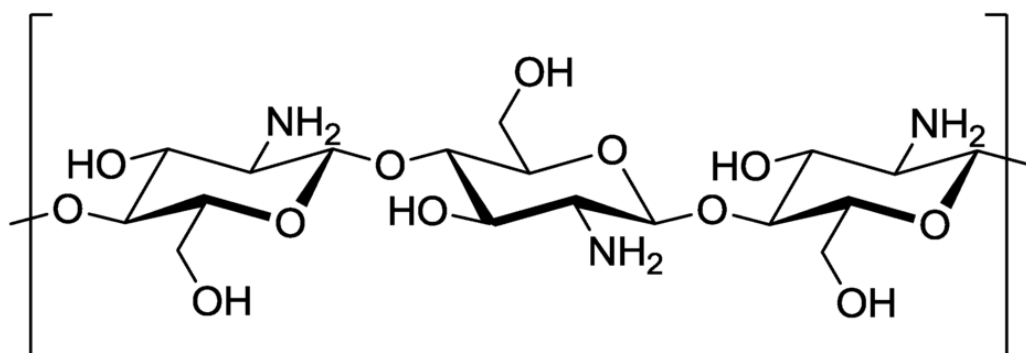


Figure 1.5 Chemical structure of chitosan

Figure 1.5 shows β -1,4 linked glucosamine units of chitosan polymer. Chitosan is the nontoxic, deacetylated, biodegradable chitin derivative which has solubility in various acid solutions and is substantially more manipulable material than chitin. As shown in table 1, Chitosan has an extensive variety of uses in various fields for the most part in medical like for drug delivery, in genetic engineering, food industries, waste-water treatment and agriculture area (Younes and Rinaudo 2015).

Following are major characteristics that make Chitosan advantageous for numerous applications:

- (1) Chitosan has a very well define the chemical structure
- (2) It is very easy to modify Chitosan chemically as well as enzymatically
- (3) It is functional both biologically and physically
- (4) It is biodegradable and biocompatible
- (5) It has the property to process into a variety of products which includes membranes, fine powders, flakes, sponges, beads, cotton, fibres, and gels.

The main source of chitosan is shells of both crab and shrimps which is generally thrown away as a byproduct by seafood industries. As a result, chitosan has a high molecular weight, gel-forming ability and cationic character, it has been extensively used in many industries especially as a flocculant to clarify wastewater and detoxify hazardous waste. In addition, chitosan increased the physical strength of cellulose paper used as a coating material in paper factories by which the printing quality of the paper was also improved while using anionic inks. Chitosan is also used in filtering beverages and in the agricultural sector. In addition, it is used as the food ingredient in many products in Japan and has also been approved as food additive in Italy, Japan and Finland. Nowadays, it can be used as an add-on supplement for losing weight and also as a cholesterol-lowering agent.

Chitosan polymer having high molecular weight and DD has shown more advantage especially in the form of microspheres, gels and microcapsules. These fabricated forms are more stable and also help in the sustainable rate of drug release. In addition, chitosan polymers help in protecting the skin against various microbial infections, moisturize the skin and offer protection against mechanical hair damage.

1.8 Biomedical applications of Chitosan

1.8.1 Antibacterial Activity

Chitosan possesses a broad spectrum of antimicrobial activity with very little toxic towards mammalian cells. The real means of inhibition is yet not fully understood but it is hypothesized as an interaction between the positively charged polysaccharide that changes the cell permeability (pH lower than 6.5).

1.8.2 Antifungal activity

It is mentioned in the literature that Chitosan has the property of reducing the *Fusarium oxysporum* infection in celery which may prevent the extent of *Sphaerotheca pannosa varrosae*, *Peronospora sparsa* and *Botrytis cinerea* on roses. Chitosan treatment was given to tomato plants resulted in the reduction of fungal growth and spore production (Huang and Hsu 2000). In addition, seed treatment with Chitosan can reduce the infection of *Colletotrichum sp.* and can improve the enactment of chilly seedlings. Depending on the mechanism it is clear that Chitosan shows the ability of forming a permeable layer by accumulating on the surface, synthesizing proteinase inhibitors or by inducing callus synthesis. Other applications of Chitosan are shown in Table 1.2.

Table 1.2 Main applications of chitosan in pharmaceutical and biomedical domains (Younes and Rinaudo 2015).

S No.	Forms	Applications
1	Beads	For Drug delivery
2	Microspheres	Used for Enzyme immobilization, Gene delivery vehicle
3	Nano particles	To encapsulate the sensitive drugs
4	Coatings	For modification and finishing of the textile surface
5	Films	Dialysis membrane, Anti-tumoral and also a semi-permeable film for wound dressing material
6	Powder	As an adsorbent for medical devices, pharmaceutical industries, Surgical gloves, enzyme immobilization etc.
7	Sponge	Drug delivery, Enzyme entrapment, Artificial skin
8	Gels	Tissue engineering, Delivery vehicle, Implants, coating, Coating for wet wound
9	Tablets	Compressed diluent, Disintegrating agent
10	Capsules	The delivery vehicle for pH or temperature-sensitive drugs

Alkaline deacetylation of chitin (figure 1.6) suffers from disadvantages such as high water footprint and environmental pollution from effluents generated from a concentrated alkaline solution and a heterogeneous and broad range of insoluble and soluble products (Younes and Rinaudo 2015).

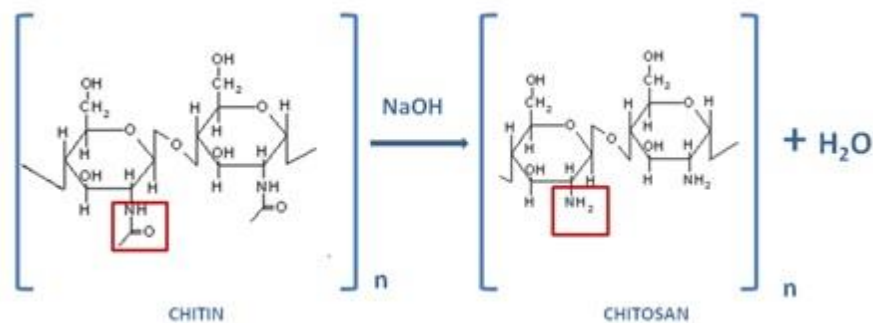


Figure 1.6. Alkaline conversion of chitin to chitosan (Carvalho, C et al. 2012)

1.9 Preparation Methods influencing the Physicochemical Characteristics

The early studies have clearly demonstrated that process conditions can adversely affect the specific characteristics (DD and molecular weight) of the sample. After demineralization, two types of products are formed, one being the collapsed chitin where the original chitin structure is lost and the other being compressed whereas the original chain and the fibrous structure are intact. Another way to damage the structure of is by brief exposure to bleaching material (Sannan et al. 1975). It is obvious that the dominant cause behind the absolute structure of Chitosan is the chemical poly dispersion of the value of acetylation degree (Younes and Rinaudo 2015). At the time of deacetylation by harsh chemicals, the polymer chain degrades along with the damage in the crystalline structure of chitosan (Rege and Block 2000).

The two major Asian countries like Japan and Korea where chitosan has been approved as one of the functional foods from the last decade. Chitin and Chitosan have been included in 2003 by Codex Alimentarius Commission but still not listed in the General Standard for Food Additives. Although there are several studies that have proved the non-toxicity of the compound yet there have been no long-term findings of human

safety reported (Galed et al. 2008). In spite of having a large no. of properties and applications, the complexity of these two polymers is difficult to control. The polymers vary from each other due to their natural origin and also the properties of the sample from the same source change depending on the manufacturing process (Rauth et al. 2006).

The above findings put forward that the well-ordered deacetylation process should be developed using an enzyme which will be an interesting alternative process that could lead to the preparation of new oligomers and polymers from chitosan.

To overcome these downsides of alkaline N- deacetylation of chitin, the proposal of an alternative enzymatic method that exploits the use of chitin deacetylation enzyme has been explored. Presently the deacetylation of chitin is being done using various chemical procedures. In contrast, using chitin deacetylases offers the probability of a controlled and non-degradable process resulting in the creation of new well-defined chitosan (Tsigos et al. 2000). CDA is an enzyme having the ability to catalyze the hydrolysis of acetamido groups in acetyl glucosamine (GlcNAc) of the polymer chitin, stimulating the conversion to Chitosan. CDA mediated deacetylation of chitin provides a natural, safe enzymatic procedure to change fungal cortical into chitosan which results in a more homogenous product for innumerable applications (Ghormade et al. 2010). CDA play a crucial role in the defence and attack systems, which has numerous uses in agriculture like for the bio-control of insect pests and fungal human pathogens (Zhao et al. 2010). Chitin deacetylases are found mainly in various fungi, marine bacteria and some insects, which catalyze chitin deacetylation. There are as such so many substrates that are available for the analysis of chitinolytic enzymes such as chitin, 3H-chitin,

chitin red®. Most substrates are generally insoluble and typically contain non-specific chemical substitutions such as amino acids, peptides, or proteins (Koga and Kramer 1983) that CDA is unable to act upon.

Thus, if we can modify enzyme such that it can directly use chitin as a substrate, we can enhance the catalytic efficiency of the process, make homogeneous Chitosan and enhance sustainability of chitosan manufacturing process. One of the possible solutions to this problem is to make CDA act on insoluble chitin. There is a chitin-binding protein (CBP) usually found in micro-organisms which has the property to bind on the insoluble chitin. This research work focuses on the fusion of the CBP with CDA so that, the fused protein complex may act upon insoluble chitin.

CHAPTER 2

LITERATURE

REVIEW

2 LITERATURE REVIEW

In the traditional deacetylation process, strong alkaline solutions at high temperatures are used producing a wide range of heterogeneous products with varying deacetylation patterns. It results in products with a low degree of polymerization and also environmentally unfriendly. Alternatively, the deacetylation of chitin using an Enzyme may provide a non-degrading and well-defined process of chitosan production.

2.1 Carbohydrate-active enzymes

Carbohydrates exist in the form of monomers, oligomers, and polymers in nature and various enzymes have evolved in such a way that can modify or break down these complex structures. In the CAZy database, these carbohydrate-active enzymes (CAZymes) are organized into different classes, according to their families, functions and amino acid sequence similarity (Levasseur et al. 2013). Currently, in the CAZy database there are six different enzyme classes. One class known as non-catalytic modules, among these six classes remain associated with carbohydrate-active enzymes. The glycosyl hydrolase (GH) class contains enzymes that can break down glycosidic bonds. Several GH enzymes also have transglycosylation activity, in which sugar acts as an acceptor, leading to forming a new glycosidic bond (Cantarel et al. 2009). Activated sugars are involved to stimulate Glycosyltransferases (GTs) to synthesize glycosidic bonds while polysaccharide lyases (PLs) cleave in a non-aqueous manner. Carbohydrate esterases (ECs) prevent changes in carbohydrate ester (Cantarel et al. 2009). The fifth class is called helper activity (AA) and contains many redox enzymes that work in conjunction with other CAZymes (Levasseur et al. 2013). Class AA comprises the lytic polysaccharide monooxygenases which was discovered by (Vaaje-

Kolstad et al. 2005) and which play a major in glycolysis. Class AA have redox enzymes that can act on lignin found within the polysaccharides plant cell. In addition, lignin promotes the activity of LPMO (Levasseur et al., 2013). In addition, the CBM includes proteins with zero enzymatic activity. They usually make covalent bonding with other enzymes and stimulate substrate-binding, which is their major role (Cantarel et al., 2009).

2.2 Chitin Deacetylase

Chitin deacetylase is an enzyme that can catalyze the acetamido group hydrolysis in chitin polymer, leading to their conversion into chitosan (Figure 2.1). CDA mediated deacetylation of chitin provides an eco-friendly approach to convert the crude chitin into chitosan. The biochemical characterization of CDA from different organisms enhances its products for commercial applications. The use of the enzyme CDA for the production of chitosan polymers and oligomers allows an enzymatic process to be developed which could potentially overcome most of the disadvantages associated with the chemical process in the future. The deacetylation process results in forming a free amino group, which in the presence of acidic pH gives the polymer a positive charge which makes it more hydrophilic. Being the only multi-coupled biopolymer, chitosan in an aqueous solution possesses a number of interesting physicochemical properties such as the formation of hydrogels and nanoparticles. It is also believed that the positive charge is at least partially responsible for a wide range of known biological functions (Raval et al. 2013). In chitin, the enzyme CDA catalyze the hydrolysis of N-acetamido bonds resulting in the production of chitosan. CDA enzyme is mostly studied in fungi *Mucor rouxii*, *Absidia coerulea*, *Aspergillus 8 nidulans* and *Colletotrichum lindemuthianum* (Martinou et al. 2003). All these enzymes are secreted either into

culture media or the periplasmic region and thermally stable at optimum temperature (508°C). Nevertheless, they have variability in carbohydrate content, molecular weight and range of pH optima and also cannot be inhibited by acetate released during deacetylation reaction. The gene corresponding for the chitin deacetylases of the fungi *M. rouxii*, *C. lindemuthianum* and *Saccharomyces cerevisiae* was cloned and characterized. In addition, the expression of the chitin deacetylase genes of *C. lindemuthianum* and *M. rouxii* was recently reported in *Escherichia coli* and *Pichia pastoris*, respectively.

2.3 Sources of chitin-deacetylases

2.3.1 Insect chitin deacetylase

Recent studies have demonstrated the presence of CDAs in arthropods (Dixit et al. 2008), (Luschnig et al. 2006), tracheal tube of *Drosophila melanogaster* (Coronel et al. 2019), insect species such as *Anopheles gambiae*, *Apis mellifera*, *Bombyx mori*, *D. melanogaster*, *Epiphyas postvittana*, *Helicoverpa armigera*, *Mamestra configurata*, *Spodoptera frugiperda*, and *Trichoplusia ni*. (Simpson et al. 1997), (Wang et al. 2006), (Dixit et al. 2008).

CDA has been found in the midgut tissues of the larvae and the importance of the enzyme helps may be in increasing nutrient uptake. In *M. configurata*, the proteins expressed in *E. coli* helped in the detection of CDA activity (Hou et al. 2008).

2.3.2 Fungal chitin deacetylase

CDAs were studied and identified in several fungi. However, in the fungus *Mucor rouxii*, the CDA was partially purified and characterized by (Araki and Ito, 1975) and

(Martinu et al., 1995). (Martinou et al. 2002) studied cobalt-activated CDA (Cda2p) from *Saccharomyces cerevisiae* and found out that there was a complete loss of enzymatic activity during deglycosylation. On adding 1 mM CoCl₂, the same enzyme activity was restored. (Alfonso et al. 1995), (Gao et al. 1995) and (Tsigos and Bouriotis 1995) studied the role of thermostable CDA in *Aspergillus nidulans*, zygomycete fungus *Absidia coerulea* and culture filtrate of *Colletotrichum lindemuthianum*.

2.3.3 Bacterial chitin deacetylase

Chitinous debris containing mainly nitrogen is mainly processed by marine and oceanic bacteria. It has been shown that the hydrolysis of chitin is carried forward by chitinase and beta-N-acetylglucosaminidase with the administration of (GlcNAc)₂ and GlcNAc, respectively as the end product (Pruzzo et al. 2008). For the catabolic cascade of chitin in *Vibrio*, the CDA gene has been seen to play the major role (Jung et al. 2007).

2.4 Biochemical studies

Chitin deacetylase is isolated and has been characterized biochemically from several fungi, including *M. rouxii* (Araki and Ito, 1975), (Martinou et al. 1995), *A. coerulea* (Gao et al. 1995), and *A. nidulans* (Alfonso et al. 1995) and cultured filtrate of *C. lindemuthianum* fungi (Kauss et al. 1995), (Tsigos and Bouriotis 1995), (Tokuyasu et al. 1996) as indicated in Table 2.1. The specificity of the CDA has been studied numerously on different substrates with varying degree of deacetylation. It has been found that soluble or colloidal forms of these polymers' deacetylate more quickly than the crystalline forms, which are more difficult to access. In the case of *M. anisopliae*, the highest CDA activity was seen on ethylene glycol chitin (Nahar et al. 2004). In addition to that the degree of polymerization of polymer is mainly responsible for the

specificity of CDA. For enzymatic deacetylation chitin oligomers with a DP greater than two are needed. It has been suggested that a minimum of 3 to 4 consecutive GlcNAc residues are necessary for CDA activity (Martinou et al. 1995), (Alfonso et al. 1995), (Tokuyasu et al. 1996).

Likewise, *S. brevicaulis* CDA have the deacetylating activity of N-acetylchito-oligosaccharides with DP from 2 to 6 (Cai et al. 2006). From previous reports, it was observed that CDA of periplasmic origin had an optimal low pH, while at high pH the extracellular CDAs were more active e.g., CDA from *M. anisopliae* showed the maximum activity at pH 8.5, the alkaline medium (Nahar et al. 2004). Likewise, CDA from *C. lindemuthianum* and *S. brevicaulis* also showed pHs of 11.5 and 7.5, respectively, optimal for CDA activity.

2.5 Molecular studies of chitin deacetylase

The CDA genes are being cloned and characterized in several fungi viz. *M. rouxii* (Martinou et al. 1995), *C. lindemuthianum* (Shrestha et al. 2004), (Tokuyasu et al. 1999), *S. cerevisiae* (Nilegaonkar 2010), *Schizosaccharomyces pombe* (Matsuo et al., 2005), *R. circinans* (Gauthier et al. 2008) and *F. velutipes* (Yamada et al. 2008) and insects viz. *D. melanogaster* (Luschnig et al. 2006), *M. configurata* (Hou et al. 2008) and *T. castaneum* (Dixit et al. 2008). The CDA gene from *C. lindemuthianum* and by using the signal sequence of the chitinase from *S. lividans*, the gene was expressed in *E. coli* (Tokuyasu et al. 1996). Additionally, the CDA gene was isolated from the human pathogenic dimorphic fungus *Cryptococcus neoformans* (Biondo et al. 2002). Several fungi have been reported to contain multiple CDA genes. RC, D2 and I3/2 are the three putative CDA genes that were isolated from cDNA library of *Rhizopus circinans*

(Gauthier et al. 2008). In insects nine CDA copies were from *T. castaneum* (Arakane et al. 2009), while two (CfCDA2a and CfCDA2b) from *Choristoneura fumiferana* (Quan et al. 2013). CE4 family members share the NodB homology domain due to its similarity to NodB proteins. The NodB domain also contains specific regions of acetylxyylanesterases and xylanases from bacteria and open reading frames (ORFs) which is not characterized in *Bacillus* species (Tsigos et al. 2000), (Coutinho et al. 2003).

2.6 Recombinant CDA

A recombinant CDA was generated in the culture media of *E. coli*, whose gene was originated from *Colletotrichum lindemuthianum*, supported by the signal sequence of chitinase gene from *Streptomyces lividans*. There was an immediate production of CDA with the maximum activity shown at 12-18th h after the induction by IPTG. According to various studies, the CDA gene from *Saccharomyces cerevisiae* was cloned and expressed in *Escherichia coli* followed by the purification and characterization of the recombinant enzyme, which showed its activity with glycol chitin as a substrate (Martinou et al. 2002).

In another research work, the Open Reading Frame (ORF) of CDA encoding 427 amino acid protein including 22 amino acid signal sequence was cloned from the *Vibrio parahaemolyticus* KN1699 genome and analysed. A plasmid was constructed containing the gene and inserted in *E. coli*. The concentration of recombinant enzyme secreted was 150 times larger than the wild type (Kadokura et al. 2007).

2.7 Molecular weight of CDA from various sources

The molecular weights of partially purified chitin deacetylases from *Mucor racemosus* and *Rhizopus nrbicans* when estimated to k between 26 kDa and 64 kDa (Phytologie and Glk 1990). (Tokuyasu et al. 1996) reported that the molecular weight of the purified chitin deacetylase from the plant pathogen *C. lindemuthianum* was 31.5 kDa and 33 kDa as observed on SDS-PAGE and gel filtration chromatography. A purified 14 chitin deacetylase from *M. rouxi* had a molecular weight of about 75 kDa by SDS-PAGE, and about 80 kDa by size-exclusion chromatography (Kafetzopoulos et al. 1993). Xiao-Dong et al., (1995) reported that the molecular weight of the purified chitin deacetylase from the *A. Coerulea* was 75 kDa by using SDS-PAGE and gel filtration chromatography the molecular weight of the purified chitin deacetylase from the *Aspergillus nidulans* was 27 kDa by using SDS-PAGE. (Deising and Siegrist 1995) reported that five isoforms of chitin deacetylase from *Uromycesviciae fabae* with molecular weight ranging from 12.7 to 48.1 were detectable by using SDS-PAGE. CDA with 53 kDa as molecular weight was purified from *Penicillium oxalicum* SAEM- 51 with optimum temperature and pH of 50 °C and 9.0 respectively (Pareek et al. 2012).

2.8 Glycerol based media for fermentation

Ongoing industrialization and dwindling oil reserves have created a global demand for the production of energy from a variety of unconventional and renewable resources (such as biohydrogen, biodiesel or bioethanol). Among these, biodiesel is one of the most valued renewable energy sources. Biodiesel is produced by chemical or enzymatic esterification of vegetable or animal fats with short-chain alcohols (mainly methanol) (Metsoviti, Paraskevaidi et al. 2012), which leads to the synthesis of alkyl esters

(biodiesel) and sub-product water, or “crude” or “raw” glycerin) (Metsoviti, Zeng et al. 2013). In the last decade, the constant demand for alternative biofuels has led to an abrupt escalation in the manufacturing of biodiesel, and thus the main problem that arose was the distribution of its main by-product, namely glycerol; in fact, when producing 10 kg of biodiesel from various oils, 1 kg of glycerin becomes available. As a result, a large amount of crude glycerin accumulated, which caused its market price to drop significantly. Thus, the transformation of this abundant source of carbon into value-added products thanks to microbiological technologies opens up important opportunities for industrial microbiology. Glycerin has been used as a component of a fermentation broth for the production of 1,3-propanediol from organisms such as *Klebsiella oxytoca* (Metsoviti, Paraskevaidi et al. 2012), *Citrobacter freundii* (Metsoviti, Zeng et al. 2013), *Clostridium butyricum* DSP1 (Sazymanowska-Powder 2014) and others, but there were no reports of the use of glycerin as the only carbon source in production environments for the production of enzymes. Compared to conventional bioprocessing substrates such as glucose and sucrose, glycerin derived from biodiesel is a class of substrates that are inexpensive, durable, and not considered a suitable food source for humans.

2.9 Characterization of CDA

The authors described a new recombinant CDA from various sources. (Martinou et al. 2002) expressed the *Saccharomyces cerevisiae* chitin deacetylase gene (CDA2) in *Escherichia coli* and reported maximum enzyme activity at pH 8 and 50 °C (Scotland Bailey 1986). *Rhizobium NodB* chitin deacetylase gene was expressed in *E. coli* cultures in soluble form (Chambon et al. 2017). Chitin deacetylase (CDA)

from *Colletotrichum lindemuthianum* was expressed in *Pichia pastoris* (Shrestha et al. 2004) and they reported the highest activity of 72 U/mg activity at 60°C and pH 8 in the presence of cobalt cofactor. Han et al., expressed a novel CDA encoding gene, *Hacda2* in *Helicoverpa armigera* (Han et al. 2015). Liu et al., identified a new CDA like enzyme from the metagenomic library of deep-sea sediments in the arctic ocean (Liu et al. 2016) and the maximum enzyme activity was reported at 28°C and pH 7.4.

Table 2.1 Biological and chemical Characteristics of reported Chitin Deacetylases

Organism	Optimum pH	Optimum Temperature (°C)	Molecular weight (kDa)	Reference
<i>A. coerulea</i>	5.0	50	75	(Gao et al. 1995)
<i>A. nidulans</i>	7.0	50	27.5	(Alfonso et al. 1995)
<i>C. lindemuthianum</i>	11.5	60	31.5-33	(Tokuyasu et al. 1996)
<i>C. lindemuthianum</i>	8.0	60	25	(Shrestha et al. 2004)
<i>F. velutipes</i>	7.0	60	31	(Yamada et al. 2008)
<i>Mortierella sp.</i>	5.5	60	50, 59	(Hemsworth et al. 2013)
<i>M. rouxii</i>	4.5	50	75-80	(Hunt et al. 2008)
<i>R. circinans</i>	5.5-6.0	37	75	(Gauthier et al. 2008)
<i>S. cerevisiae</i>	8.0	50	43	(Martinou et al. 2002)

Organism	Optimum pH	Optimum Temperature (°C)	Molecular weight (kDa)	Reference
<i>S. brevicaulis</i>	7.5	55	55	(Cai et al. 2006)

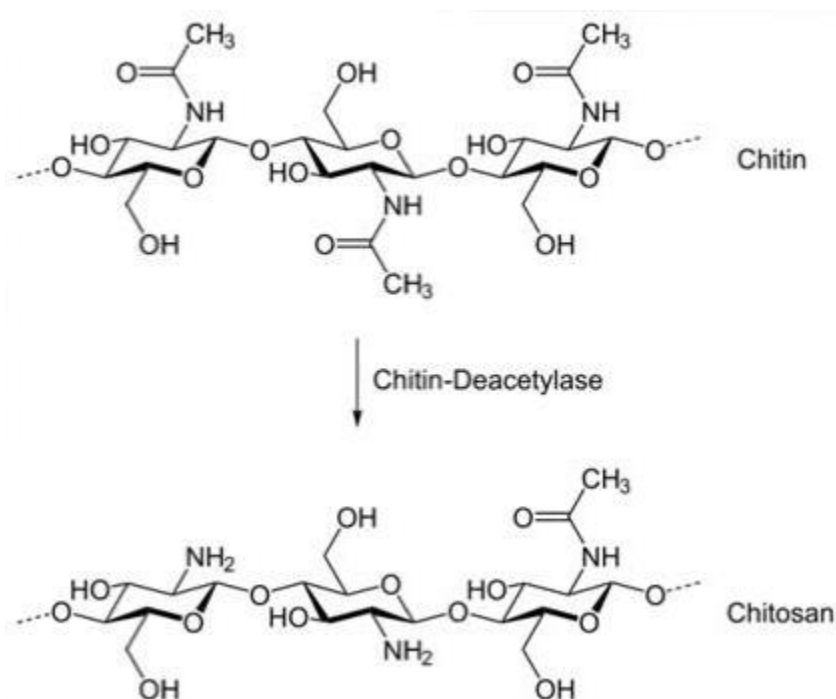


Figure 2.1 Mechanism of action of Chitin Deacetylase

The main disadvantage of using chitin deacetylases is the low efficiency of the enzyme when applied to the substrate which are highly crystalline in nature. The enzymes are highly effective when applied to polymers of chitin and oligosaccharides with high water solubility. (Martinou et al. 1995) observed deacetylation of strong acetylated c chitin both crystalline and amorphous, as well as two samples of chitosan with DDA 72 and 58% by chitin deacetylase. It was observed that CDA does not effectively destroy both the chitin substrates i.e., amorphous as well as crystalline which are

insoluble in water. These two substrates resulted in causing only 0.5 to 9.5% deacetylation, respectively. Although the water-soluble chitosan achieved a degree of deacetylation (DDA) between 97-98% (Tsigos et al. 2000). Similarly, other authors such as (Cai et al. 2006) described the activity of chitin deacetylase on both the chitin materials and concluded that crystalline chitin has less activity than amorphous materials. In highly crystalline chitin, the acetamido groups are inaccessible due to which there is decrease in the enzyme activity. Through the pretreatment of the crystalline chitin substrate, attempts have been made to increase the availability of these groups. However, the conditions necessary to achieve this often led to degradation of the polymer chain (Manjeet et al. 2013a).

2.10 Current limitations

Briefly to say, there are three major challenges that need to be addressed.

- The first challenge is the scarcity of well characterized CDAs which has the ability to produce desired chitosan or COS products.

So far, it has been reported that there are only fewer fungal CDAs which are partially or fully characterized (Zhao et al. 2010). There are many environmental microbes that are responsible for the primary source of enzyme activity and have enormous metabolic capacity, many of which remain intact today. Thus, it is important to study new CDAs with unique properties, as it is believed that the more effective the enzyme, the higher the productivity and hence the lower the costs.

- The second challenge is to derive the structure of chitosan which is enzymatically in order to illustrate the catalytic mechanism of diverse CDAs (Martinou et al. 1995).

Till today minimal data is available in the literature to describe or briefly explain the catalytic mechanism of CDA on chitin substrates (Tokuyasu et al. 1999), (Tsigos et al. 2000).

- The third and final challenge is to find out the novel way to destroy the highly crystalline chitin that cannot easily be broken down by CDA.

There are two ways to consider in this case, either by the pre-treatment of chitin substrate through physiochemical means or by integrating CBM/CBP along with CDA.

2.11 Exploring novel CDAs and their biological roles

To date, a very small number of microbes produce CDA which are discovered either by identifying CDA encoding genes or determining the CDA activity invitro. There is a large no. of microorganisms that still remain unexplored for the discovery of Novel CDAs. It is apparently clear that CDAs produced from various sources vary in potency, stability, efficacy, and specificity. A large number of well-characterized chitooligosaccharide products have been synthesized through unique CDAs from various organisms. CDA from *C. lindemuthianum* (Tokuyasu et al. 1996), *Thermococcus kodakaraensis* KOD1 (Tanaka et al. 2004), and *Vibrio cholerae* can convert GlcNAc-GlcNAc to GlcN-GlcNAc (Tanaka et al. 2004) (Li et al. 2007). *M. rouxii* and *Absidia corulea* CDA have no ability to deacetylate GlcNAc-GlcNAc at all (Gao et al. 1995). Finding the right enzyme depends on a sensitive and efficient

screening process using a variety of genes and organisms. Recently, two *Mortierella* sp. DY-52 (Kim et al. 2008) and *Absidia corymbifera* DY-9 (Zhao et al. 2010) can produce extracellular CDA and is much more effective than CDA from *Mucor rouxii*. (Pareek et al. 2012) discovered a new CDA-producing strain *Penicillium oxalicum* ITCC 6965, isolated from residues of seafood processing plants. Molecular technologies (Hess et al. 2011) as the approach Metagenomics are the most viable method today for finding these new enzymes, and these enzymes have been proven successful in the cosmetic and pharmaceutical industries (Lorenz and Eck 2005). The process involves extracting all genetic material and then transferring it to surrogate organisms to create a library of metagenome clones. In addition, clones can be tested for a specific enzyme involved in a specific activity.

2.12 Biological roles of novel CDA

The biological roles of CDA can be understood by examining the new CDA. These enzymes have been biologically important for spore formation (Matsuo et al. 2005), (Christodoulidou et al. 1996) cell wall reliability (Baker et al. 2007) and self-defence in converting the resulting chitin polymer into chitosan polymer (Hadrami et al. 2010), (Blair et al. 2006).

In *Saccharomyces cerevisiae* (Christodoulidou et al. 1996) and *Cryptococcus neoformans* (Baker et al. 2007), two and four CDA genes have been identified, respectively. Consideration of the biological role of CDAs of several phytopathogenic and human fungi, namely *C. lindemuthianum* (Eddine et al. 2002) and *Cryptococcus neoformans* (Baker et al. 2007), has the ability to protect from host attack by modifying cell wall chitin of the pathogen (Blair et al. 2006).

2.13 Catalytic mechanism of Novel CDA

The most important factor is the substrate specificity and the catalytic mechanism of the new CDA. The mechanism of action on partially acetylated chitosan has been studied by many authors (Itsigos et al. 1995). (Caufrier et al., 2003) studied an enzyme attributed to carbohydrates of the esterase 4 family and reported that *M. rouxii* and *Streptomyces lividans* CDAs (both native and truncated) were active against xylan, glycol-chitin, chitin-50 and (GlcNAc)₄ substrates. There is very little literature on the catalytic mechanism of CDA.

2.13.1 Multiple attack mechanism

In this mechanism, when CDA binds to a chitin chain, a chain deacetylation reaction is initiated (Fig.2.2A). The mechanism of action of enzyme from *M. rouxii* has been studied on partially N-acetylated chitosan (Martinou et al. 1995) and N-acetyl chito-oligosaccharides (Itsigos et al. 1995). It was found out that only chitin oligomers were effectively deacetylated and the first reaction started at the non-reducing end of the residue.

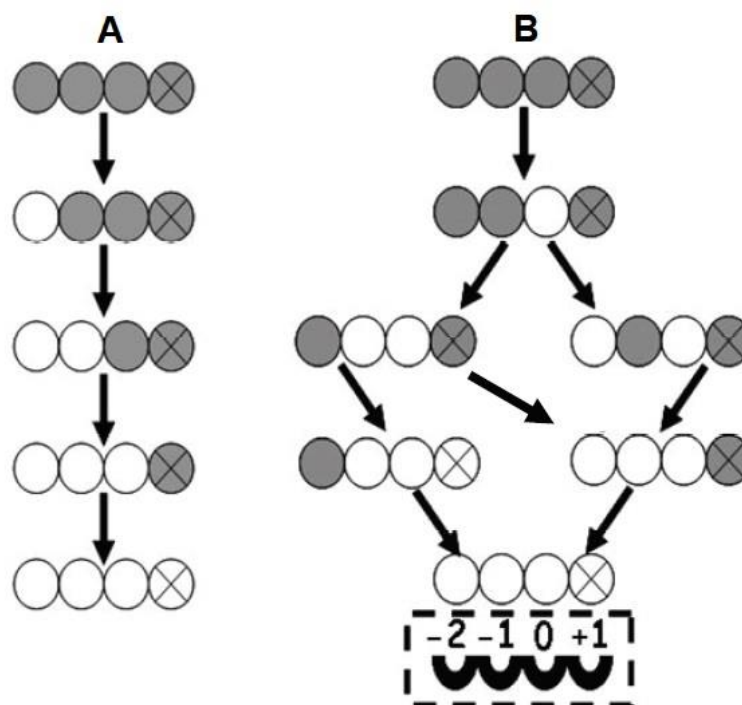


Figure 2.2 The pathway of (GlcNAc)₄ deacetylation by an exo-type chitin deacetylase from *M. rouxii* (A) and an endo-type chitin deacetylase from *C. lindemuthianum* (B)

The shaded and the open circles represent GlcNAc and GlcN respectively. The circles with the X inside indicate the reducing end residue. The arrows indicate the sequence of deacetylation.

Figure. 2.2 A represent the non-reducing end deacetylation by *M. rouxii* CDA in a progressive multiple attack mode. Figure 2.2 B represent the deacetylation by *C. lindemuthianum* CDA through Multiple chain mode. Among the four subsites (-2, -1, 0, +1) 0 is the only subsite which is responsible for catalysis (Liu et al. 2014).

2.13.2 Multiple chain mechanism

The extracellular CDA from *C. lindemuthianum* (ATCC 56676) was responsible for hydrolyzing acetamido groups through this mechanism. In this case, an active complex

is formed which initiates the hydrolysis and there is the formation of a new active complex (Figure 2.3 B). (Tokuyasu et al. 1997)

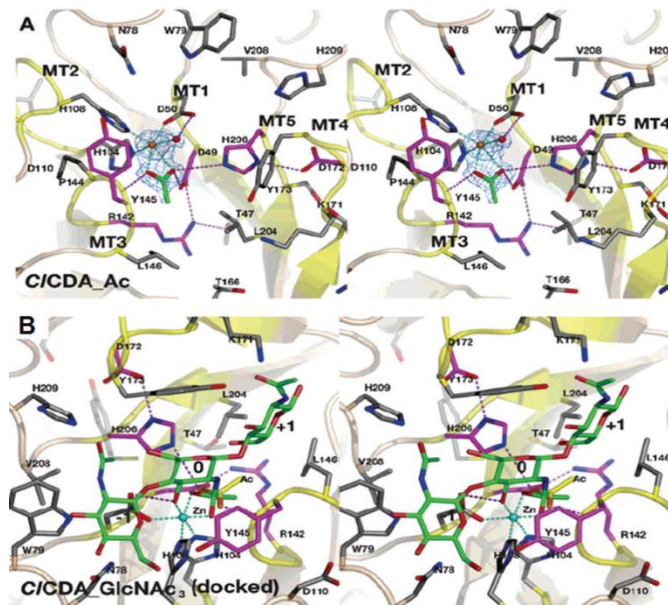


Figure 2.3 Details of the *CICDA* active site

The figure showing the active sites in complex with acetate product. Sticks with green carbons represent the acetate molecules. The active site is shown in the ribbon diagram. Sticks with magenta carbons and yellow carbons indicate the conserved site and experimentally observed acetate respectively. (Blair et al. 2006).

2.14 Dealing with the crystalline chitin

Insoluble polysaccharides like cellulose, chitin, xylan, glucan, starch and mannan are a big problem. the polymers available on Earth and their enzymatic degradation are one of the most important reactions to be carried out. These glycoside hydrolases effectively attack these polysaccharides due to the inaccessibility of the active site of the corresponding enzyme.

There are many glycoside hydrolases that use insoluble substrates by non-catalytic CBMs which can help to overcome these problems. The major role of these accessory domains is to bind polysaccharides with subsequent approximation of the biocatalyst to the substrate, which ensures hydrolysis of carbohydrates (Boraston et al. 2004).

2.15 Carbohydrate binding modules (CBMs)

CBMs are often found connected to GH18 domains sometimes *via* one or more FnIII domains. These CBMs are non-catalytic and play a role in efficient polysaccharide recognition. CBMs were previously defined as cellulose-binding domains (CBDs), as the first known binding modules were known to bind primarily to cellulose. Further, as these binding domains were found to bind to a wide range of carbohydrates, they are referred to as CBMs (Boraston et al. 2004).

Most of the CBMs consist of β -sheets as their most important secondary structure element. There are three different classes of CBMs differentiated on the basis of the topology of ligand binding sites. Type A CBMs have a flat hydrophobic surface which is composed of only aromatic residues. These planar surfaces interact with crystalline chitin or cellulose like substrates. In type B CBMs, aromatic residues in ligand binding site interact with a single chain of polysaccharide and display a cleft arrangement. Type B CBMs recognize substrates like β -1,3-glucans, mixed β -(1,3)/(1,4) - glucans, β -1,4-mannans, galactomannan and glucomannan. Type C CBMs bind only to mono, di or trisaccharides. This is due to steric interaction in ligand binding sites.

CBMs have been differentiated into 69 different families on the basis of amino acid sequence similarity. They were previously known as the CBM33 family and have now

been placed under family AA10 of LPMOs in the CAZy database. Mostly, these CBMs are found tethered to GH domains, where they help GH to degrade insoluble substrates. Some CBMs target plant cell walls where they bind to insoluble starch which is a storage polysaccharide in plants. CBMs may play divergent roles of targeting function and a disruptive function. The CBMs also play a role in root colonization, pathogen defence, plant development and polysaccharide biosynthesis (Guillen et al. 2009).

Due to efficient substrate recognition and binding ability, CBMs bring the enzyme (especially hydrolytic domain to which CBM is attached) in close proximity of substrate. This results in

fast and efficient degradation of insoluble polysaccharides. CBMs thus help hydrolytic domain of the enzyme to come closer to the substrate. Usually, CBMs bind to the polysaccharides which are substrates for their associated hydrolytic domain. N-terminal CBM2a of Cel6A from *Cellulomonas fimi* was reported to carry out non-catalytic disruption of crystalline cellulose. When CBMs occur independently they are referred as binding proteins. CBMs which were previously placed in family 33 of CAZy database bind to chitin and thus referred to as chitin-binding proteins (CBPs). These CBPs are now known to oxido-hydrolyze crystalline substrates.

2.16 Sources

2.16.1 Carbohydrate-Binding Module from *Trichoderma reesei*

Cryptococcus sp. S-2-carboxymethyl cellulase (CSCMCCase) has no binding domain. Due to the absence of a binding domain, the enzyme remains ineffective against cellulose substrates. To improve the affinity towards insoluble cellulose substrates, the

CBD of *Trichoderma reesei* cellobiohydrolase, belonging to the CBM 1 family, was fused to the C-terminus of carboxymethylcellulose. This recombinant fusion protein had a pH similar to that of the native enzyme (Thongekkaew et al. 2013).

2.16.2 Carbohydrate-Binding Module from *Clostridium thermocellum*

In 2015 a study examined the chance of increasing the activity of family 1 carbohydrate esterase by its fusion with family 3 carbohydrate-binding module (CBM). The CtCBM3 from *Clostridium thermocellum* was fused to (AnAXE), the carboxyl terminus of acetylxylanesterase from *Aspergillus nidulans*. There was a significant increment in the activity of AnAXE-CtCBM3 cellulose acetate by 2-4 folds. Notably, it was suggested that the fusion with CtCBM3 increases the association between the substrate and the enzyme (Mai-gisoni et al. 2015).

2.16.3 Chitin Binding Protein from *Serratia proteamaculans*

CBPs along with chitinases have been shown to act synergistically in order to degrade the natural crystalline chitin variants in *Serratia proteamaculans* 568 (Arora et al. 2013). CBP from different sources (Table 2.1) showcases their divergence of preference to bind with the chitin substrate (Horn et al. 2012).

2.16.4 Cloning and amplification of Chitin Binding Protein from *S. proteamaculans* 568

S. proteamaculans 568 gDNA was used as a template to amplify three Sp CBP genes and was expected to contain an N-terminal leader peptide. The gene cloning took place without the part that encodes the signal peptide. Three CBP Sp were overexpressed by the His C-terminal marker in *E. coli*. The expressed CBP Sp was separated and purified

by Ni-NTA agarose chromatography. 18.6, 28.0 and 50.0 kDa was the approximate molecular weight of the *Sp* CBP21, *Sp* CBP28, and *Sp* CBP50, respectively revealed by SDS-PAGE analysis. The hydrolysis efficacy of four species of chitinases was estimated on original chitin variants in the presence as well as the absence of CBP. It was resulted that the addition of CBP21 increased the efficacy of hydrolysis of α - and β -chitin, especially in the presence of reduced glutathione.

2.16.5 Chitin Binding Protein from *Serratia marcescens*

S. marcescens secretes an 18.8 kDa protein, CBP21, when grown on chitin (Suzuki et al. 1998). It is known to bind to chitin and belongs to CBM family 33. Its three-dimensional structure has recently been solved (Vaaje-Kolstad et al. 2005). It was reported that CBP21 upon binding to the native chitin disrupts the crystal structure of the substrate and leads to the significant increase in the chitinase enzyme efficiency. A study revealed that CBP21 has a pH-dependent affinity towards chitin (Suzuki et al. 1998).

2.17 CBPs increase substrate accessibility and efficiency of chitinases

CBPs were earlier known to be non-catalytic proteins that aid chitinases in hydrolyzing crystalline chitin. Efficient chitin degradation in *S. marcescens* was shown to be dependent on the action of CBP21 (Vaaje-Kolstad et al. 2005). CBP21 accelerates hydrolysis of β -chitin by chitinase A and C and was essential for complete degradation of chitinase B. CBPs from other organisms were also found to show synergism with chitinases (Eijsink et al. 2008). It clearly illustrates that in the presence of CBPs, accessibility of substrate is increased, which increases chitinase efficiency. Hence, chitin degradation is faster in presence of CBPs as compared to when only chitinases

were present. It means that chitinases and CBPs work in synergy with each other for efficient chitin degradation. CBPs from different organisms showed differential binding preferences. Some CBPs bind specifically α -chitin, some to β -chitin and some CBPs bind to both α - and β -chitin. *SpCBP28* from *S. proteamaculans* 568 does not bind to α -chitin, β -chitin, colloidal chitin or advice. Also, there are some chitinases which are self-efficient and do not need support of CBPs for chitin degradation. For example, *BliChi* from *Bacillus licheniformis* did not show increased product concentration when incubated with chitin substrates in presence of *BliCBP/BtCBP/SpCBP21* (Manjeet et al. 2013b). As some CBPs showed binding and synergistic action with chitinases towards crystalline chitin and some do not, the role of these CBPs could be different under different conditions.

2.18 Antifungal activity of CBPs

There are many chitin degrading bacteria which show antagonistic effect on fungal pathogens namely *Enterobacter agglomerans*, *S. marcescens* and *Xanthomonas maltophilia* (Kobayashi et al. 1997) and *Stenotrophomonas maltophilia*. (Someya et al. 2010) reported the synergistic effect of the enzyme from *S. marcescens*. Since the fungal cell wall is mainly composed of chitin, plant and bacteria CBPs have been explored for their antifungal activity (Huang and Hsu 2000). *Streptomyces tendae* Tu901 CBP interferes with the polarity of growth in fungi (Raps et al. 1999).

2.19 CBPs are oxido-hydrolytic

(Vaaje-Kolstad et al. 2005) described for the first time an enzyme (*SmCBP21*: previously CBM33 now belongs to AA10 type) that generated oxidized CHOS due to its oxido-hydrolytic activity. Due to oxido-hydrolytic activity, CBM33s have been

reclassified under auxiliary activity (AA) family of LPMOs. LPMOs are divided into three families and named as AA9, AA10 and AA11. LPMOs belonging to family AA9 (previously GH61) are mainly found in fungi, AA10 (previously CBM33) occur in bacteria and viruses and those which have a mixed character of AA9 and AA10 are grouped under AA11. *EfCBM33A* from *Enterococcus faecalis*, *B1AA10A* from *B. licheniformis*, *TfAA10B* from *Thermobifida fusca*, *BaAA10A* from *B. amyloliquefaciens* (Hemsworth et al. 2013) were oxido-hydrolytic.

The three-dimensional structure of AA10 type LPMOs from *S. marcescens* (*SmCBP21*; AAU88202.1), *E. faecalis* (*EfCBM33A*; AAO80225.1), *B. amyloliquefaciens* DSM7 (*BaCBM33* DSM7; CBI42985.1), *Burkholderia pseudomallei* 1710b (*BpAA10A*; ABA49030.1), *Vibrio cholerae* 01 biovar E1 Tor str. N16961 (*GbpA*; AAF96709.1) and *Thermobifida fusca* (*E7*; AAZ55306.1) are available. Table 2.2 shows the details of CBP, which have been identified in different organisms.

Table 2.2 Details of bacterial CBPs and their binding preferences (Purushotham et al. 2012)

CBP name	Source	Binding substrates
CBP21	<i>S. marcescens</i>	Showed high preference to β -chitin
ChbB	<i>B. amyloliquefaciens</i>	Showed less preference to α -chitin than β -chitin substrate

CBP name	Source	Binding substrates
LICBP33A	<i>Lactococcus lactis</i>	Equally preferable to both α and β -chitin
CHB1	<i>St. olivaceoviridis</i>	Firmly to α -chitin
CHB2	<i>St. reticuli</i>	Firmly to α -chitin
CHB3	<i>St. coelicolor</i>	More bound towards α -chitin than to β -chitin
CbpD	<i>P.aeruginosa</i>	Only colloidal chitin
E7	<i>Thermobifida fusca</i>	Equally preferable to α and β -chitin substrate
E8	<i>Thermobifida fusca</i>	More towards β -chitin than on α -chitin substrate
Cbp50	<i>B. thuringiensis</i>	Mostly to β -chitin
EfCBM33A	<i>E. faecalis</i>	More to β -chitin.

2.20 Mode of action of CBP

The mode of action of CBP21 from *S. marcescens* was described by (Horn et al. 2012). Disruption of chitin by CBP21 was shown to occur in two steps: hydrolysis and oxidation. CBP21 introduces chain breaks in the most inaccessible regions of crystalline chitin substrates. These chain breaks resulted in oxidation of chitin chain ends. Oxidation of chitin and introduction of charge disrupt the normal chair conformation of NAG residues. CBP21 thus generated oxidized CHAOS. Using NMR and isothermal calorimetry, it was shown that CBP21 is an overall rigid molecule. However, there is a metal-binding site which shows high local flexibility. Binding of

CBP21 to crystalline chitin was metal-dependent. Metal-binding studies further confirmed that ions, preferably Cu¹⁺ followed by Cu²⁺, bind to a site which is present in between His28 and His114 (Aachmann et al. 2012). For glycoside hydrolases to bind and degrade crystalline chitin polymorphs, the use of CBM plays an important role (Oriyoshi et al. 2010). However, so far in the literature, almost no mention has been made of any CDAs having such CBMs. Therefore, the only way to stimulate effective enzymatic deacetylation of insoluble chitin is to integrate CBM / CBP with CDA using a genetic approach, or to research a new CDA that contains CBM.

Three different chitinases that belong to family 18 are produced by the bacterium *Serratia marcescens* to degrade chitin. It has been studied that the efficient degradation of chitin is completely based on non-catalytic protein, CBP21, which has the ability of binding to the insoluble crystalline substrate chitin, which further results in the structural changes of the substrate and helps the enzyme with enhanced substrate accessibility. CBP21 has already promoted the hydrolysis of crystalline -chitin when combined with chitinases A and C. In most of the chitin-degrading microorganisms there are various homologues of CBP21, which suggests a global mechanism by which CBPs can help in enhancement of chitinolytic activity. (Vaaje-Kolstad et al. 2005).

2.21 Synthesis of the fusion protein

The enzymatic deacetylation which involves CDA offers a possibility to prepare new specific chitosan oligomers and polymers. The paucity of an effective method to degrade the crystal structure of chitin, which is too resistant to be easily treated by CDAs is also a major problem to overcome. Binding of CBM to crystalline substrate results in the disruption and disruption of polysaccharide chains and increased substrate

availability. An example of the degradation of the substrate is provided by CBP21 of the CBM 33 family. CBP 21 is produced by *Serratia marcescens* (Vaaje-Kolstad et al. 2005) and it was earlier proposed in an article that CBP21 is a non-catalytic protein, however, Vaaje-Kolstad and colleagues reported it as an oxidizing enzyme that can catalyze the breaking of glycosidic bonds in crystalline as well as amorphous chitin (Horn et al. 2012). Therefore, an effective role for CBP21 in stimulating the effective degradation of crystalline chitin can be expected in the future through the integration of CBM / CBP with CDA using a genetic engineering approach or the study of new CDA containing CBM.

The above results suggest that the advancement of a well-controlled deacetylation process of chitin substrates using an enzyme is an alternative as well as an eye-catching process that can lead to the production of new chitosan oligomers and polymers.

As per the literature available till now, there is no such research available on the fusion of the two proteins CDA and CBP21. Herein, we propose the fusion of the two proteins, which may enhance the catalytic efficiency of CDA on insoluble chitin.

The main objective of the research work is the enzymatic deacetylation of insoluble chitin by the fusion of CDA and CBP21. Based on this the following specific objectives are derived.

Objective I : Cloning and expression of CDA gene in recombinant *E.coli*.

Objective II : Identification and cloning of CBP from suitable microorganism.

Objective III : Fusion of CBP gene with CDA gene.

Objective IV : Expression of fused protein in recombinant *E. coli* followed by its purification

Objective V: Comparison of activities of fusion protein and native protein on various chitin substrates.

CHAPTER- 3

MATERIALS AND

METHODS

3. MATERIAL AND METHOD

All the above-performed experiments were performed in triplicate and the graphs which are plotted in the thesis are their mean values indicated in the legend of the figures.

Chemicals used

Luria-Bertani broth (LB) and Nutrient Broth (NB) were obtained from Hi-Media laboratory, India. Inorganic salts such as NaCl, CaCl₂, MgCl₂, MnCl₂, CoCl₂, and ZnCl₂ were used from Nice laboratories, India.

Materials Used

Thermo-cycler (Hi-Media), UV-Vis Spectrophotometer (Hi-Media), Incubator Shaker (Orbitek), Centrifuge (Remi), Vortex, Magnetic Stirrer, Gel Doc, Electrophoresis Set up, SDS-PAGE, Lyophilizer, pH meter (LabMan), 96 well plate reader, sonicator.

3.1 Cloning of BI-CDA gene in pET22b and its expression in E. coli Rosetta

pLysS cells.

3.1.1 Cloning of BI-CDA gene.

The gene for BI-CDA was obtained from metagenomics library. The raw sequence was submitted to the Gen-Bank under accession No. PRJEB6317 (Stöveken et al. 2014). In order to amplify the gene, forward and reverse primers were designed specific to gene and obtained from Sigma Aldrich India given in Table 3.1.

Table 3.1 Specific primers designed for BI-CDA gene

Primers	Sequence 5' to 3'	T _m (°C)
Forward Primer	GGATGGGCCCAAAGCAGGAACCG	62
Reverse Primer	GTCGACGGAGCTCGAAATTCCATCTG	62

The gene was amplified using Polymerase Chain reaction (PCR). A master mix of 25 μ L was prepared and accordingly PCR program was set as shown in table 3.2 and 3.3 respectively.

Table 3.2. PCR components

Components	25 uL Reaction	50 uL reaction	Final concentration
Q5 Reaction Buffer (5X)	5	10	1X
dNTPs (10 mM)	0.5	1	200 μ M
Forward Primer (10 μ M)	1.25	2.5	0.5 μ M
Reverse Primer (10 μ M)	1.25	2.5	0.5 μ M
Template DNA	Variable	Variable	<1,000 ng
Q5 High-Fidelity DNA Polymerase	0.25	0.5	0.02 U/ μ L
Q5 High GC Enhancer (5X) (optional)	5	10	(1X)
Nuclease-Free Water	To 25	To 50	

Table 3.3. Thermo-cycling conditions for routine PCR

Steps	Temperature	Time
Initial Denaturation	98°C	30 seconds
25–35 Cycles	98°C 50–72°C 72°C	5–10 seconds 10–30 seconds 20–30 seconds/kb
Final Extension	72°C	2 minutes
Hold	4–10°C	

After the trial and error, the PCR components and conditions were optimized which includes 200 ng of DNA, 1 uL of 10 M of each primer, 1 X reaction buffer, 2.5 mM dNTP's (Nucleotide tri phosphate) and 0.02 U/ μ L Taq. Polymerase. The PCR program was set with an initial DNA denaturation at 95 °C for 2 minutes, followed by 30 cycles with denaturation at 95 °C for 30 seconds, annealing of primers at 60 °C for 45 seconds, and final extension at 72 °C for 1 minute as given by the Table 3.4 and 3.5.

Table 3.4 Optimized PCR components

Components	25 uL Reaction	Final concentration
Q5 Reaction Buffer (5X)	5	1X
dNTPs (10 mM)	2 ul	200 uM
Forward Primer (10 μ M)	1 ul	0.5 uM
Reverse Primer (10 μ M)	1 ul	0.5 uM
Template DNA	2 ul	200 ng
Q5 High-Fidelity DNA Polymerase	0.25	0.02 U/uL
Nuclease-Free Water	13.75	

Table 3.5 Optimized Thermo-cycling conditions for routine PCR

Steps	Temperature	Time
Initial Denaturation	95°C	2 minutes
25–35 Cycles	95°C 60°C 72°C	30 seconds 45 seconds 30 seconds
Final Extension	72°C	1 minutes
Hold	4–10°C	

After the PCR, the amplified product with already incorporated sites for NdeI (NEB, Germany) and Sall (NEB, Germany) was ligated within the pET 22b vector after being digested with the above-mentioned set of enzymes at 37°C for 3 hours. T4 DNA Ligase (NEB, Germany) was used to perform ligation at 16 °C for 16 hours.

3.1.2 Vector Transformation in *E. coli* Rosetta pLysS cells. (Heat Shock Transformation method)

3.1.2.1 Competent Cell Preparation: CaCl₂ Method

E. coli Rosetta cells were made competent for transforming them with a pET 22b vector containing CDA gene, for carrying out the gene expression studies.

Pre-requisites:

Sterile LB broth, 35 mg/ml sterile chloramphenicol - inoculated with bacterial cells to prepare starter culture, incubated at 37°C overnight. 100 mM and 85 mM CaCl₂ solution, 100 mM MgCl₂ solution and Glycerol. These solutions are chilled at 4°C overnight.

- Sterile 25 ml of LB broth was prepared followed by the addition of 25 µl of 35 mg/ml chloramphenicol.
- 0.25 ml of starter culture was added to it and kept for incubation at 37°C at 250 rpm.
- Checked for the O.D. and after approximately 2-3 hours it reached to 0.4. Immediately the cells were kept on on ice and the culture was chilled for 20-30 minutes.

- 25 ml of the culture was poured in an ice-cold centrifuge tube and centrifuged at 4000 rpm for 15 minutes at 4°C. The supernatant was decant and the pellet was re-suspended in about 10 ml of ice-cold 100 mM MgCl₂.
- Again the mixture was centrifuged at 3000 rpm for 15 minutes at 4°C, and the pellet was again re-suspended in about 20 ml of ice-cold 100 mM CaCl₂.
- The suspension was kept on ice for at least 20 minutes again centrifuged and the pellet was re-suspended in 5 ml of ice-cold 85 mM CaCl₂.
- In order to wash the pellet, it was centrifuged at 2100 rpm for 15 minutes and the pellet was re-suspended in 2ml of ice-cold 85 mM CaCl₂ along with 15% glycerol (300 µl).
- For long term the aliquot was stored in -80°C.

3.1.2.2 Transformation Protocol: Heat Shock Method

Following are the steps to follow for the transformation process using Heat shock method:

- LB-agar plates were prepared with antibiotics Ampicillin and chloramphenicol in the concentration of 100 mg/ml and 35 mg/ml respectively.
- Competent cells were removed from -80°C freezer and was kept for thawing on wet ice for 10-20 minutes. 50 µl of the cells were added to the chilled culture tube.
- The cells were mixed with 1-4 µl of DNA sample and was slowly mixed with a pipette tip.

- The mixture was incubated on ice for 30 minutes. Immediately after the cells were heat shocked by placing them in a 42°C water bath for 30 seconds, the tube was returned ice for 2 minutes.
- 950 µl of recovery medium or LB broth was added to the culture tube and was placed in incubator shaker at 250 rpm for 1 hour at 37°C.
- Almost 100 µl of transformed cells were spread on LB agar plates containing appropriate antibiotics and the plates were incubated at 37°C overnight.

3.1.3. Study of cell biomass and growth curve studies.

3.1.3.1. Plasmid Extraction

Plasmids from the broth culture were isolated as per the protocol provided by QIAprep Spin Miniprep Kit (QIAGEN).

- 5 ml of bacterial overnight culture (known as starter culture) was pelleted down by centrifuging at 8000 rpm for 3 minutes at 15-25°C.
- 0.25 ml of buffer P1 was added to re-suspend the pellet and was then transferred to microcentrifuge tube. It was followed by adding 0.25 ml of buffer P2 and 0.35 ml of buffer N3 and the mixture was mixed thoroughly by inverting the tubes 4-6 times until the solution became clear.
- The above formed mixture of about 0.8 ml was then transferred to the spin column and was centrifuged for 1 minute at 13,000 rpm followed by washing with 0.5 ml buffer PB and 0.75 ml of buffer PE. The flow through was discarded by centrifuging the tube at 13,000 rpm for 1 minute.

- The spin column was then placed in a new microcentrifuge tube and in order to elute the plasmid DNA, 0.05 ml of buffer EB was added to the centre of the spin column. Tubes were incubated for 1 minute at room temperature followed by centrifugation at 13,000 rpm for 1 minute.

3.1.3.2. Growth curve studies

The *E. coli* Rosetta pLysS cells were revived on the LB agar medium, antibiotics added to the medium at a conc. of 0.1% Ampicillin (100 mg/ml in distilled water) and Chloramphenicol (35 mg/ml in ethyl alcohol). Incubated at 37°C. Starter culture of 3ml volume prepared from LB broth which contained 1% glycerol inoculated with the *E. coli* cells and incubated at 37°C, 250 rpm until the O.D. reached 0.4-0.5. This was used to inoculate media for bacterial growth studies. Here 15 ml LB broth was prepared in 250 ml flask and 1% glycerol, 0.1% antibiotics & IPTG was added to a final concentration of 1 mM in the media just before inoculation. Inoculum added was 2% of the volume. Flasks were incubated at 37C, 250 rpm. Culture O.D. recorded after every 2 hours at 600 nm.

3.1.4 Expression of CDA in *E. coli* Rosetta pLysS cells

Starter culture was prepared by inoculating the LB broth media with single colony of bacteria taken from the culture plate. The flask was kept in an incubator shaker at 37°C under observation until the O.D of the culture reached 0.4-0.6.

80 ml media was prepared in 250 ml flask and was inoculated with 5% inoculum from the starter culture. The flask as then induced by 1 mM IPTG and incubated at 37°C at 120 rpm. To analyze the biomass and CDA activity, samples were collected at regular

time intervals. The correlation between O.D₆₀₀ and biomass was obtained as, Biomass (g/L) = 0.503 · O.D₆₀₀.

3.1.5 Study of enzyme (CDA) activity.

Following are the steps for MBTH assay (3-methyl-2-benzothiazoline hydrazone) which was used to study the enzyme activity.

- The cells were pelleted down by centrifuging at 10,000 rpm for 15 minutes and was then mixed with 1 mL of Tris-HCl buffer having pH 6.5.
- Probe type sonicator was used for the cells to be lysed and the pulse was set as 5 seconds on and 1 second off for 5 minutes with 20% amplitude.
- The cell lysate obtained after sonication was centrifuged at 10,000 rpm for 15 minutes. The supernatant was collected and was filtered through a 0.45 µm syringe filter.
- 250 µL each Glycol chitin (1 mg/mL) and Tris-HCl buffer (pH 6.5) along with 100 µL of the supernatant was added to the assay mixture as a source of the enzyme. For enzyme-substrate binding, the mixture was kept in the incubator shaker at 37°C for 1 hour.
- In order to stop the reaction, 500 µL of 5% KHSO₄ was added to the sample and was kept for 5 minutes. This was followed by adding 500 µL of 5 % NaNO₂ and was incubated for 6 hours in the fume hood to release all the NO₂ gas.
- 0.5 mL of ammonium sulphamate (12% by wt.) and 0.5 mL of 0.5 % MBTH was added and was given 1 hour incubation. 0.5% FeCl₃ was prepared in 0.1 N HCl and 0.5 mL of the preparation was added in the reaction mixture.

- The reaction mixture was kept for 1 hour incubation at room temperature in the dark and the absorbance was measured at O.D 656 nm.

One Unit of the CDA activity is defined as the activity, which releases 1 μmol of glucosamine from Glycol chitin per minute. Both MBTH assay and enzymatic acetate assay kit (Sigma Aldrich, Catalog no. MAK086) was used to calculate the enzyme activity of the sample.

3.1.6 Optimization of processing parameters

Optimization of processing parameters play an important role in the development of any fermentation process owing to their impact on the economy and efficacy of the process. The conventional approach of optimizing parameters one-factor-at-a-time provide a systematic basis for further optimization. The development of a bioprocess for CDA (from *Bacillus licheniformis*) production in recombinant *E. coli* pLysS, may improve the productivity of the CDA biosynthesis.

3.1.6.1 Effect of rotational speed

The 250 mL conical flasks with 80 mL medium volume were incubated in orbital shaker at 120, 200 and 250 rpm to investigate the effect of rotational speed on biomass and CDA activity.

3.1.6.2 Effect of medium filling volume on biomass growth and CDA production

The 250 mL conical flasks were filled with different amounts of medium volumes to study the effect of medium volumes on biomass and enzyme activity. The flasks were operated at 250 rpm and 37°C in an orbital shaker.

3.1.6.3 Study of the CDA production in different media

The CDA production was studied in three different media namely Luria Bertani Broth (Tryptone 10 g/L, Yeast extract 5 g/L and NaCl 10 g/L), Nutrient Broth (Peptic digest of animal 5 g/L, NaCl 5 g/L, Beef extract 1.5 g/L and yeast extract 1.5 g/L) and Tryptic Soy Broth (Pancreatic digest of casein 17 g/L, NaCl 5 g/L, paptic digest of soya bean meal 3 g/L, Di-potassium hydrogen phosphate 2.5 g/L and Dextrose 2.5 g/L). The flasks were filled with 12 mL medium volume and operated at 250 rpm and 37°C for 8 hours.

3.1.6.4 Study of the effect of different nitrogen sources on CDA production

The organic nitrogen sources such as yeast extract, beef extract, bacteriological peptone, and tryptone were added at 10 g/L concentration to the LB broth. The flasks were filled with 12 mL medium volume and operated at 250 rpm and 37°C for 8 hours.

3.1.7 Optimization of Glycerol Based Media

In order to enhance the biomass and CDA production of recombinant E. coli, the LB media was supplemented with glycerol as a carbon source. The concentrations ranging from 0.1 – 2 % v/v of glycerol were added to the medium and was experimented for biomass and CDA production.

3.1.7 Purification of CDA protein by Ni-NTA chromatography

Ni-NTA column was chosen for the purification of the recombinant protein because of the presence of His-tag which has affinity towards Nickel and binds to it strongly while the rest of the contaminants were washed out.

The general method is that the protein is batch absorbed onto the column. The Ni-NTA beads are mixed with the sample and then pouring into the column. The low concentrations of phosphate and imidazole are used to remove low affinity bound proteins. Finally, the imidazole concentrations are increased to elute the protein from the NTA-beads.

- 1 ml and 4 ml of the Ni-NTA slurry and cleared lysate respectively were mixed and kept for shaking on a rocker at 4°C for at least 3-4h.
- The lysate and slurry mixture was then loaded into a column and was left in the column overnight. Afterwards, the bottom cap was removed and the column flow-through was collected.
- 4 bed volumes of wash buffer was used to wash the column twice. The wash fractions were also collected.
- Then the samples were eluted with Elution Buffer 1 (in a volume of 0.5ml) each for 2-bed volumes. The sample is next eluted with Elution Buffer 2 (in a volume of 0.5 ml) for 2-bed volumes.
- SDS PAGE was run to check purity and protein concentration measured. CDA activity was also calculate for the samples. The composition of different buffers is given in table 3.6.

Table 3.6 Buffer preparation for protein purification

Lysis buffer	Wash Buffer	Elution buffer 1	Elution Buffer 2
NaH ₂ PO ₄ (50 mM)	NaH ₂ PO ₄ (50 mM)	NaH ₂ PO ₄ (50 mM)	NaH ₂ PO ₄ (50 mM)
NaCl (300 mM)	NaCl (300 mM)	NaCl (300 mM)	NaCl (300 mM)
Imidazole (5 mM)	Imidazole (100 mM)	Imidazole (250 mM)	Imidazole (500 mM)
10 % Glycerol	10 % Glycerol	10 % Glycerol	10 % Glycerol

3.1.7.1 SDS PAGE

The supernatant containing the intracellular enzymes were also subjected to SDS page to confirm the production of chitin deacetylase enzyme. 7.5% separating gel and 5% stacking gel was used. The sample and loading buffer was taken in the ratio of 1:1. A protein marker of mid-range 14.3 – 97.4 kDa was used. The gel was run at 50V, 7mA approximately.

3.1.8 Characterization of enzymatic reaction catalysed by BI-CDA

3.1.8.1 Effect of co-factors on CDA activity

All the co-factors i.e., Ca²⁺, CO²⁺, Mg²⁺, Mn²⁺ and Zn²⁺ studied here were prepared as their respective chloride salts. The enzyme and substrate (glycol chitin) mix were incubated for 60 minutes along with co-factors at 37°C in Bis-Tris buffer 50 mM, pH 7.0. The enzyme activity was calculated using acetate assay kit.

3.1.8.2 Effect of concentration of Co ion on CDA activity

Later the CO^{2+} ion concentration was tested with a range from 0.5-10 mM and was calculated using acetate assay kit.

3.1.8.3 Effect of pH on CDA activity

Later the pH range was taken from 3 to 10. An overlap at pH 8 was genuinely taken to study the effect of buffer too along with pH. The different buffer solutions used were Na-citrate buffer (pH 3-6), Tris-Cl (pH 7-8), Borate buffer (pH 8-10) with 50 mM concentration. The reaction was carried out at 37°C for 60 minutes and the activity was calculated using acetate assay kit.

3.1.8.4 Effect of temperature on CDA activity

In the end the effect of different temperatures i.e., 20, 37, 50, 70 and 90° C on the CDA activity was checked using acetate assay kit.

One unit of enzyme activity is defined as the release of 1 μmol of glucosamine from the glycol chitin substrate per minute. The enzyme activity of the sample was calculated accordingly.

3.1.9 Estimation of production cost

The raw material cost was calculated as,

$$C_T = \sum_{i=1}^n c_i y_i \dots\dots\dots 1$$

C_T = Total raw material cost in USD

c_i = Unit cost of raw material “i” in USD

y_i = Quantity of raw material used “i” in bioprocess

According to Bailey and Ollis, the raw material cost is the 30% to 40% of the total production cost, also the overhead charges and the labour cost are 15% each of the total production cost, therefore,

Total cost = Production cost + overhead charges + labour cost.

3.2 Identification of CBP from suitable microorganism

The bacterial culture of *Serratia marcescens* ATCC 13880 was procured from MTCC Chandigarh.

3.2.1 Genomic DNA extraction

Genomic DNA of *Serratia marcescens* ATCC 13880 was extracted using the extraction kit procured from Hi-media.

- 1.5 ml of the overnight bacterial culture was pelleted down in 2 ml Eppendorf tube by centrifuging at 13,000-16,000 rpm for 2 minutes.
- The pellet was resuspended in 180 μ l of lysis solution, 20 μ l of proteinase K solution (20 mg/ml) and was incubated for 30 minutes at 55°C.
- 200 μ l of ethanol (95-100%) was added to the lysate and mixed thoroughly by vortexing for a few minutes.
- The lysate thus obtained was transferred onto the spin column and centrifuge at 10,000 rpm for 1 minute. The flow through was discarded.

- 500 µl of the pre-wash solution was added to the column and centrifuged at 10,000 rpm for 1 minute.
- 500 µl of diluted wash solution was added and centrifuged at 12,000-16,000 rpm for 3 minutes and the flow-through was discarded.
- Finally the column was transferred to the fresh uncapped collection tube and 0.05 ml of elution buffer was added. The column was incubated for 5 minutes at room temperature and centrifuged at 10,000 rpm for 1 minute to elute the DNA.

3.2.2 Designing of primer pair

Gene-specific primers were designed using an online tool, Benchling. Input reference sequence for CBP was taken from ENA (EMBL-EBI). ID - ENA/BAA31569.1 reported from *Serratia marcescens* 2170 (Taxon 615). Basic aspects of primer designing - In order for DNA polymerase to bind to the 3' end of the primer and to continue synthesizing DNA in that direction, the last base of the primer should be G/C as it has 3 hydrogen bonds, which helps in strong annealing between the primer and the template. Total GC content: 50% desirable. Forward Primer - Sequence will be complementary to sense strand. Reverse Primer - Have to take the reverse complement of the DNA sequence to get into right orientation.

This primer sequence was again analyzed using an online oligo analyzer tool from IDT (Integrated DNA Technology) to check for secondary structure like hairpin, homodimers, and heterodimers (<https://eu.idtdna.com/calc/analyzer>)

Table 3.7 Primer specifications

Oligo Name	Sequence (5' to 3')	Length	Tm	MW (g/mol)	GC content
CBP_F	AAACTTCCCGTACCCTGCTCTC	22	62.1	6566	54.5%
CBP_R	ACGTCGATCGCCTGATAGAAGG	22	62.1	6784	54.5%

3.2.3 Polymerase Chain Reaction

Reaction Setup from NEB Protocol for Q5 High Fidelity was followed.

According to the protocol, all reaction components need to be assembled on ice (Table 3.1) and the reactions were immediately transferred to a thermocycler which was preheated to 98°C.

3.2.3.1 PCR optimization

Designed primer pair was then used for amplification of CBP from *Serratia marcescens* ATCC 13880, in order to identify the sequence. Amplified product was obtained after optimization of the polymerase chain reaction. Components which were optimized include DNA concentration, dNTP concentration, Primer concentration, High Fidelity Taq. Polymerase (M0491) from NEB was used instead of conventional Taq. polymerase as the region to be amplified was GC-rich (GC content was greater than 50%). In addition, PCR products generated using High Fidelity Taq. Polymerase has blunt ends as this polymerase will cleave any overhangs generated. Appropriate PCR

cycling conditions were also finalized by optimizing the denaturation, elongation and annealing temperature and the time required.

Starting with the cycling conditions - According to the NEB protocol, the time for denaturation temp. given was 30 seconds only, but as our gene to be amplified is GC rich, we increased the time for denaturation from 30 seconds to 3 minutes for efficient separation of strands to occur. Time for annealing temp. was kept for 20 seconds but to finalize the annealing temperature, a temperature gradient was setup which included temperatures ranging from 61.8°C, 63.1°C and 64.3°C. Suitable product was obtained at temp. of 63.1°C Recommended cycling time for elongation was 20-30 seconds/ kb but as the gene to be amplified had a size less than a kb, 10 seconds was kept for this step. Final elongation was 1 minute. Also, no. of cycles was kept as 28 to reduce non-specific bands as 35 cycles gave multiple bands.

Varying DNA concentration: Initially 150 ng template DNA was used with the above cycling conditions, but the intensity of the band obtained was too low thus the DNA conc. was increased to 200 ng to improve the yield along with dNTP conc. which was increased to 250 μ M but still it did not make any significant difference. So, the focus was shifted on primer conc. and the primer conc. was increased from 0.5 μ M to 0.75 μ M and 1 μ M for each forward and reverse primer. Specific bands were obtained with following component and conditions.

3.2.4 Optimized PCR

Amplified product was obtained after optimization of the polymerase chain reaction. Components which were optimized include DNA concentration, dNTP concentration,

Primer concentration, High Fidelity Taq. Polymerase (M0491) from NEB was used instead of conventional Taq. polymerase as the region to be amplified was GC-rich (GC content was greater than 50%). In addition, PCR products generated using High Fidelity Taq. Polymerase has blunt ends as this polymerase will cleave any overhangs generated. Appropriate PCR cycling conditions were also finalized by optimizing the denaturation, elongation and annealing temperature and the time required.

Starting with the cycling conditions - According to the NEB protocol, the time for denaturation temp. given was 30 seconds only, but as our gene to be amplified is GC rich, we increased the time for denaturation from 30 seconds to 3 minutes for efficient separation of strands to occur. Time for annealing temp. was kept for 20 seconds but to finalize the annealing temperature, a temperature gradient was setup which included temperatures ranging from 61.8°C, 63.1°C and 64.3°C. Suitable product was obtained at temp. of 63.1°C Recommended cycling time for elongation was 20-30 seconds/ kb but as the gene to be amplified had a size less than a kb, 10 seconds was kept for this step. Final elongation was 1 minute. Also, no. of cycles was kept as 28 to reduce non-specific bands as 35 cycles gave multiple bands.

Varying DNA concentration: Initially 150 ng template DNA was used with the above cycling conditions, but the intensity of the band obtained was too low thus the DNA conc. was increased to 200 ng to improve the yield along with dNTP conc. which was increased to 250 μ M but still it did not make any significant difference. So, the focus was shifted on primer conc. and the primer conc. was increased from 0.5 μ M to 0.75 μ M and 1 μ M for each forward and reverse primer.

Specific bands were obtained under following optimized components and conditions:

Table 3.8. Optimized PCR

Components	Volume (μL)	Final Concentration
Sterile D/W	16.4	-
Q5 Reaction buffer (5X)	10	1X
dNTPs (2.5 mM)	4	200 μM
Forward primer (10 μM)	3.75	0.75 μM
Reverse primer (10 μM)	3.75	0.75 μM
Template DNA	1.6	200 ng/μL
High Fidelity Taq. pol.	0.5	0.02 U/μL
GC Enhancer	10	1X
Total Reaction	50	

Reaction buffer contains 2.0 mM Mg^{++} at the final conc. of 1X

Table 3.9 Optimized PCR cycling conditions

Temperature Cycle	Time
98°C	3 min
98°C	10 sec
63.1°C	20 sec

Temperature Cycle	Time
72°C	10 sec
72°C	1 min

3.2.5 PCR product purification

After the PCR was carried out the resultant mixture was subjected to purification to obtain the PCR product in a purified form, free from other components of the mixture. The PCR product purification kit was procured from Hi Media. 225 µl of PCR binding solution was added to 45 µl of the PCR sample and was mixed well by pipetting. PCR product along with the binding solution was added in the miniprep spin column and centrifuged at 13,000 rpm for 1 minute. The column was then transferred to the new clean 2 ml uncapped collection tube. 30 µl of elution buffer was poured to the center of the column and was incubated at room temperature for 1 minute, centrifuged and the purified product was checked on Agarose gel electrophoresis.

3.2.6 Gel elution

PCR product obtained after the gel electrophoresis was purified using the gel elution kit from Hi-media.

- The DNA band were excised from the gel and its weight was determined accordingly and 3 volumes of the gel binding buffer was added.
- The mixture was incubated at 55-60°C for 7 minutes until the gel melted completely.

- Lysate was loaded onto spin column and centrifuged at 12,000 rpm for 1 minute at room temperature. Flow through was discarded.
- 300 µl of gel binding buffer was added into the column and centrifuged for 1 minute at 12,000 rpm at room temperature.
- Ethanol (96-100%) was added to the column. Also 700 µl of diluted gel wash buffer was added too. It was centrifuged for 1 minute at 12,000 rpm at room temperature. Discarded the flow-through.
- 30-50 µl of elution buffer was added onto the column. Incubated for 1 minute at room temperature, centrifuged and the DNA was collected in the fresh eppendrf tube.

3.2.7 Sanger sequencing

The extracted PCR products were purified using the purification kit and lyophilized in order to send it for sequencing. PCR product sequencing was carried out Eurofins Genomics India Pvt. Ltd., Bengaluru, India.

3.3 Fusion of CDA gene with CBP gene

3.3.1 Restriction digestion and ligation method

This study was carried with the help of Benchling software available online.

Input sequences were pET22b-CDA vector and CBP sequence of *Serratia marcescens* 2170 from EMBL. SacII and NdeI are the two restriction sites used to insert the CBP gene. If the vector sequence is double digested with these restriction enzymes, we can fuse the amplified CBP sequence (Table. 3.10) which also contains the same restriction sites.

This will result in N-terminal fusion of CDA with CBP. These restriction sites upon fusion are restored and the fusion protein when expressed will have intact His-tags.

Table 3.10 Modified CBP Primers designed for fusion

Primer Pair	Length	GC Content	Tm (°C)	Rest. Sites	Sequence (5' To 3')
F.P CBP fusion	51	47.00%	86.7°C	SacII	TCC CCGCG GAATTTTCTTTTATC GGTTCCTGCTTTGGGCCATGAACAAAAC
R.P CBP fusion	54	46.00%	88.6°C	NdeI	GAATTCC CATATG TTATTGCTCAGG TTGACGTCGATCGCCTGATAGAAGGCGT

3.3.2 Optimization of PCR parameters

Designed primer pair having NdeI and SacII sites was then used to amplify the CBP gene in order to attach the two restriction sites. The amplified product was obtained after optimization of the PCR parameters and concentration of the components. The DNA and primer concentration were optimized. High fidelity Taq. Polymerase was used. PCR cycling conditions were also optimized specifically by changing the annealing time and temperature of the primers.

According to NEB protocol, the initial denaturation temperature was given as 30 seconds, as the CBP gene is a GC rich sequence so we increased the time to 2 minutes for efficient separation of the two strands. The annealing time was kept as 15 seconds but to optimize the annealing temperature, the gradient was setup ranging from 70 °C

to 74 °C. The recommended cycling time for the elongation step by NEB was 20-30 seconds, but the gene to be amplified had a size less than 1 kb, hence the time decided for the step was 15 seconds for 30 cycles. Final elongation time was set as 1 minute. (Table 3.11 and 3.12)

Table 3.11 Components for Fusion PCR-I

Components	Volume (μL)	Final Concentration
Sterile D/W	23	-
Q5 Reaction buffer (5X)	10	1X
dNTPs (2.5 mM)	4	200 μM
Forward primer (100 μM)	0.25	0.5 μM
Reverse primer (100 μM)	0.25	0.5 μM
Template DNA	2	180 ng/μL
High Fidelity Taq. pol.	0.5	0.02 U/μL
GC Enhancer	10	1X
Total Reaction	50	

Table 3.12 Optimizing parameters for the Fusion PCR-I

Temperature Cycle	Time
95 °C	2 min
95 °C	20 sec

Temperature Cycle	Time
70-74 °C	15 sec
72°C	15 sec
72°C	1 min

The reaction was setup accordingly and there wasn't any band present when the product was checked on Agarose gel electrophoresis.

Now in the next step of optimization, the concentration of the PCR components was not changed. The annealing temperature was taken as 75°C and the annealing time was also increased from 15 seconds to 45 seconds. This step resulted in multiple bands but the very light band at the specific position.

Again, the temperature gradient (76,78,80,82,84 and 86 °C) was set up and the annealing time was also reduced from 45 to 30 seconds. The above setup resulted in the specific as well as nonspecific bands at all temperatures except 86 °C. The melting temperature for the Forward primer was 86.7 °C, so the reaction didn't take place at 86 °C and hence there wasn't any band. The complete focus was now shifted towards the annealing time, which in the next step was decreased from 30 seconds to 20 seconds in order to remove the nonspecific bands while keeping concentration of each component unchanged. Table 3.13 and 3.14 shows the optimized PCR components and parameters respectively which resulted in the desired band.

Table 3.13 Optimized Fusion PCR-I

Components	Volume (μL)	Final Concentration
Sterile D/W	23	-
Q5 Reaction buffer (5X)	10	1X
dNTPs (2.5 mM)	4	200 μM
Forward primer (100 μM)	0.25	0.5 μM
Reverse primer (100 μM)	0.25	0.5 μM
Template DNA	2	180 ng/μL
High Fidelity Taq. pol.	0.5	0.02 U/μL
GC Enhancer	10	1X
Total Reaction	50	

Table 3.14 Optimized Fusion PCR-I parameters

Temperature Cycle	Time
95 °C	2 min
95 °C	20 sec
78 °C	20 sec
72°C	15 sec
72°C	1 min

3.3.3 Optimizing Ligation of CBP gene into pET22b CDA plasmid

The reaction temperature was set according to the NEB protocol. Four set of reactions were kept which were deactivated at different time intervals (5, 10, 16 and 20 hrs). Table 3.15 and Table 3.16 shows the optimized parameters and components for appropriate ligation.

Table 3.15 Optimized Ligation components. (CBP gene in pET22b CDA plasmid)

Components	Volume (μl)
Reaction Buffer	4
Digested Plasmid	2
CBP gene	4
Water	8
Ligase Enzyme	2
Total	20

Table 3.16 Optimized Ligation Parameters. (CBP gene in pET22b CDA plasmid)

Parameters	Temperature ($^{\circ}$C)	Time
Incubation	37	20 hours
Inactivation	65	10 minutes

3.3.4 Designing Primers for CDA-CBP fused gene.

The primer pair for the fused gene were also designed using online tool benchling.

Table 3.17 gives the primer specifications for the CDA-CBP fused gene.

3.17 Specifications of the fused Primer pair.

Primer Name	Sequence	Melting Temperature (T _m) (°C)	GC content	Length
Forward Primer	TTGTCGACGGAGCTCGAAATTC	69.4	50	22
Reverse Primer	TGTTATTTGCTCAGGTTGACGTC	65	43.4	23

The fused gene was amplified at an initial denaturation temperature of 95°C for 2 minutes. Primer annealing temperature was set as 60°C for 45 seconds and the cycling time for elongation was given as 72°C for 3 minutes. The final elongation of 72°C was set for 5 minutes. The whole reaction was set for 30 number of cycles.

3.4 Expression and purification of the recombinant fused protein

The CDA-CBP pET22b plasmid was transformed in BL21 *E. coli* cells according to the standard Heat Shock Transformation procedure. The transformants were then selected on the antibiotic (Ampicillin) agar plates.

3.4.1 Fused protein purification.

Supernatant from the IPTG induced BL21 cultures expressing the fused protein was harvested by centrifugation at 6000g for 10 minutes and then sonicated to release the intracellular protein. The protein was purified through Ni-NTA resin (Qiagen).

Fractions were eluted with 250mM and 500mM imidazole. The protein concentration was checked using Bradford assay (Hi Media) and enzyme purity was verified by SDS PAGE.

3.5 Efficiency of recombinant fused protein on Soluble and Insoluble chitin substrates.

The acetate assay kit (Sigma) was used to detect and measure the acetate production. To measure the activity, the enzyme substrate reaction was performed using two soluble substrates (Glycol and Colloidal Chitin) and two insoluble substrates (Chitin powder and Chitin flakes). Chitosan as substrate was also taken as a control to check the false activity.

The enzyme substrate reaction contains 0.130 mg of enzyme, 0.1 M Tris buffer (pH 8) and 1 mg of each substrate. Reactions without enzyme were served as negative controls or blanks. The final reaction volume in all the cases was 1 ml kept at 35 °C for 16 hours. The production of acetate was detected at 650 nm. All experiments were performed in triplicates.

One unit of enzyme activity was defined as the amount of enzyme required to produce 1 μ mol of acetate per minute.

3.5.1 Activity time profile of the fused protein

The activity of the protein was monitored at different time intervals i.e., 4, 8, 12, 16, 20, 24 hours with chitin powder used as substrate kept at 35 °C which was further calculated using acetate assay kit.

3.5.2 Characterization of the enzymatic reaction catalysed by CDA-CBP fused protein.

3.5.2.1 Effect of cofactors

The cofactors Mn^{2+} , Mg^{2+} , Ni^{2+} , Co^{2+} and Ca^{2+} (5 mM) used in the study were in the form of their respective chloride salts. The enzyme was incubated for 16 hours with the substrate (chitin powder) along with cofactors at 37°C in Tris Buffer 0.1 M (pH 8). The activity was calculated using acetate assay kit.

3.5.2.2 Effect of concentration of Ca^{2+} ions.

The concentration of Ca^{2+} ions was later tested with a range from 1mM to 10 mM and later the activity was calculated using acetate assay kit.

3.5.2.3 Effect of pH.

The pH ranges from 3 to 10 was taken and the buffers used were of 0.1 M concentration. The reaction was carried out at 37°C for 16 hours and the activity was calculated using acetate assay kit.

3.5.2.4 Effect of Temperature.

In the end the effect of different temperatures ranging from 25°C, 30°C, 35°C, 40°C and 50°C was checked and activity was calculated using acetate assay kit.

CHAPTER 4

Results and Discussion

4. Results and Discussion

4.1 Cloning of *Bicda* in pET22b and its expression in *E. coli* Rosetta pLysS

The BICDA gene which was incorporated with the *Nde*I site and *Sal*I site at 5' and 3' ends respectively was amplified using PCR.

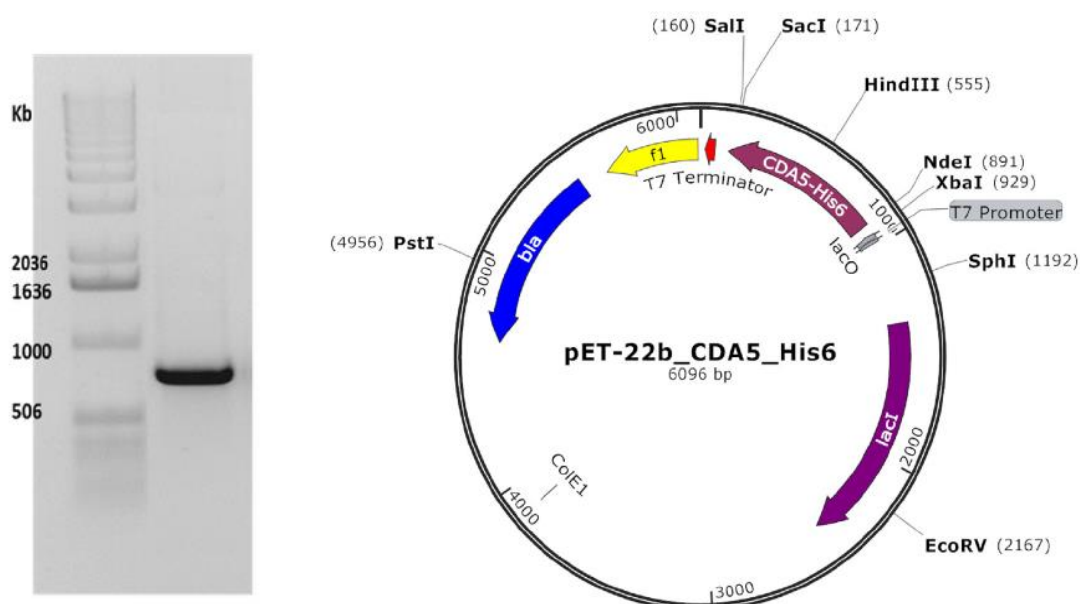


Figure 4.1. (a) The amplified product of CDA gene. (b) The vector map of the pET 22b (+) with the chitin deacetylase gene cloned

The CDA gene which corresponds the size of ~750 bp was further cloned into pET22 b (+) vector within multiple cloning sites using the above-mentioned set of enzymes as shown in figure 4.1 (a) (b) respectively.

In order to ensure the ligation of CDA gene, the vector was double digested with the same set of restriction enzymes (*Nde*I and *Sal*I). The digested product was run on the agarose gel electrophoreses and two bands corresponding to 750 bp and 5346 bp were observed as shown in figure 4.2.

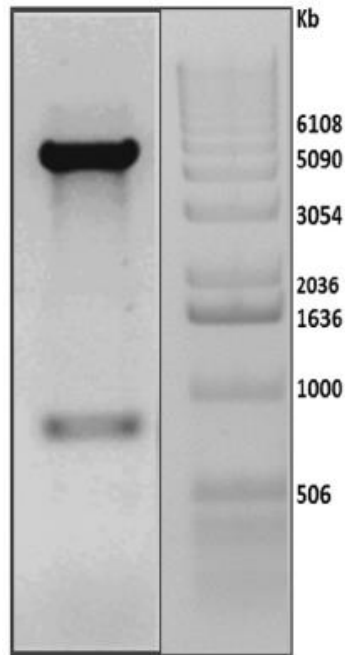


Figure 4.2. Gel picture showing the double digested vector to ensure the size of the gene.

4.2 Vector transformation in *E. coli* Rosetta pLysS

The ligated vector was transformed into *E. coli* pLysS cells by standard heat shock transformation method.

The resulting product was plated on LB agar plates supplemented with antibiotics and incubated at 37° C. Figure 4.3 depicts the transformed colonies obtained after incubating the plates overnight.

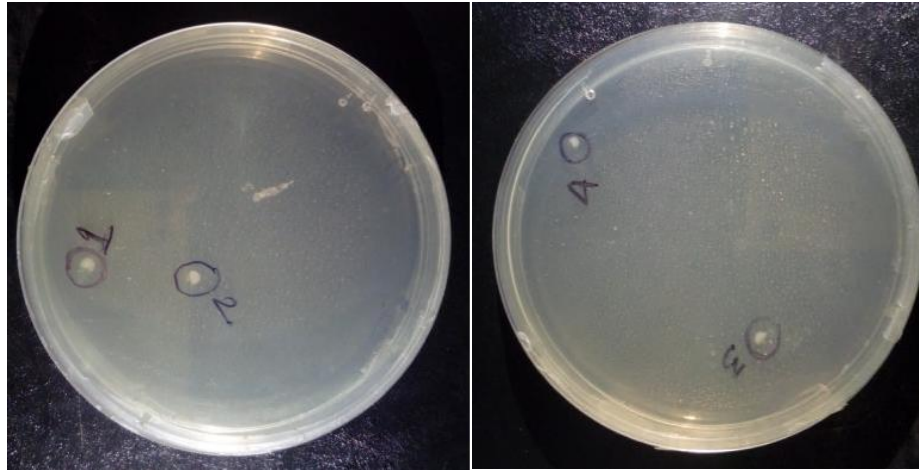


Figure 4.3. Transformed colonies of *E. coli* Rosetta cells on LB agar plates

4.3 Effect of operating condition on CDA production

Figure 4.4 shows effect of rotational speed and filling volume on the growth and CDA production in recombinant *E. coli* pLysS cells. As rotational speed increased (Figure 4.4, solid lines), the growth rate improved in the LB medium due to which the time required to attain the maximum biomass reduced. The culture grown at 250 rpm reached the maximum biomass of about 1 g/L in about 30 to 34 h, whereas the culture grown at 120 rpm achieved maximum biomass at about 60 h. Further, reduction in the medium filling volume in the flask reduced the time required to achieve maximum biomass. Figure 4.4 demonstrates the effect of medium filling volume on the growth of the microbial culture (dashed lines). As filling volume reduced from 40mL to 12mL, the time required to reach the maximum biomass concentration of about 1 g/L reduced from about 30 to 34 hours to only about 8 hours. The oxygen transfer rate in shake flask cultures is proportional to (rotational speed)^{1.18} and (medium volume)^{-0.74} (Sarkar et al. 2017). Thus, increasing the rotational speed of the shaker and reducing the medium filling volume improved the oxygen transfer rate from the air to the medium.

Higher oxygen transfer rate improved the growth and hence reduced the time required to reach the maximum biomass concentration. The maximum enzyme activity in the LB medium varied between about 80 and 84 U/mL in above study.

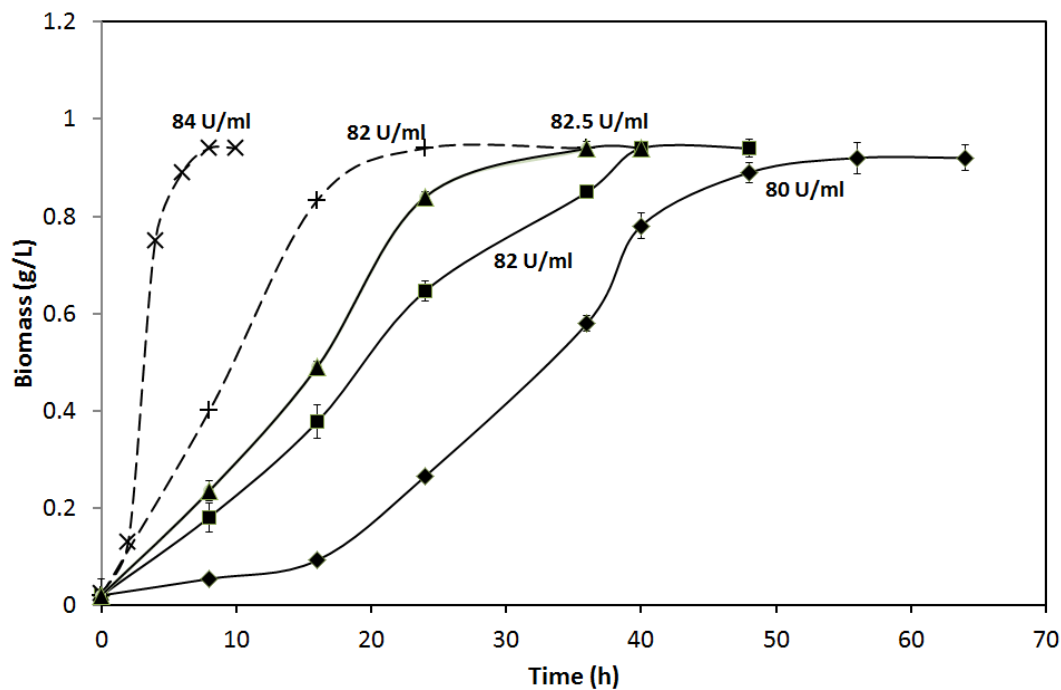


Figure 4.4 Effect of rotational speed (solid line - (◆) 120, (■) 200, (▲) 250 rpm) and medium volume (dashed line - (+) 40 ml, (X)12 ml) on recombinant E. coli growth in LB medium.

Figure 4.5 shows the effect of different types of media on CDA activity. The cultures grown in TSB medium exhibited the maximum CDA activity as compared to the other investigated media. TSB medium contains 17 g/L of complex nitrogen source and 2.5 g/L of glucose. Whereas, the other two media do not contain glucose. The amount of complex nitrogen source available in other two media is also less as compared to TSB medium. Therefore, TSB medium produced more biomass of about 3 g/L as compared

to about 1 g/L biomass in LB and NB medium, respectively. However, the time required to achieve the maximum CDA activity increased from about 8 h in LB/NB medium to 15 h in TSB medium. The CDA expressing plasmid has lac operon for expression of CDA gene where IPTG acts as an inducer. According to Mondin et al., glucose concentration as low as 2mM repress the lac operon which was the reason behind delayed expression of recombinant CDA in TSB medium (Hoßbach et al. 2018). Since, glucose was repressing the expression of the CDA, glycerol was chosen as the carbon source for medium development. Moreover, glycerol does not compete with the human food chain which makes it an ideal carbon source for bioprocess development. The effect of the different nitrogen sources on the CDA production was investigated.

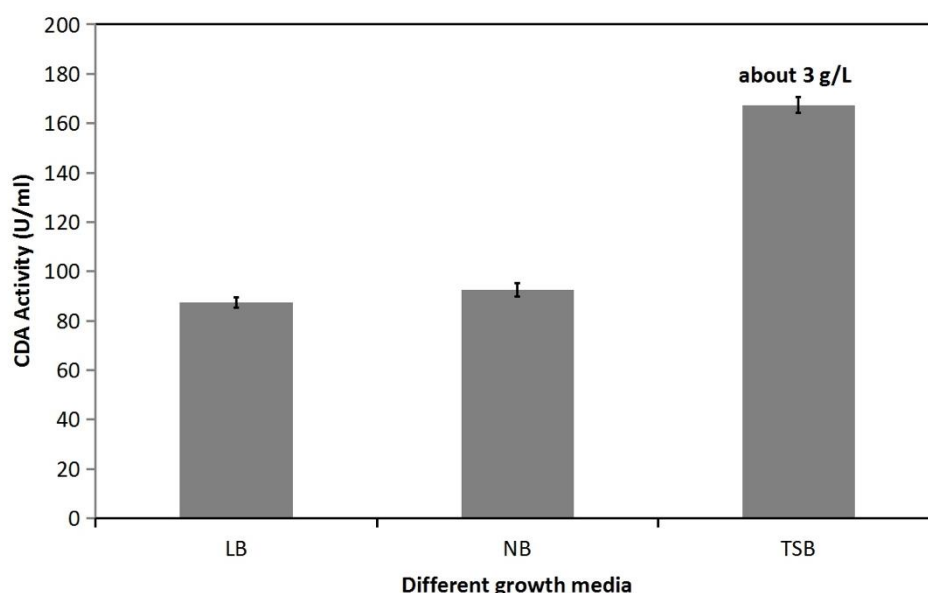


Figure 4.5 Effect of different growth media on CDA activity

Figure 4.6 (A) and 4.6 (B) demonstrates the effect of the different nitrogen sources and different glycerol concentrations on the CDA expression. Yeast extract and beef extract exhibited almost similar enzyme expression of about 160 U/mL, followed by peptone

and tryptone. The enzyme activity almost doubled in cultures supplemented with the different nitrogen sources as compared to the control culture grown in LB medium. The addition of glycerol further improved enzyme production and hence activity. As glycerol supplementation increased in the medium, the enzyme activity improved. The crude filtered supernatant gave the maximum enzyme activity of about 320 U/mL and the specific activity of about 256 U/mg in 2% (w/V) glycerol. Higher concentrations (3%) of the glycerol resulted in similar CDA activity at 10 h and therefore were not used in further studies.

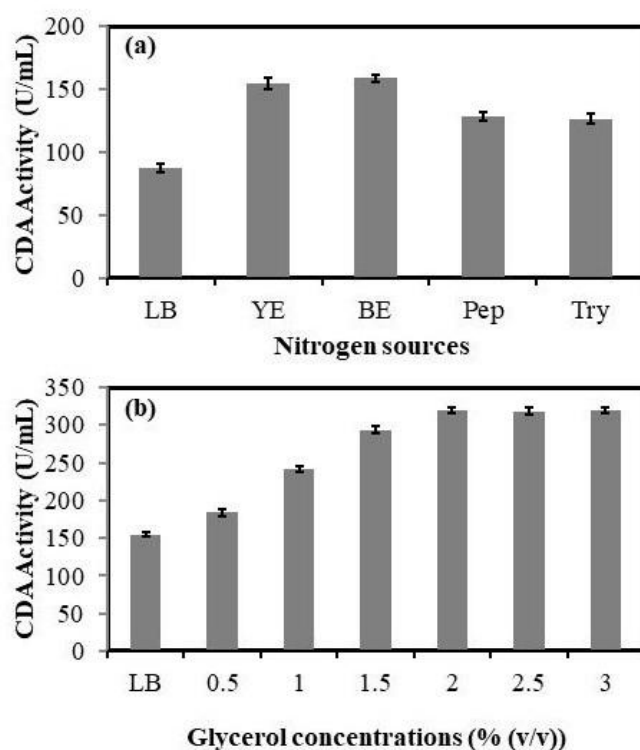


Figure 4.6 (A) Effect of different nitrogen sources (LB: Luria-Bertani, YE: Yeast Extract, BE: Beef Extract, Pep: Peptone, Try: Tryptone), (B) Effect of different glycerol concentrations (0.5 – 2%) on CDA activity

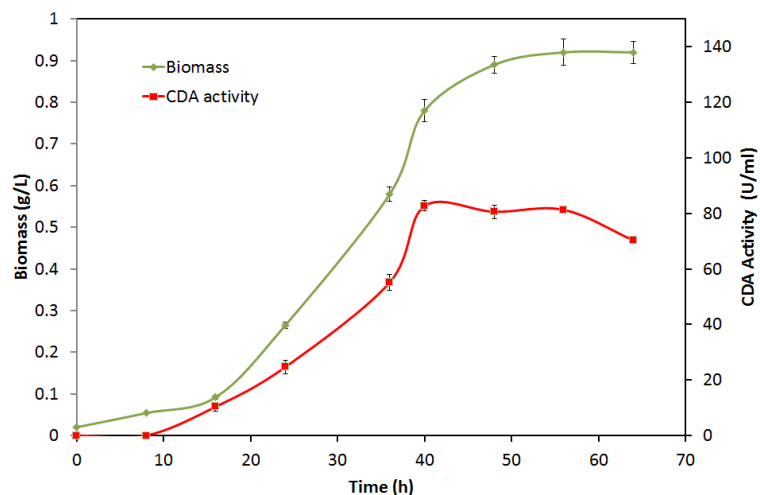


Figure 4.7. Study of the enzyme activity in LB media (250 ml flask, 5% inoculum, 80 ml medium volume, 120 rpm)

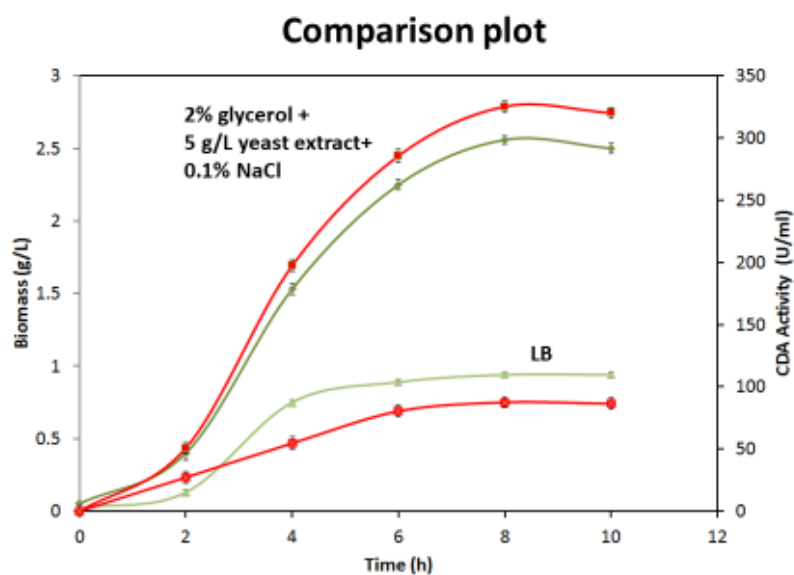


Figure 4.8. Biomass growth and CDA activity in control conditions and under optimized conditions (250 ml flask, 2% glycerol, 5% inoculum, 12 ml medium volume and 250 rpm)

4.4 Study of cell biomass and enzyme activity

Figure 4.7 demonstrates the cell biomass (g/L) and CDA activity (U/mL) with respect to time. The culture grown in LB medium reached the maximum biomass of about 1

g/L in about 60 hours. The maximum enzyme activity in the LB medium varied between about 80 to 84 U/mL.

Figure 4.8 compares the biomass and CDA activity in the control medium before and after addition of glycerol as a carbon source in the medium. There was about 6-fold improvement in the CDA activity in optimized medium containing 2% glycerol, 10 g/L yeast extract and 1 g/L NaCl. Moreover, the bioprocess time reduced substantially from about 48 h to just 8 h. The increase in CDA activity and reduction in cultivation time increased volumetric productivity of CDA from 1.67 U/mL/h to 40 U/mL/h.

4.5 Purification of CDA

The CDA thus produced was purified by Ni-NTA matrix column (Qiagen, Germany).

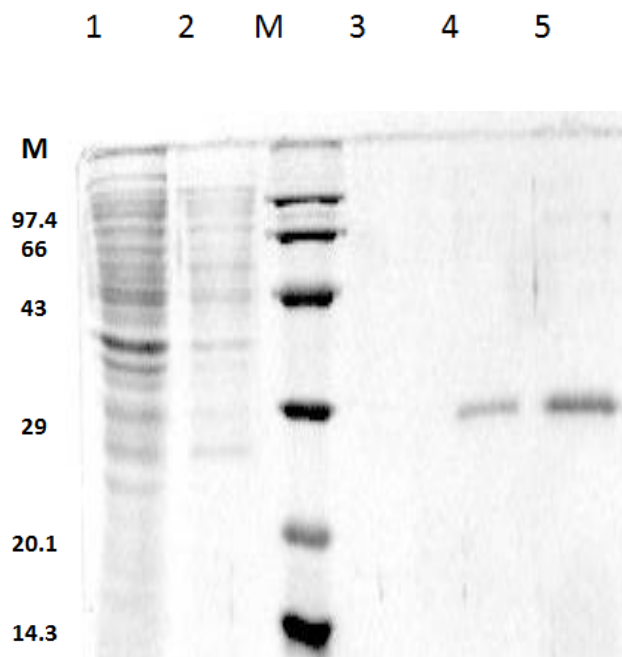


Figure 4.9. SDS PAGE of CDA purification stages. Here, “M” represents molecular weight marker, Lanes 1: flow through, 2: wash, 4: 250 mM imidazole buffer, 5: 500 mM imidazole buffer

4.6 Characterization of enzymatic reaction catalysed by BI-cda

4.6.1 Effect of co-factors on CDA activity.

The co-factors used (Ca^{2+} , CO^{2+} , Mg^{2+} , Mn^{2+} and Zn^{2+}) were incubated along with the enzyme and substrate (glycol chitin) for 60 minutes at 37°C in Bis-Tris buffer and pH 7.0. The enzyme activity was highest in the presence of Co as the co-factor as shown in figure 4.10 (A).

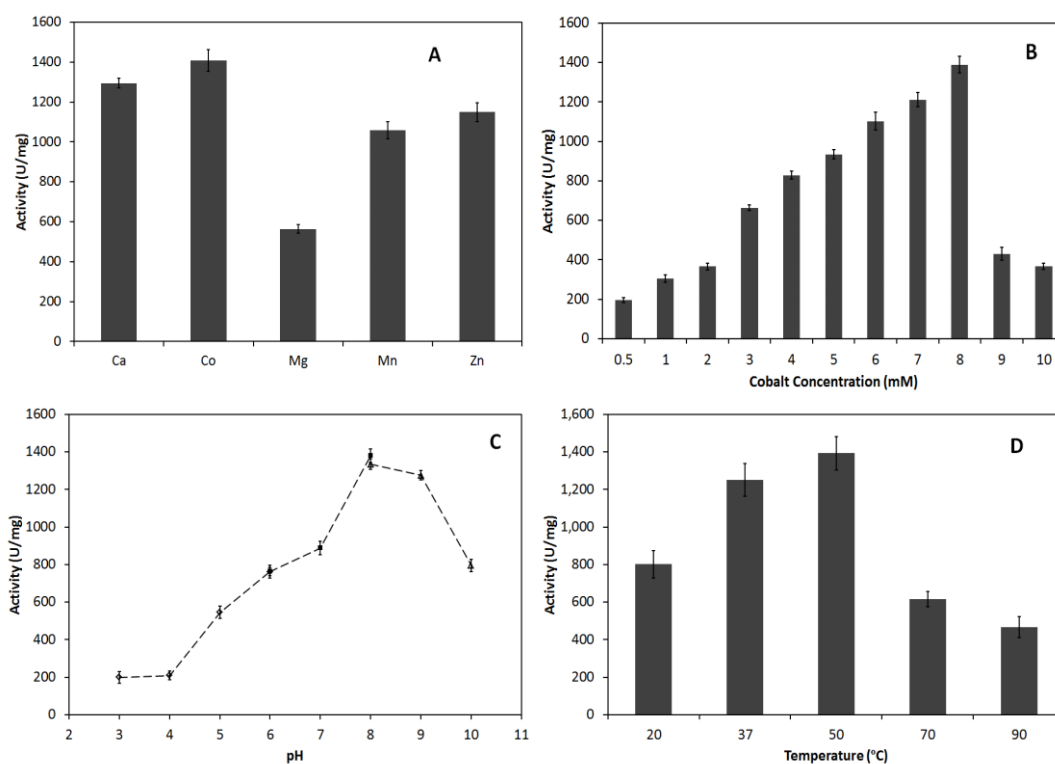


Figure 4.10. Effect of (A) Cofactors, (B) Cobalt concentration, (C) pH and (D) temperature on the purified CDA activity.

4.6.2 Effect of concentration of Co ion on CDA activity.

The concentration of the Co was later tested with a range from 0.5-10 mM. It can be observed that a concentration of 8 mM Co yielded the best activity of the enzyme as shown in figure 4.10 (B).

4.6.3 Effect of pH on CDA activity.

Later the effect of pH range from 3 to 10 was observed on CDA and it was found out that the enzyme was showing the highest activity at pH 8 as shown in figure 4.10 (C).

4.6.4 Effect of temperature on CDA activity.

In the end the effect of different temperatures i.e. 20, 37, 50, 70 and 90° C on the CDA activity was checked. It was found that the enzyme worked well with the substrate at 50° C as shown in figure 4.10 (D). The enzyme was incubated with the substrate for 60 minutes. The purified enzyme activity was about 1400 U/mg under optimum conditions.

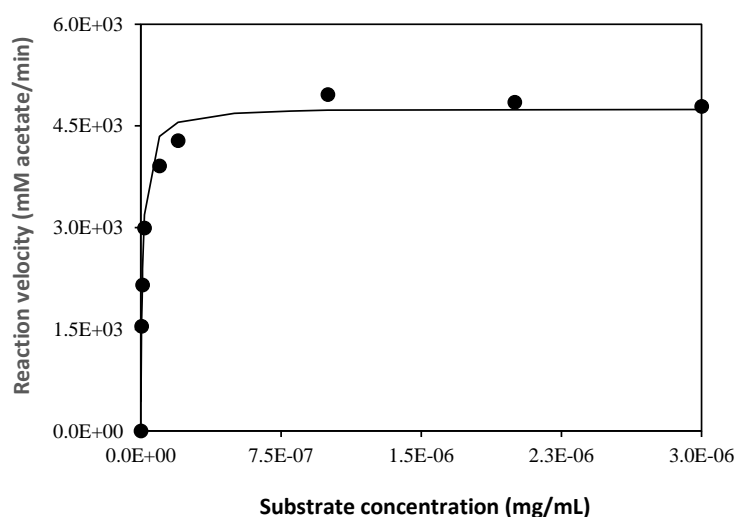


Figure 4.11 The Michaelis-Menten plot for the enzymatic deacetylation of glycol chitin.

Figure 4.11 represents the relation between the reaction velocity with respect to substrate concentration. The data were fitted with nonlinear regression using MS Excel solver and the K_m , V_{max} and K_{cat} values were obtained as $9.96E+03$ mM acetate/minute and $5.18E+03$ 1/s respectively as given in Table 4.1.

Table 4.1 The below calculations are based on 100mg purified protein obtained from 5L of culture broth as per the method given in Biochemical Engineering Fundamentals by Bailey and Ollis, McGraw Hill.

Raw material for 100 mg purified CDA Cost obtained from alibaba.com	Unit cost USD (c_i)	Quantity (y_i)	Cost USD (c_i*y_i)
Yeast extract (per Kg)	6	0.1 kg	0.6
Glycerol (per Kg)	2	0.1 kg	0.2
Ni-NTA (per ml)	15	5 ml	75
Other chemicals (per Kg)	20	0.1 kg	2
Total raw material (RM) cost $C_T = \sum_{i=1}^n c_i y_i$	-	-	77.8
Production cost (basis: 30% of production cost is RM cost)	-	-	259.3
Overheads (15% of production cost)	-	-	38.9
Labour Cost (15% of production cost)	-	-	38.9

Raw material for 100 mg purified CDA Cost obtained from alibaba.com	Unit cost USD (c_i)	Quantity (y_i)	Cost USD (c_i*y_i)
Total cost	-	-	337.1

In a bioprocess, the raw material cost share in the total production cost is usually in the range of 30 to 40%. The raw material cost for CDA production using the mentioned process is about 77.8 USD. If conservative estimate is taken and assume raw material cost is 30% of the production cost, then the production cost value is USD 259.3, which was calculate as total raw material cost/0.3. Adding labour cost and overhead charges (15% each of the total production cost), the total CDA production cost reaches to about 337 USD. Overall, the cost of production of 100 mg of purified CDA is mentioned in Table 4.1. The production cost is calculated based on the method given by Bailey and Ollis (Scotland Bailey 1986).

4.7 Identification of CBP

4.7.1 Design of primer pairs

Gene-specific primers were designed using an online tool, Benchling. Input reference sequence for CBP was taken from ENA (EMBL-EBI). ID - ENA/BAA31569.1 (Fig. 4.12), reported from *Serratia marcescens* 2170 (Taxon 615).

Coding: BAA31569.1

Serratia marcescens CBP21 precursor

View: [TEXT](#) [FASTA](#) [XML](#)

Organism Serratia marcescens	Molecule type genomic DNA	Topology linear	Data class STD
Sequence length 594	Sequence Version 1		

Lineage
Bacteria, Proteobacteria, Gammaproteobacteria, Enterobacterales, Yersiniaceae, Serratia

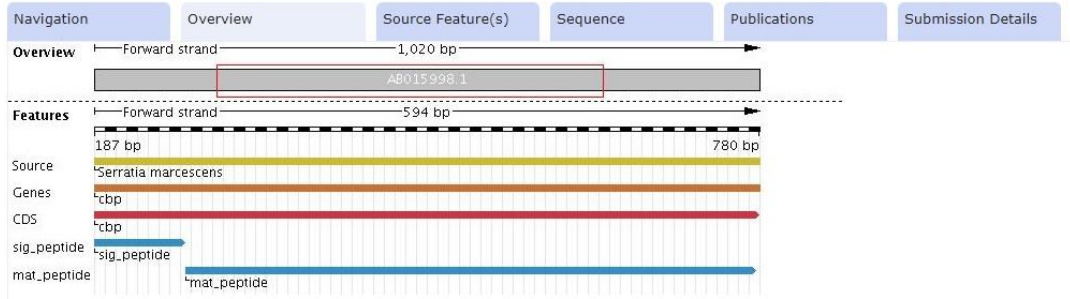


Figure 4.12 Serratia marcescens CBP 21 precursor

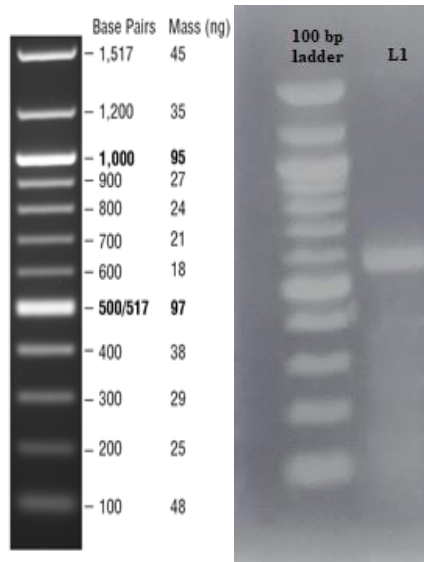
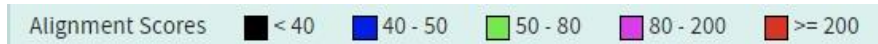


Figure 4.13 Agarose gel displaying CBP gene.



Distribution of the top 9 Blast Hits on 9 subject sequences



Serratia marcescens strain EL1 chromosome

Sequence ID: [CP027796.1](#) Length: 5201791 Number of Matches: 1

Range 1: 1771709 to 1772247 [GenBank](#) [Graphics](#)

[▼ Next Match](#) [▲ Previous Match](#)

Score	Expect	Identities	Gaps	Strand
944 bits(511)	0.0	531/540(98%)	4/540(0%)	Plus/Plus

Features: [chitin-binding protein](#)

Query	7	gCTGA-CGCGGCC-TGTTGCGCGTTTTCGC-ACAGGCGAATGCCACGGTTATGTCGAGTC	63
Sbjct	1771709	GCTGAGCGCGGCCATGTTGCGCGTTTTCGCAACAGGCGAATGCCACGGTTATGTCGAATC	1771768
Query	64	GCCGGCCAGCCGCGCCTATCAGTGCAAAGTGCAGCTCAACACCCAGTGCAGGCGAGCGTGCA	123
Sbjct	1771769	GCCGGCCAGCCGCGCCTATCAGTGCAAAGTGCAGCTCAACACCGAGTGCAGGCGAGCGTGCA	1771828
Query	124	GTACGAACCGCAGAGCGTCGAAAGGCTTCCCGCAGGCCGGCCCGGCTGACGG	183
Sbjct	1771829	GTACGAACCGCAGAGCGTCGAAAGGCTTCCCGCAGGCCGGCCCGGCTGACGG	1771888
Query	184	CCATATCGCCAGCGCCGACAAGTCCACTTTCTTGAAGTGGATCAGCAAACGCCGACGCG	243
Sbjct	1771889	CCATATCGCCAGCGCCGACAAGTCCACTTTCTTGAAGTGGATCAGCAAACGCCGACGCG	1771948
Query	244	CTGGAACAAGCTCAACCTGAAAACCGGCCGAACTCCTTTACCTGGAAGCTGACCGCGCG	303
Sbjct	1771949	CTGGAACAAGCTCAACCTGAAAACCGGTCGAACTCCTTTACCTGGAAGCTGACCGCGCG	1772008
Query	304	TCACAGCACCACAGCTGGCGCTATTTATCACCAGCCGAACTGGGACGCTTCGCAGCC	363
Sbjct	1772009	TCACAGCACCACAGCTGGCGCTATTTATCACCAGCCGAACTGGGACGCTTCGCAGCC	1772068
Query	364	GCTGACCCGCGCTTCCCTTTGACCTGACGCGTTCTGCCAGTTCAACGACGGCGGCCAT	423
Sbjct	1772069	GCTGACCCGCGCTTCCCTTTGACCTGACGCGTTCTGCCAGTTCAACGACGGCGGCCAT	1772128
Query	424	CCCTGCCGACAGGTCACCCACAGTGAACATACCGGACAGATCGCAGCGGTTTCGCACGT	483
Sbjct	1772129	CCCTGCCGACAGGTCACCCACAGTGAACATACCGGACAGATCGCAGCGGTTTCGCACGT	1772188
Query	484	GATCCTTGCCGTGTGGGACATAGCCGACACCGCTAACGCCTTCTATCAGGCGAATCGACG	543
Sbjct	1772189	GATCCTTGCCGTGTGGGACATAGCCGACACCGCTAACGCCTTCTATCAGGCGA-TCGACG	1772247

Figure 4.14 Alignment scores in BLAST

4.7.2 Gene amplification and sequencing

Designed primer pair was then used for amplification of CBP from *Serratia marcescens* ATCC 13880, in order to identify the sequence. Amplified product was obtained after optimization of the polymerase chain reaction cycling conditions as well as process parameters.

The obtained sequence of Sm CBP consisted of 594 bp as shown in figure 4.13. The sequence obtained from Eurofins Genomics Pvt. Ltd. was subjected to similarity sequence analysis using NCBI-BLAST tool and the results revealed that the nucleotide sequence of Sm CBP showed 99% homology and alignment score of > 200, grouped with other *Serratia* gene such as *Serratia marcescens* strain EL1 as shown in figure 4.14.

4.8 In-silico studies of CDA-CBP fusion

4.8.1 Restriction digestion and ligation method

This study was carried with the help of Benchling software available online. Input sequences were pET22b-CDA vector and CBP sequence of *Serratia marcescens* 2170 from EMBL.

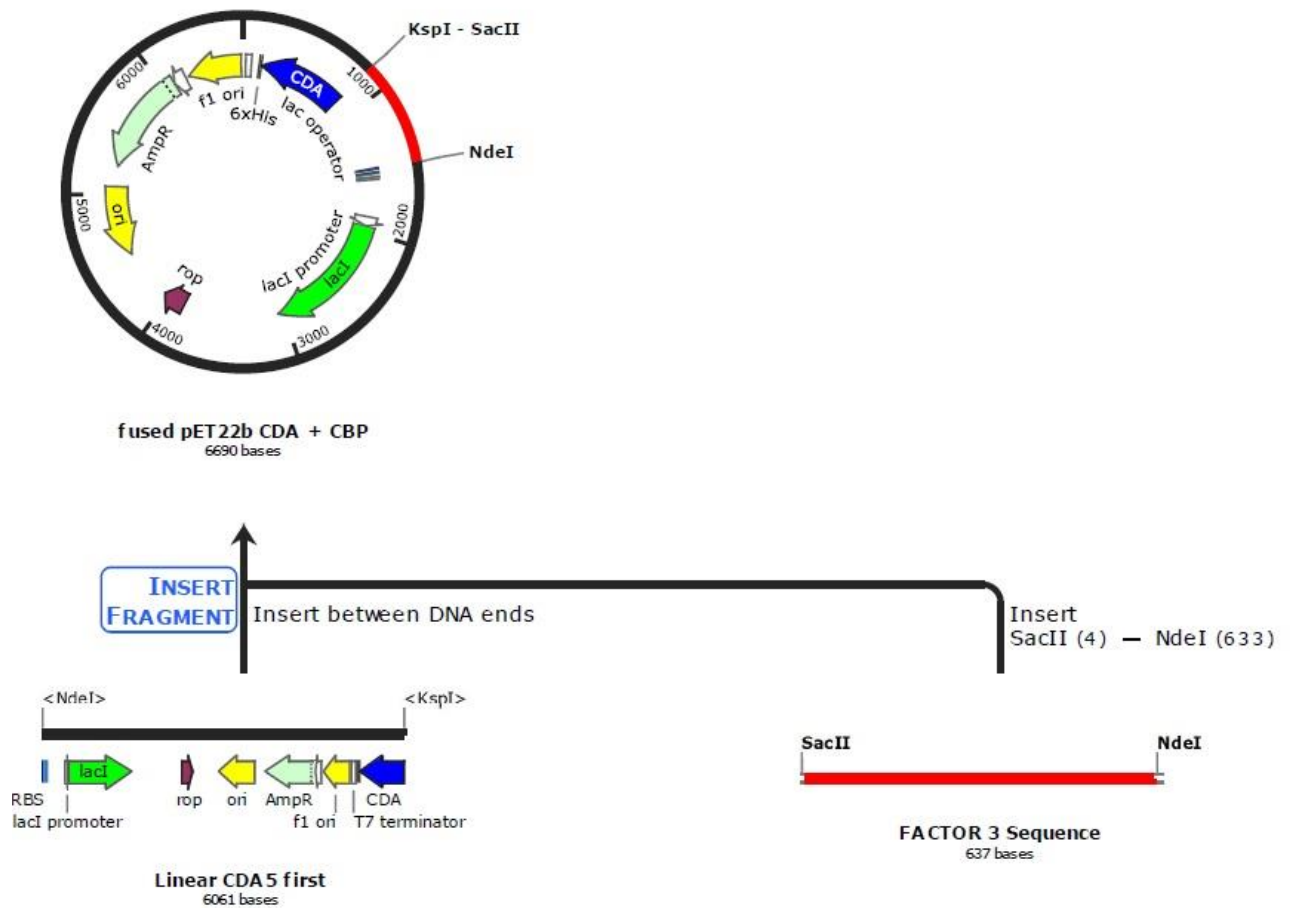


Figure 4.15 Schematic diagram showing fusion of BI-CDA and Sm-CBP genes.

In Fig. 4.16 SacII and NdeI sites are visible, when the vector sequence is double digested with these restriction enzymes, we can fuse the amplified CBP sequence (Fig. 4.13) which also contains the same restriction sites. This will result in N-terminal fusion of CDA with CBP. These restriction sites upon fusion are restored and the fusion protein when expressed will have intact His-tags.

4.8.2 Fusion primer pair

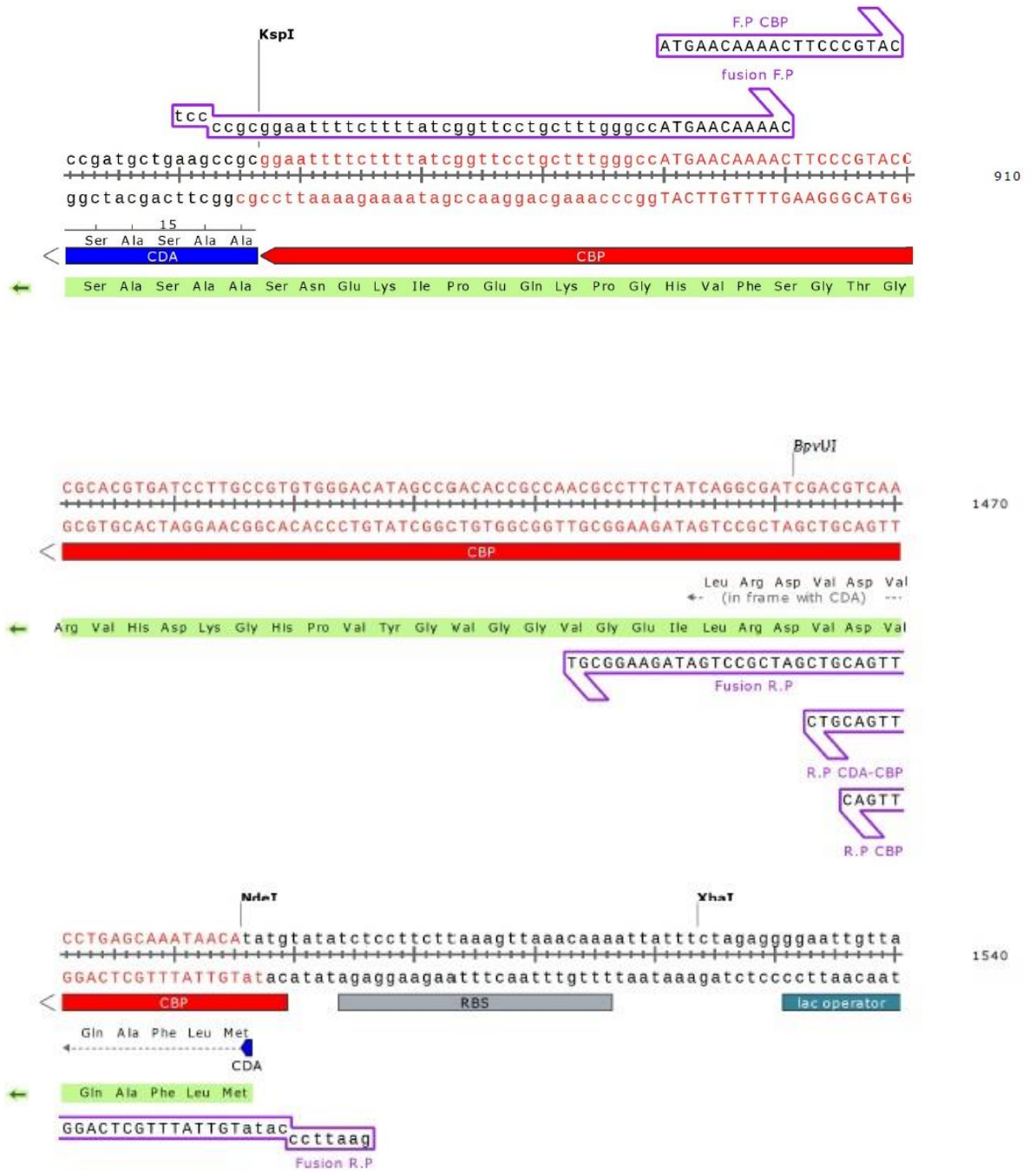


Figure 4.16 Fusion primer pair with restriction sites

4.8.3 Fusion Product

Restriction digestion technique can be used for making CDA-CBP fusion (Fig. 4.15) and then the resulting construct (Figure 4.17) with six His tag and the fused CDA-CBP gene was transformed into *E.coli* BL21 cells, where it can be expressed.

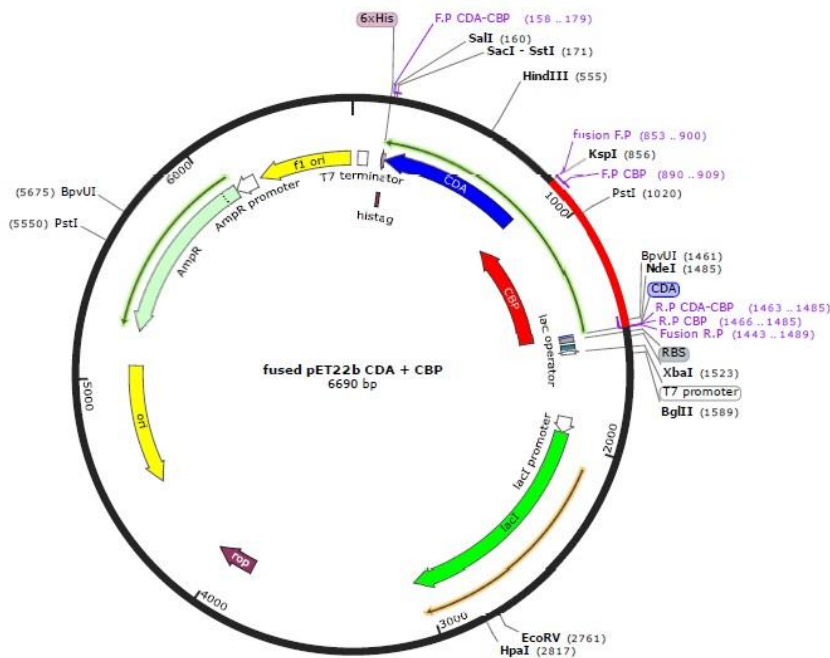


Figure 4.17 SmCBP 21 gene fused with CDA in pET22b vector

4.9 In-Vitro study of CDA-CBP fusion.

4.9.1 Fusion PCR I

The CBP gene obtained was then amplified using the gradient PCR method. The amplified product corresponding to the size of 600 bp depicts the incorporation of NdeI site on the 5' end and SacII site on the 3' end of the gene as shown in figure 4.18. The desired band along with other non-specific bands were obtained at all the annealing

temperatures except at 86 °C. This is because the forward primer has the same melting temperature i.e., $T_m = 86$ °C and the reaction might not have taken place.

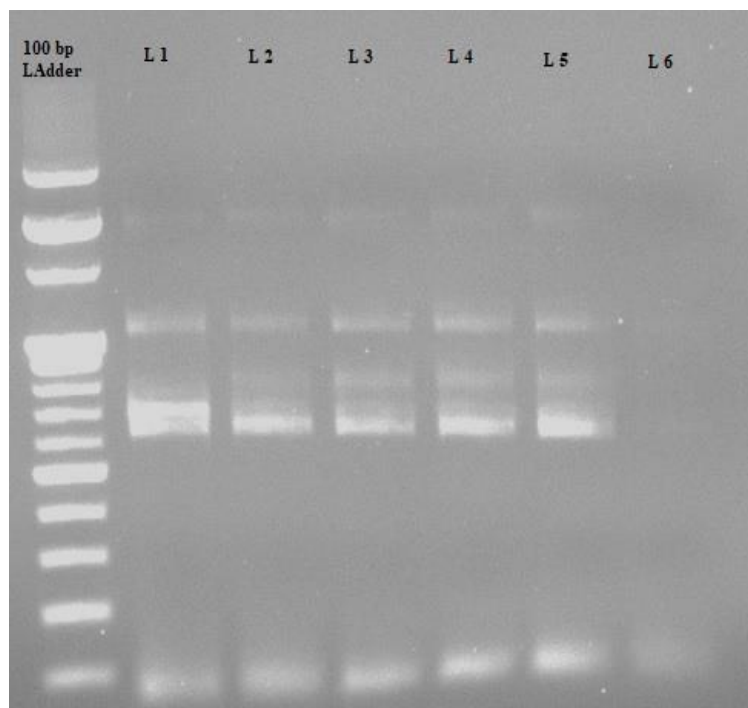


Figure 4.18. Gradient PCR for CBP gene. L1, L2, L3, L4, L5 and L6 shows the amplified gene at annealing temperatures 76, 78, 80, 82, 84 and 86 resp.

4.9.2 Optimized Fusion PCR I

From the above results, randomly 78°C was chosen as the best annealing temperature. After annealing time was decreased from 30 seconds to 20 seconds, agarose gel picture (figure 4.19) shows only the specific band at 600 bp and all other non-specific bands were removed.



Figure 4.19 Agarose gel displaying desired band

4.10 Cloning of *Sm* CBP gene in pET22b_CDA_His6 plasmid

The CBP gene corresponding to the size of 600 bp was then cloned into the pET22b_CDA_His6 vector using the same set of enzymes as shown in figure 4.15.

To ensure the fusion of both *Bli* CDA and *Sm* CBP gene, the vector was double digested with NdeI and SalI restriction enzyme. The digested product was run on the agarose gel, two bands corresponding to approximately 1350 bp and 5340 bp were observed as shown in figure 4.20.

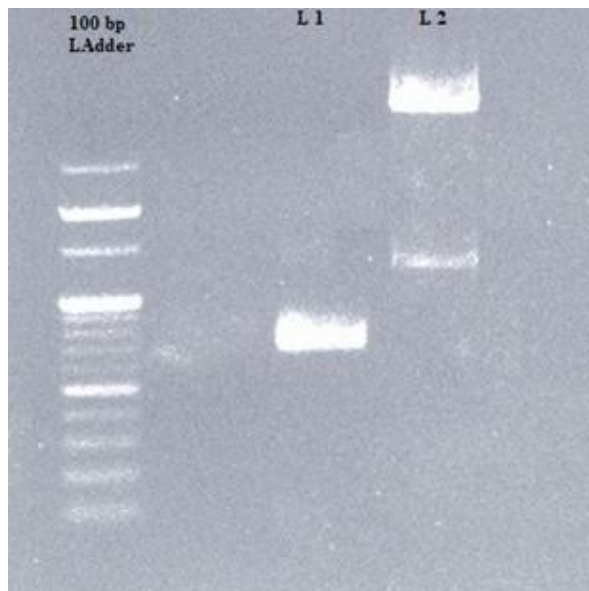


Figure 4.20. Agarose gel showing double digested fused plasmid. L1 shows the CDA gene (752 bp) and L2 shows the double digested fused plasmid with Sall and NdeI enzymes

The band obtained at 1350 bp was cross verified by amplifying the fused gene with the corresponding set of primers. Figure 4.21 shows the gel picture of the amplified product corresponding to the size of 1350 bp which is the exact size of the fused gene.



Figure 4.21. Agarose gel showing amplified fused CDA-CBP gene

4.11 Vector transformation in *E. coli* BL21

The ligated vector was transformed into *E. coli* BL21 cells by standard heat shock transformation method.

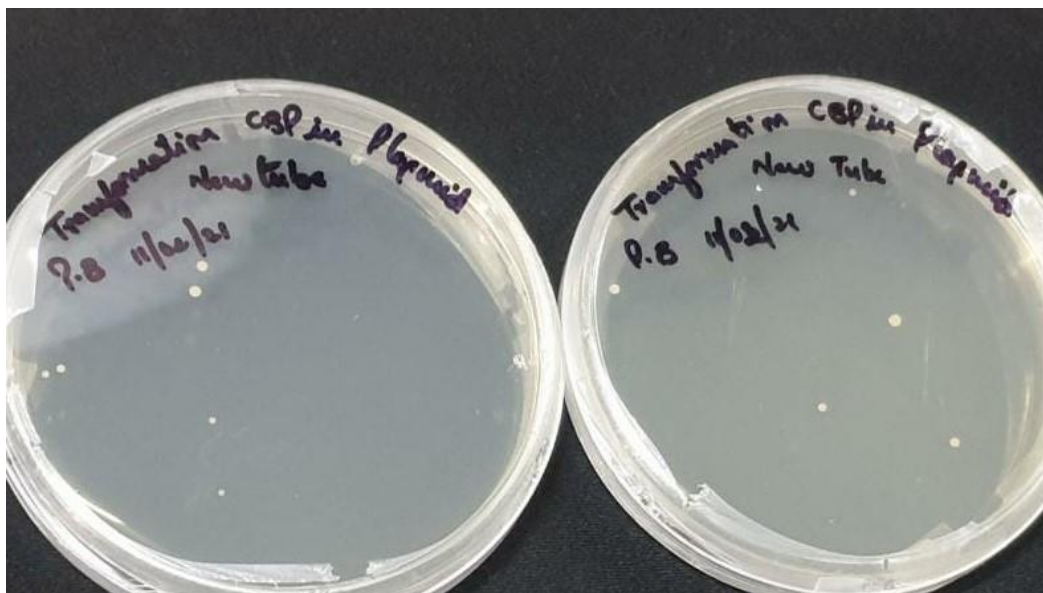


Figure 4.22. Transformed colonies of *E. coli* BL21 cells on LB agar plates

The resulting product was plated on LB agar plates supplemented with antibiotic (ampicillin) and incubated at 37°C. Figure 4.22 depicts the transformed colonies obtained after incubating the plates overnight.

4.12 Expression and Purification of the fused protein

In order to express the protein, the *E. coli* BL21 bacterial culture containing pET22b CDA_CBP_His6 plasmid was induced with 2% IPTG and kept in incubator shaker for 24 hours at 18°C. On characterization of the microorganism by the biochemical test such as Indole, the test result here showed the orange-red color in the surface alcohol layer on the top of the broth which indicated the positive result towards the presence of *E. coli* as shown in figure 4.23.



Figure 4.23. Indole test showing positive result for *E. coli*

The product thus produced was purified using Ni-NTA column. Figure 4.21 demonstrates the SDS-PAGE analysis of the purified fused protein revealed an approximate molecular weight of 51 KDa which is similar to the expected size.

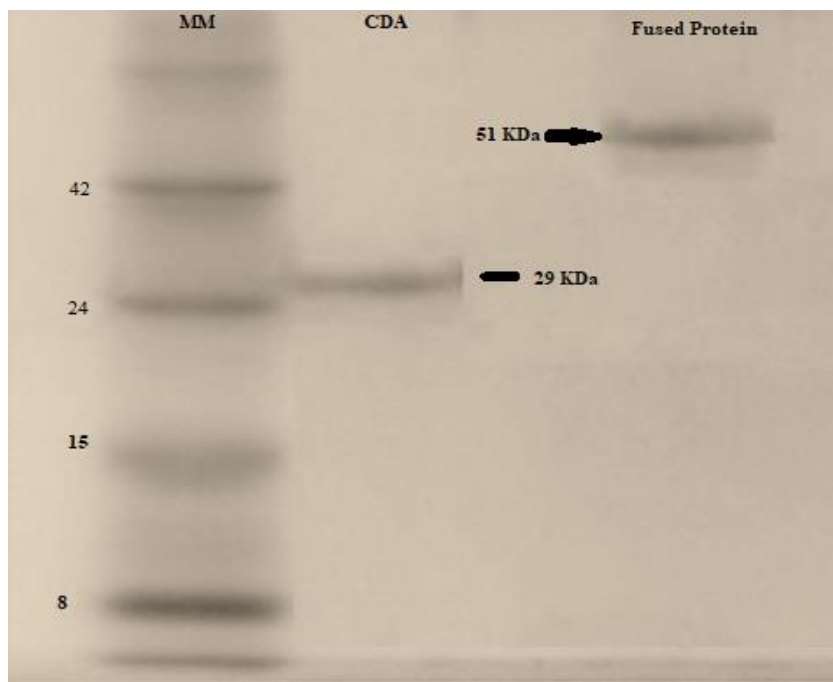


Figure 4.24. SDS PAGE of the purified fused protein. MM represents the molecular marker, S1, S2, S3 and S4 are the purified samples collected in four different tubes.

4.13 Catalytic efficiency of recombinant fused protein on soluble and insoluble chitin substrates.

The catalytic efficiency of the fused chimera (CDA-CBP) was analyzed for the degradation of the soluble substrates (Glycol chitin & Colloidal chitin) and insoluble substrates (Chitin powder & chitin flakes). Chitosan (DA > 90%) as a substrate was taken as the control to check the false positive activity. The chimeric enzyme was highly active on chitin powder substrate as compared to chitin flakes under the standard reaction conditions as shown in figure 4.25. The activity of the enzyme of chitosan substrate was close to negligible.

Enhanced hydrolytic activity of CBP21 fused chimera on insoluble chitin powder can be explained in terms of intramolecular synergism. This mechanism was initially reported for endoglucanase A (Cen A) from *Cellulomonas fimi* that had a catalytic domain and a non-hydrolytic cellulose-binding domain which can interact synergistically in the disruption and hydrolysis of cellulose fibers (Claeysens and Henrissat 1992) Thus the addition of CBP21 for improving catalytic efficiency of CDA can be considered as an example of intermolecular synergism. Inter-molecular synergism can be explained as the competition for the binding sites in substrate between the two individual protein molecules which may decrease the overall catalytic efficiency (Claeysens and Henrissat 1992).

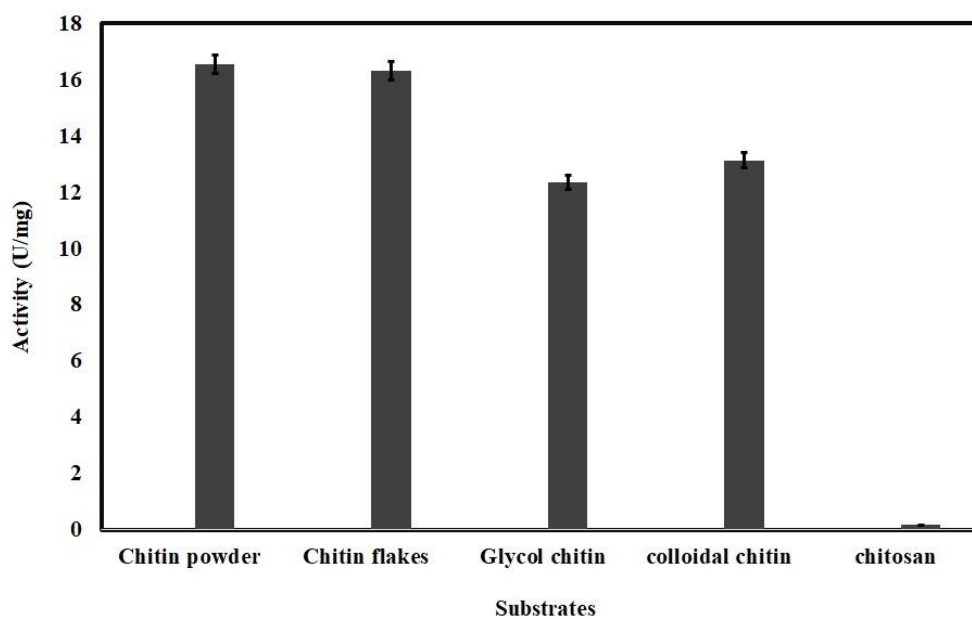


Figure 4.25 Effect of fusion chimera on different Chitin substrates

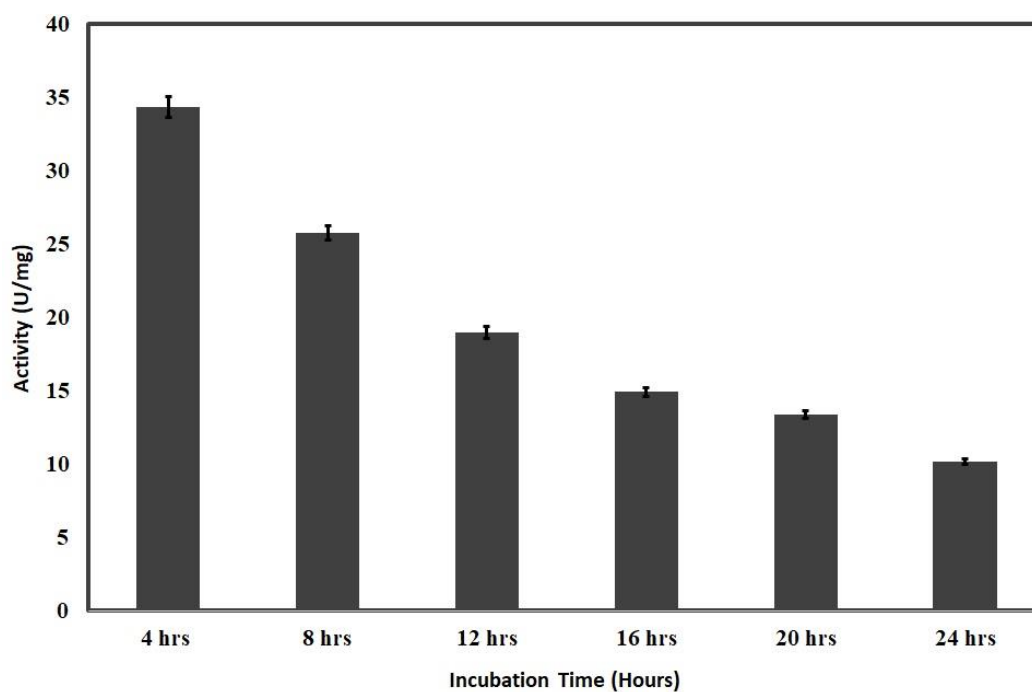


Figure 4.26 Activity time profile of the fusion chimera

4.14 Activity time profile of the fused protein

The efficiency of the fusion chimera in degrading insoluble chitin powder was tested in a time-course study. After 4 hours of incubation, the protein showed the highest activity. The activity started gradually decreasing after 8, 12, 16, 20 and 24 hours of incubation as shown in figure 4.26.

4.15 Characterization of the enzymatic reaction catalyzed by the fusion chimera (CDA-CBP)

(A) Effect of co-factors on (CDA-CBP) activity

All the co-factors with the concentration of 5 mM were used in the form of their respective chloride salts. After 4 hours of incubation with the substrate (chitin powder) and co-factors at 37 °C, the enzyme activity was highest in the presence of Ca²⁺ ions as shown in figure 4.27 (A).

(B) Effect of concentration of Ca²⁺ ions on (CDA-CBP) activity

The concentration of the Ca²⁺ was later tested with a range from 1mM to 10mM. As figure 4.27(B) depicted that the concentration of 3mM Ca²⁺ ion yielded the best activity of the enzyme. After this the activity started decreasing and there was not much difference in the activity between 9mM and 10mM Ca²⁺ concentration.

(C) Effect of pH on CD-CBP activity.

The pH ranges from 3 to 10 was taken to study the effect of pH on the enzyme. Na-citrate buffer was used for pH 3-6, Tris-Cl buffer was used for pH 7 & 8 and borate

buffer was used for pH 9 & 10. After 4 hours of incubation, the enzyme showed the best activity at pH 8 as shown in figure 4.27(C).

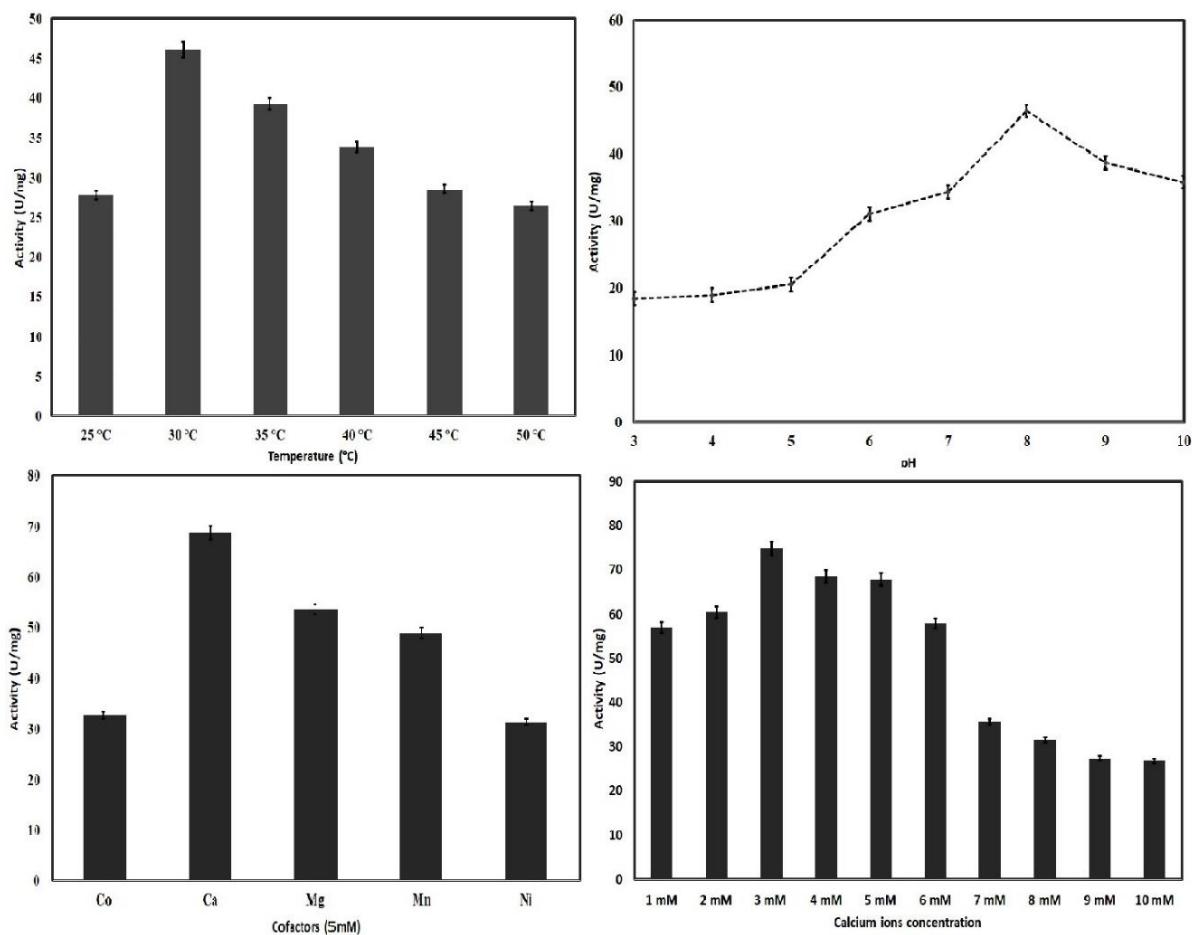


Figure 4.27 Effect of (A) Temperature (B) pH (C) Cofactors (D) Ca²⁺ ion concentration on the Fusion chimera activity

(D) Effect of temperature on CDA-CBP activity.

In the end the effect of different temperatures on enzyme activity ranging 25, 30, 35, 40, 45 and 50 °C was checked. It was seen that at 30 °C the enzyme showed the highest activity after 4 hours of incubation as shown in figure 4.27(D).

The activity of the purified fusion chimera was approximately 70 U/mg under standard conditions.

CHAPTER 5

SUMMARY AND

CONCLUSION

5 Summary and Conclusion

The present work aimed to advance the development of the controllable process using the enzymatic deacetylation of insoluble chitinous substrates that can result in the preparation of novel chitosan polymers and oligomers. Taking this into consideration, work presented in this thesis referred to the preparation of two genes for fusion i.e. CDA from *Bacillus licheniformis* cloned in pET 22b vector and CBP gene from *Serratia marcescens* ATCC 13880 strain. The fused chimera was then characterized and the results revealed its compatibility in enzymatic deacetylation of the insoluble chitinous substrate and can be potentially used for biomedical applications. The major findings of the present study are listed below:

BI-CDA gene was obtained from metagenomics library which was amplified and cloned in pET22b (+) vector and ligated after digesting with NdeI and SalI restriction enzymes.

The vector was thus transformed in *E. coli* pLysS cells through Heat Shock method and was expressed using 1 mM IPTG.

The addition of 2% glycerol and optimization of process parameters improved the biomass growth and hence the CDA yield.

The protein was purified by Ni-NTA chromatography with a M.W of 29 KDa depicted by SDS-PAGE and the optimum operating conditions for enzymatic activity was pH 8, cobalt ion as cofactor at 8 mM concentration at 50 °C.

The purified enzyme activity was about 1400 U/mg under optimum conditions.

Further the study was carried out to identify the CBP gene from *Serratia marcescens* ATCC 13880 strain. PCR components and conditions were optimized to get an amplified CBP21 gene.

Amplified product was sent for Sanger sequencing and the sequence obtained gave the alignment score of > 200 with CBP gene of *Serratia marcescens* strain EL1.

CDA-CBP fusion schematics were designed In-silico through an online tool (Benchling).

The pET22b_CDA vector was double digested with NdeI and SacII restriction enzymes and the CBP gene was amplified with the modified primers containing the same set of enzymes.

After ligation, the vector with the fused gene was then transformed in *E. coli* BL21 cells and protein was expressed through IPTG induction.

The product thus produced was purified using Ni-NTA column and the SDS-PAGE analysis revealed the approximate M.W of 51 KDa.

The fusion chimera was highly active on the insoluble chitin substrate (Chitin powder) under standard reaction conditions.

The efficiency of the fusion chimera in degrading insoluble chitin powder was tested in a time course study and after 4 hours of incubation, the enzyme showed the highest activity.

Further the fusion chimera was characterized and the optimum operating conditions for the enzymatic activity was pH 8, calcium ion as a cofactor at 3 mM concentration at 30 °C.

The purified enzyme activity was approximately 70 U/mg under standard conditions.

5.2 Future Scope

The production of the protein can be easily scaled up by optimizing the process parameters.

The fused protein produced in this study can be used to treat various insoluble chitinous substrates through enzymatic deacetylation.

The chitosan produced through such ecofriendly and cost-effective technologies will be a great help in various fields from food industry to health care and biomedical industry etc.

REFERENCES

REFERENCES

- Aachmann, F. L., Sørli, M., Skjåk-bræk, G., Eijsink, V. G. H., and Vaaje-kolstad, G. (2012). "NMR structure of a lytic polysaccharide monooxygenase provides insight into copper binding , protein dynamics , and substrate interactions." 109(46).
- Aam, B. B., Heggset, E. B., Norberg, A. L., Sørli, M., Vårum, K. M., and Eijsink, V. G. H. (2010). "Production of chitooligosaccharides and their potential applications in medicine." *Mar. Drugs*, 8(5), 1482–1517.
- Alfonso, C., Nuero, O. M., Santamarfa, F., Reyes, F., and Aplicada, D. M. (1995). "Purification of a Heat-Stable Chitin Deacetylase from *Aspergillus nidulans* and Its Role in Cell Wall Degradation." 30, 49–54.
- Arakane, Y., Dixit, R., Begum, K., Park, Y., Specht, C. A., Merzendorfer, H., Kramer, K. J., Muthukrishnan, S., and Beeman, R. W. (2009). "Analysis of functions of the chitin deacetylase gene family in *Tribolium castaneum*." *Insect Biochem. Mol. Biol.*, 39(5–6), 355–365.
- Arora, N., Sachdev, B., Gupta, R., Vimala, Y., and Bhatnagar, R. K. (2013). "Characterization of a Chitin-Binding Protein from *Bacillus thuringiensis* HD-1." 8(6).
- Baker, L. G., Specht, C. A., Donlin, M. J., and Lodge, J. K. (2007). "Chitosan, the

Deacetylated Form of Chitin , Is Necessary for Cell Wall Integrity in *Cryptococcus neoformans* □ †.” 6(5), 855–867.

Batista, Z., and Roberts, G. A. R. (1990). “A novel , facile technique for deacetylating chitin.” 434, 429–434.

Biondo, C., Beninati, C., Delfino, D., Oggioni, M., Mancuso, G., Midiri, A., Bombaci, M., Tomaselli, G., and Teti, G. (2002). “Identification and Cloning of a Cryptococcal Deacetylase That Produces Protective Immune Responses.” 70(5), 2383–2391.

Blair, D. E., Hekmat, O., Schu, A. W., Shrestha, B., Tokuyasu, K., Withers, S. G., and Aalten, D. M. F. Van. (2006). “Structure and Mechanism of Chitin Deacetylase from the Fungal Pathogen.” 9416–9426.

Boraston, A. B., Bolam, D. N., Gilbert, H. J., and Davies, G. J. (2004). “Carbohydrate-binding modules: fine-tuning polysaccharide recognition.” 781, 769–781.

Cai, J., Yang, J., Du, Y., Fan, L., Qiu, Y., Li, J., and Kennedy, J. F. (2006). “Purification and characterization of chitin deacetylase from *Scopulariopsis brevicaulis*.” 65, 211–217.

Cantarel, B. L., Coutinho, P. M., Rancurel, C., Bernard, T., Lombard, V., and Henrissat, B. (2009). "The Carbohydrate-Active EnZymes database (CAZy): an expert resource for Glycogenomics." 37(October 2008), 233–238.

Caufrier, F., Martinou, A., and Dupont, C. (2003). "Carbohydrate esterase family 4 enzymes: substrate specificity." 338, 687–692.

Chambon, R., Pradeau, S., Fort, S., Cottaz, S., and Armand, S. (2017). "High yield production of Rhizobium NodB chitin deacetylase and its use for in vitro synthesis of lipo-chitinoligosaccharide precursors." *Carbohydr. Res.*, 442, 25–30.

Chem, J. B. (1995). "Enzymology: Purification and Characterization of Chitin Deacetylase from *Colletotrichum lindemuthianum* Iason Tsigos and Vassilis Bouriotis Purification and Characterization of Chitin Deacetylase from *Colletotrichum lindemuthianum* *."

Chemistry, C. W., and Fungp, T. O. F. (1968). "Copyright 1968."

Christodoulidou, A., Bouriotis, V., and Thireos, G. (1996). "Two Sporulation-specific Chitin Deacetylase-encoding Genes Are Required for the Ascospore Wall Rigidity of *Saccharomyces cerevisiae* *." 271(49), 31420–31425.

- Coronel, J., Behrendt, I., Bürgin, T., Anderlei, T., Sandig, V., Reichl, U., and Genzel, Y. (2019). "Influenza A virus production in a single-use orbital shaken bioreactor with ATF or TFF perfusion systems." *Vaccine*, 37(47), 7011–7018.
- Coutinho, P. M., Stam, M., Blanc, E., and Henrissat, B. (2003). "Why are there so many carbohydrate-active enzyme-related genes in plants?" 8(12), 563–565.
- Deising, H., and Siegrist, J. (1995). "Chitin deacetylase activity of the rust."
- Dhillon, N. K. (2008). "Chitosan Nanoparticles: A Boon for drug delivery." 752–765.
- Dixit, R., Arakane, Y., Specht, C. A., Richard, C., Kramer, K. J., Beeman, R. W., and Muthukrishnan, S. (2008). "Domain organization and phylogenetic analysis of proteins from the chitin deacetylase gene family of *Tribolium castaneum* and three other species of insects." 38(4), 440–451.
- Eddine, N., Gueddari, E., Rauchhaus, U., Moerschbacher, B. M., Deising, H. B., and Moerschbacher, B. M. (2002). "Developmentally regulated conversion of surface-exposed chitin to chitosan in cell walls of plant pathogenic fungi." 103–112.
- Eijsink, V., (2008). "Towards new enzymes for biofuels: lessons from chitinase research Towards new enzymes for biofuels: lessons from chitinase research." 26(5), 228-35.

Ferrer, J., and Goajira, A. (1996). "Acid hydrolysis of shrimp-shell wastes and the production of single cell protein from the hydrolysate." 57, 55–60.

Formation, C. (1975). "A Pathway of Chitosan Formation in *Mucor rouxii*." 78, 71–78.

Galed, G., Diaz, E., Goycoolea, F. M., and Heras, A. (2008). "Natural Product Communications Influence of N -Deacetylation Conditions on Chitosan Production from α -Chitin."

Gao, X., Katsumoto, T., and Onodera, K. (1995). "Purification and Characterization of Chitin Deacetylase from *Absidia coerulea*." 117(2), 257–263.

Gauthier, C., Clerisse, F., and Dommes, J. (2008). "Characterization and cloning of chitin deacetylases from *Rhizopus circinans*." 59, 127–137.

Ghormade, V., Kulkarni, S., Doiphode, N., Rajamohanam, P. R., and Deshpande, M. V. (2010). "Chitin deacetylase: A comprehensive account on its role in nature and its biotechnological applications." *Curr. Res. Technol. Educ. Top. Appl. Microbiol. Microb. Biotechnol.*, (Chart 1), 1054–1066.

Gooday, G. W., and Occurrence, I. (1990). "The Ecology of Chitin Degradation." 387–

430.

Guillen, F., Folch-mallol, J., Quiroz-cast, R., and Eijsink, V. (n.d.). "Carbohydrate-binding domains: multiplicity of biological roles Related papers."

Hadrami, A. El, Adam, L. R., Hadrami, I. El, and Daayf, F. (2010). "Chitosan in Plant Protection." 968–987.

Hamed, I., Özogul, F., and Regenstein, J. M. (2016). "SC." *Trends Food Sci. Technol.*

Han, G., Li, X., Zhang, T., Zhu, X., Li, J., and Swale, D. (2015). "Cloning and tissue-specific expression of a chitin deacetylase gene from *Helicoverpa armigera* (Lepidoptera: Noctuidae) and Its Response to *Bacillus thuringiensis*." *J. Insect Sci.*, 15(1), 1–7.

Hekmat, O., Tokuyasu, K., and Withers, S. G. (2003). "Subsite structure of the endo-type chitin deacetylase from a Deuteromycete, *Colletotrichum lindemuthianum*: an investigation using steady-state kinetic analysis and MS." 380, 369–380.

Hemsworth, G. R., Taylor, E. J., Kim, R. Q., Gregory, R. C., Lewis, S. J., Turkenburg, J. P., Parkin, A., Davies, G. J., and Walton, P. H. (2013). "The Copper Active Site of CBM33 Polysaccharide Oxygenases."

- Hjerde, R. J. N., Varum, K. M., Grasdalen, H., Tokura, S., and Smidsm, O. (1997). "Chemical composition of O- (carboxymethyl) - chitins in relation to lysozyme degradation rates." 8617(97), 131–139.
- Horn, S. J., Vaaje-kolstad, G., Westereng, B., and Eijsink, V. G. H. (2012). "Novel enzymes for the degradation of cellulose Novel enzymes for the degradation of cellulose."
- Hou, X., Coutu, C., and Hegedus, D. D. (2008). "A chitin deacetylase and putative insect intestinal lipases are components of the *Mamestra configurata* (Lepidoptera : Noctuidae) peritrophic matrix." 17, 573–585.
- Huang, M., and Hsu, C. (2000). "The Proneural Gene *amos* Promotes Multiple Dendritic Neuron Formation in the *Drosophila* Peripheral Nervous System." 25, 57–67.
- Jang, M., Kong, B., Jeong, Y., Lee, C. H., and Nah, J. (2004). "□ -Chitin Separated from Natural Resources." 3423–3432.
- Jung, W. J., Jo, G. H., Kuk, J. H., Kim, Y. J., Oh, K. T., and Park, R. D. (2007). "Production of chitin from red crab shell waste by successive fermentation with *Lactobacillus paracasei* KCTC-3074 and *Serratia marcescens* FS-3." 68, 746–750.

Kadokura, K., Sakamoto, Y., Saito, K., Ikegami, T., Hirano, T., Hakamata, W., Oku, T., and Nishio, T. (2007). "Production of a recombinant chitin oligosaccharide deacetylase from *Vibrio parahaemolyticus* in the culture medium of *Escherichia coli* cells." *Biotechnol. Lett.*, 29(8), 1209–1215.

Kafetzopoulos, D., Thireos, G., Vournakis, J. N., and Bouriotis, V. (1993). "The primary structure of a fungal chitin deacetylase reveals the function for two bacterial gene products." *Proc. Natl. Acad. Sci. U. S. A.*, 90(17), 8005–8008.

Kauss, H., and Bauch, B. (1988). "Chitin deacetylase from *Colletotrichum lindemuthianum*." *Methods Enzymol.*, 161(C), 518–523.

Kobayashi, A., Numayama-tsuruta, K., and Fujii-kuriyama, Y. (1997). "CBP / p300 Functions as a Possible Transcriptional Receptor Nuclear Translocator (Arnt) 1 Coactivator of Ah." 122(4), 703–710.

Koga, D., and Kramer, K. J. (1983). "Hydrolysis of glycol chitin by chitinolytic enzymes." *Comp. Biochem. Physiol. -- Part B Biochem.*, 76(2), 291–293.

Levasseur, A., Drula, E., Lombard, V., Coutinho, P. M., and Henrissat, B. (2013). "Expansion of the enzymatic repertoire of the CAZy database to integrate auxiliary redox enzymes." 1–14.

- Li, Y., Lopez, P., Durand, P., Ouazzani, J., and Badet, B. (2007). "An enzyme-coupled assay for amidotransferase activity of glucosamine-6-phosphate synthase." 370, 142–146.
- Liu, J., Jia, Z., Li, S., Li, Y., You, Q., Zhang, C., Zheng, X., Xiong, G., Zhao, J., Qi, C., and Yang, J. (2016). "Identification and characterization of a chitin deacetylase from a metagenomic library of deep-sea sediments of the Arctic Ocean." *Gene*, 590(1), 79–84.
- Liu, Y., Liu, B., Joshi, J., and Nie, L. (2014). "Multi-level cervical disc arthroplasty (CDA) versus single-level CDA for the treatment of cervical disc diseases : a meta-analysis Multi-level cervical disc arthroplasty (CDA) versus single-level CDA for the treatment of cervical disc diseases : a meta-analysis." (December 2016).
- Luschnig, S., Ba, T., Armbruster, K., Krasnow, M. A., Tracheal, R., and Elongation, T. (2006). "Report serpentine and vermiform Encode Matrix Proteins with Chitin Binding and Deacetylation Domains that Limit Tracheal Tube Length in *Drosophila*." 186–194.
- Mai-gisoni, G., Turunen, O., Pastinen, O., Pahimanolis, N., and Master, E. R. (2015). "Enzyme and Microbial Technology Enhancement of acetyl xylan esterase activity on cellulose acetate through fusion to a family 3 cellulose binding module." *Enzyme Microb. Technol.*, 79–80, 27–33.

Manjeet, K., Purushotham, P., Neeraja, C., and Podile, A. R. (2013a). "Bacterial chitin binding proteins show differential substrate binding and synergy with chitinases." *Microbiol. Res.*, 168(7), 461–468.

Manjeet, K., Purushotham, P., Neeraja, C., and Podile, A. R. (2013b). "Bacterial chitin binding proteins show differential substrate binding and synergy with chitinases." *Microbiol. Res.*, 1–8.

Margaret, Matt W., and Zola, H. (1967). "THE ASSOCIATION BETWEEN CHITIN AND PROTEIN IN SOME CHITINOUS TISSUES Chitin-protein ratios Residual amino acids Treatment of complexes with hydroxylamine and with lithium borohydride." 20, 993–998.

Martinou, A., Kafetzopoulos, D., and Bouriotis, V. (1995). "Chitin deacetylation by enzymatic means: monitoring of deacetylation processes." 273, 235–242.

Martinou, A., Koutsioulis, D., and Bouriotis, V. (2002). "Expression, Purification, and Characterization of a Cobalt-Activated Chitin Deacetylase (Cda2p) from *Saccharomyces cerevisiae*." *Protein Expr. Purif.*, 24(1), 111–116.

Martinou, A., Koutsioulis, D., and Bouriotis, V. (2003). "Cloning and expression of a

chitin deacetylase gene (CDA2) from *Saccharomyces cerevisiae* in *Escherichia coli*: Purification and characterization of the cobalt-dependent recombinant enzyme.” *Enzyme Microb. Technol.*, 32(6), 757–763.

Matsuo, Y., Tanaka, K., Matsuda, H., and Kawamukai, M. (2005). “*cda1 +*, encoding chitin deacetylase is required for proper spore formation in *Schizosaccharomyces pombe*.” 579, 2737–2743.

Muzzareui, R.A.A. (1993). “Biochemical significance of exogenous chitins and chitosans in animals and patients.” 20, 7–16.

Nilegaonkar, P.M.S.K.S.S.S. (2010). “Extracellular chitinase production by some members of the saprophytic Entomophthorales group.”

No, H. K., and Meyers, S. P. (n.d.). “Journal of Aquatic Food Product Preparation and Characterization of Chitin and Chitosan — A Review.” (September 2012), 37–41.

No, H. K., and Meyers, S. P. (1995). “Preparation and characterization of chitin and chitosan - A review.” *J. Aquat. Food Prod. Technol.*, 4(2), 27–52.

Oriyoshi, K. M., Oma, D. K., Amanaka, H. Y., Hmoto, T. O., and Akai, K. S. (2010). “Functional Analysis of the Carbohydrate-Binding Module of an Esterase from *Neisseria sicca* SB Involved in the Degradation of Cellulose Acetate.” 74(9),

1940–1942.

Pareek, N., Vivekanand, V., Saroj, S., Sharma, A. K., and Singh, R. P. (2012).

“Purification and characterization of chitin deacetylase from *Penicillium oxalicum* SAEM-51.” *Carbohydr. Polym.*, 87(2), 1091–1097.

Percot, A., Viton, C., and Domard, A. (2003). “Optimization of Chitin Extraction from Shrimp Shells.” 12–18.

Phytologie, D., and Glk, C. (1990). “Detection of Chitin Deacetylase Activity Polyacrylamide Gel Electrophoresis.” 253, 249–253.

Prophages, S. (2005). “Metagenomics and industrial applications.” 3(June), 510–516.

Pruzzo, C., Vezzulli, L., and Colwell, R. R. (2008). “Minireview Global impact of *Vibrio cholerae* interactions with chitin.” 10, 1400–1410.

Purushotham, P., Arun, P. V. P. S., Prakash, J. S. S., and Podile, A. R. (2012). “Chitin binding proteins act synergistically with chitinases in *Serratia proteamaculans* 568.” *PLoS One*, 7(5), 1–10.

Quan, G., Ladd, T., Duan, J., Wen, F., Doucet, D., Cusson, M., and Krell, P. J. (2013).

“Characterization of a spruce budworm chitin deacetylase gene: Stage- and tissue-specific expression, and inhibition using RNA interference.” *Insect Biochem.*

Mol. Biol., 43(8), 683–691.

Raps, C., Bormann, C., Baier, D., Ho, I., Biotechnologie, M., Chemie, O., and Tu, D.-. (1999). "Characterization of a Novel , Antifungal , Chitin-Binding Protein from *Streptomyces tendae* Tu " 901 That Interferes with Growth Polarity." 181(24), 7421–7429.

Raval, R., Raval, K., and Bm, M. (2013). "Enzymatic Modification of Chitosan Using Chitin Deacetylase Isolated." 2(1), 2–5.

Rege, P. R., and Block, L. H. (2000). "Chitosan processing : influence of process parameters during acidic and alkaline hydrolysis and effect of the processing sequence on the resultant chitosan 's properties." 321(1999), 235–245.

Rojsitthisak, P., and Stevens, W. F. (2014). "Effect of Chemical Treatment on the Characteristics of Shrimp Chitosan. Effect of Chemical Treatment on the Characteristics of Shrimp Chitosan Bioprocess Technology, Asian Institute of Technology Present address : Center for Chitin-Chitosan Biomaterials ,." (May).

Sannan, T., Kurita, K., and Iwakura, Y. (1975). "Studies on Chitin , 2 *)." 3600, 3589–3600.

Scotland Bailey, J. E. and O. D. F. (1986). "CHARLES F A BRYCE Department of Biological Sciences Napier College of Technology Edinburgh , Scotland Bailey ,

J E and Ollis D F A Course in Biochemical Engineering Gibbs , G Exercises to Improve Laboratory Report Writing . Course to Correlate Basic Scien.” 14(3), 1986.

Shrestha, B., Blondeau, K., Stevens, W. F., and Hegarat, F. L. (2004). “Expression of chitin deacetylase from *Colletotrichum lindemuthianum* in *Pichia pastoris*: Purification and characterization.” *Protein Expr. Purif.*, 38(2), 196–204.

Society, A. M. (2014). “The Chemical Nature of the Cyst Membrane of *Pelomyxa illinoisensis* Author (s): Irving B. Sachs Source: Transactions of the American Microscopical Society, Vol. 75, No. 3 (Jul., 1956), pp.” 75(3), 307–313.

Someya, S., Kakuta, M., Morita, M., Sumikoshi, K., Cao, W., Ge, Z., Hirose, O., Nakamura, S., Terada, T., and Shimizu, K. (2010). “Prediction of Carbohydrate-Binding Proteins from Sequences Using Support Vector Machines.” 2010.

Stöveken, J., Singh, R., Kolkenbrock, S., Zakrzewski, M., Wibberg, D., Eikmeyer, F. G., Pühler, A., Schlüter, A., and Moerschbacher, B. M. (2014). “Successful heterologous expression of a novel chitinase identified by sequence analyses of the metagenome from a chitin-enriched soil sample.” *J. Biotechnol.*

Supe, N., Tolaimate, A., Alagui, A., Vottero, P., Rhazi, M., and Desbrie, J. (2000). “Investigation of different natural sources of chitin: influence of the source and

deacetylation process on the physicochemical characteristics of chitosan.”
344(November 1999), 337–344.

Suzuki, T., Park, H., Kitajima, K., Lennarz, W. J., Suzuki, T., Park, H., Kitajima, K.,
and Lennarz, W. J. (1998). “CELL BIOLOGY AND METABOLISM : Peptides
Glycosylated in the Endoplasmic Reticulum of Yeast Are Subsequently
Deglycosylated by a Soluble Peptide : N -Glycanase Activity Peptides
Glycosylated in the Endoplasmic Reticulum of Yeast Are Subsequently
Deglycosylated by a Soluble Peptide : N -Glycanase Activity *.” 1–6.

Tanaka, H., Takasu, E., Aigaki, T., and Kato, K. (2004). “Formin3 is required for
assembly of the F-actin structure that mediates tracheal fusion in *Drosophila*.” 274,
413–425.

Thongekkaew, J., Ikeda, H., Masaki, K., and Iefuji, H. (2013). “Enzyme and Microbial
Technology Fusion of cellulose binding domain from *Trichoderma reesei* CBHI
to *Cryptococcus* sp . S-2 cellulase enhances its binding affinity and its cellulolytic
activity to insoluble cellulosic substrates.” *Enzyme Microb. Technol.*, 52(4–5),
241–246.

Tokuyasu, K., Kaneko, S., Hayashi, K., and Mori, Y. (1999). “Production of a
recombinant chitin deacetylase in the culture medium of *Escherichia coli* cells.”
FEBS Lett., 458(1), 23–26.

Tokuyasu, K., Ohnishi-Kameyama, M., and Hayashi, K. (1996). “Purification and

characterization of extracellular chitin deacetylase from *Colletotrichum lindemuthianum*.” *Biosci. Biotechnol. Biochem.*, 60(10), 1598–1603.

Tokuyasu, K., Ono, H., Ohnishi-kameyama, M., Hayashi, K., and Moil, Y. (1997). “Deacetylation of chitin oligosaccharides of dp 2-4 by chitin deacetylase from *Colletotrichum lindemuthianum*.” 303, 353–358.

Tsigos, I., Martinou, A., Kafetzopoulos, D., and Bouriotis, V. (2000). “Tsigos2000.” 7799(1999), 129–135.

Vaaje-Kolstad, G., Horn, S. J., Aalten, D. M. F. Van, Synstad, B., and Eijsink, V. G. H. (2005). “The non-catalytic chitin-binding protein CBP21 from *Serratia marcescens* is essential for chitin degradation.” *J. Biol. Chem.*, 280(31), 28492–28497.

Wang, S., Jayaram, S. A., and Hempha, J. (2006). “Report Septate-Junction-Dependent Luminal Deposition of Chitin Deacetylases Restricts Tube Elongation in the *Drosophila* Trachea.” 180–185.

Webster, A., Osifo, P. O., Neomagus, H. W. J. P., and Grant, D. M. (2006). “A comparison of glycans and polyglycans using solid-state NMR and X-ray powder diffraction.” 30, 150–161.

Yamada, M., Kurano, M., Inatomi, S., Taguchi, G., and Okazaki, M. (2008). "Isolation and characterization of a gene coding for chitin deacetylase specifically expressed during fruiting body development in the basidiomycete *Flammulina velutipes* and its expression in the yeast *Pichia pastoris*." 289, 130–137.

Younes, I., and Rinaudo, M. (2015). "Chitin and chitosan preparation from marine sources. Structure, properties and applications." *Mar. Drugs*, 13(3), 1133–1174.

Zhao, Y., Park, R. D., and Muzzarelli, R. A. A. (2010). "Chitin deacetylases: Properties and applications." *Mar. Drugs*, 8(1), 24–46.

APPENDICES

APPENDICES

Appendix I

A.1 Biomass standard values:

Table A.1 Biomass and enzyme activity values

TIME	BIOMASS	O.D	Enzyme Activity
0	0	0.008	0
2	0.054	0.027	1990.57
4	0.513	0.180	2113.154
6	0.783	1.119	2247.525
8	1.277	1.755	2820.386
10	1.406	2.040	2950.024
12	1.656	2.220	2836.869

A.2 Glucosamine Standard

Determination of glucosamine STD concentration by using MBTH

Protocol for Determination of Glucosamine Std. conc. using MBTH

1M stock solution of glucosamine hydrochloride was prepared in 2.48% (v/v) sulphuric acid (8.4 ml of distilled water mixed with 0.3 ml of 72% sulphuric acid).

A working concentration of 0.1mM to 5mM glucosamine hydrochloride was prepared using 2.48% (v/v) sulphuric acid, 0.5 ml of glucosamine was taken in an Eppendorf tube and 0.5ml of 1M NaNO₂ is added and mixed by pipetting. The resultant mixture is kept

for six hours at room temperature. After this step, the Eppendorf tube is opened (in fume hood) and kept overnight to remove NO₂. The blank is prepared using water in place of glucosamine as well as NaNO₂.

To the above 0.5 ml of ammonium sulfamate (12 at %) was added and carefully mixed by pipetting. The solution is incubated for an additional 5 minutes. To the blank and the reaction mixture 0.5ml of 0.5%, MBTH is added and mixed and kept for 1 hour. After the eppendorf is cooled to room temperature 0.5ml of 0.5% FeCl₃ (prepared in 0.1N HCl) is added to each well and mixed. The eppendorf are incubated for 1 hour. Samples are diluted 100 times and the absorbance measured at 656 nm.

The standard graph of concentration versus absorbance at 656 nm is plotted and this graph is used to find the glucosamine concentration in the samples. The concentration was 0.5 mM to 5mM.

Table A.2. Glucosamine std. values

Sr. No.	Conc. (mM)	Average (Absorbance)
1	0.5	0.058333
2	1.0	0.075
3	1.5	0.100
4	2.0	0.125
5	2.5	0.150
6	3.0	0.180
7	3.5	0.206

Sr. No.	Conc. (mM)	Average (Absorbance)
8	4.0	0.228
9	4.5	0.259
10	5.0	0.305

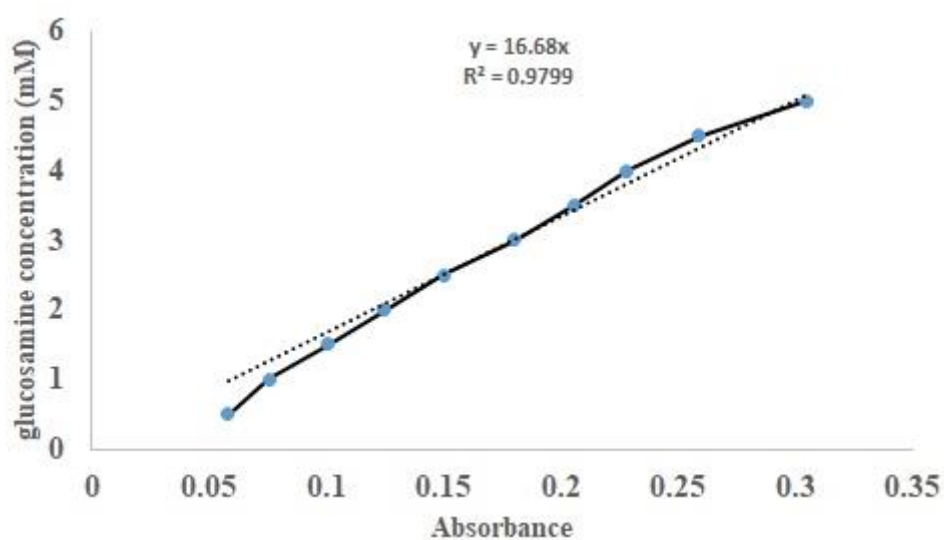


Figure 10.1 Glucosamine Standard graph

A.3 Glycol chitin preparation.

1g Glycol chitosan was dissolved in 20 ml 10% acetic acid with O/N stirring in a covered beaker and It forms a viscous suspension. The suspension is washed with 90 ml Methanol (Added slowly dropwise with constant stirring). This is filtered using a Vacuum pump. The retentate is discarded and to the filtrate 1.5 ml Acetic anhydride is added (Slowly with stirring). It is left at room temperature for 30min. It turns into a gel. It is then made into pieces and homogenized using a warring blender or mortar and pestle (methanol can be added while homogenizing). It is centrifuged at 27000g for 15

min at 4 C. If 27000g is not available, then centrifuge at lower rpm with longer centrifugation time. The supernatant is thrown away and the pellet is washed with 1V Methanol. The centrifugation step is repeated again in order to wash the pellet. To the pellet 100 ml, distilled water is added. It is suspended with shaking. This forms a suspension with end conc. of 1 % (1 g/100 mL or 10 mg/mL). This is then diluted to the required concentration depending on the desired assay.

A.4 Reference sequence for CBP

>ENA|BAA31569|BAA31569.1 *Serratia marcescens* CBP21 precursor :

Location:1..594

```
ATGAACAAAACCTTCCCGTACCCTGCTCTCTCTGGGCCTGCTGAGCGCGGCC
ATGTTTCGGCGTTTCGCAACAGGCGAATGCTCACGGTTATGTCGAGTCGCC
AGCCAGCCGCGCCTACCAGTGCAAACCTGCAGCTCAACACGCAGTGCGGCA
GCGTGCAGTACGAACCGCAGAGCGTCGAAGGCCTGAAAGGCTTCCCACAG
GCCGGCCCCGGCTGACGGCCACATCGCCAGCGCCGACAAGTCCACCTTCTT
CGAACTGGATCAGCAAACGCCGACGCGCTGGAACAAGCTCAACCTGAAA
ACCGGCCCCGAACTCCTTTACCTGGAAGCTGACCGCCCGTCACAGCACCAC
CAGCTGGCGCTATTTTCATCACCAAGCCGAACTGGGACGCTTCGCAGCCGC
TGACCCGCGCTTCCTTTGACCTGACGCCGTTCTGCCAGTTCAACGACGGCG
GCGCCATCCCTGCCGCACAGGTCACCCACCAGTGCAACATACCGGCAGAT
CGCAGCGGTTTCGCACGTGATCCTTGCCGTGTGGGACATAGCCGACACCGC
CAACGCCTTCTATCAGGCGATCGACGTCAACCTGAGCAAATAA
```


Gene sequence of CBP21 from *S. marcescens* which is used as a reference sequence

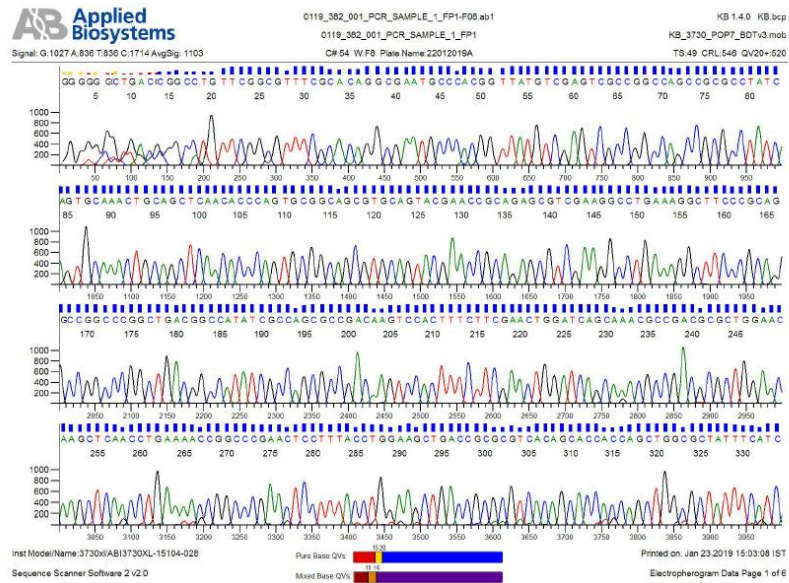


Figure A.5. Electropherogram data CBP21

A.6 Acetate Assay Standard values.

Concentration (n moles)	Absorbance
0.2	0.255
0.4	0.455
0.6	0.679
0.8	0.906
1	1.112

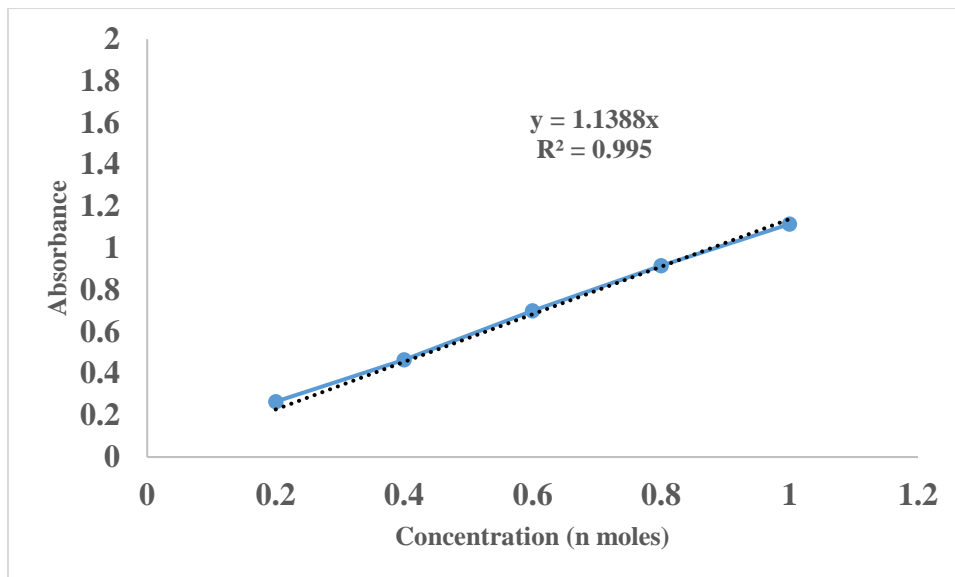


Figure A.6. Acetate assay standard graph

A.7 Chimeric Recombinant Fused Protein Sequence.

HHHHHHQRRLEFNWRFHVPKISDHIPKMEYGNEQFYKLLKELHAATTPKEH
 MLVVLPEVGLNNVQQIVNNVFGNTNASKWDESDVTWDWLNFDHDKIVE
 QFPGTIYPKSGYPSRILHTDVNTTEKIAKLTDNMEAASFSEPSKYIKSVQHTVGH
 SGVSHGNEVMKKVIDPNQEINPKLMFFTAKAHYKDLLSLIKDSAAPNPGDDF
 SLYVVKGIEPATQKSEKKEAKHKGGPVSASAASNEKIPEQKPGHVFSGTGQER
 QAQQARGHEANRLLRISVTIDLRWGAAGVLAQFQLEVRLAAAHLVFRLADFA
 QFAEWLGARSVAVDGAGVLGGEEFQILLRRRAPVLEVQFGARVGKGPLQGG
 TVAGGAPAIEDGLRVPVSRLRQGASGKVQRREALEVVAAGDRGCLDGVLA
 YRCIAATRVDKGHVPVYGGVGEILRDVDVQAFLM

Research Publications

P Bhat., GM Pawaskar., R Raval., S Cord-Landwehr., B Moerschbacher (2019). Expression of *Bacillus licheniformis* chitin deacetylase in *E. coli* pLysS: Sustainable production, purification and characterization. *International journal of biological macromolecules* 131, 1008-1013

Conferences

Priyanka Bhat, Keyur Raval, Ritu Raval (Title: Chitosan through Chitin deacetylase: Past, Present and Future) at international Conference on Crystal Ball Vision on Science and Engineering for Societal Upliftment held at CSIR-National Institute of Oceanography, Goa, India. August 2017

Priyanka Bhat, Keyur Raval, Ritu Raval (Title: Sustainable bioprocess development and optimization for Chitin-deacetylase production) at 14th International Chitin and Chitosan conference (14th ICCS) and 12th Asia-Pacific chitin and Chitosan Symposium (12th APCCS) held at Senriyama campus of Kansai university, Osaka, Japan. August 2018

Priyanka Bhat, Keyur Raval (Title: Chitosan through Chitin deacetylase: Past, Present and Future) and won best presentation award at National Symposium on Environmental Pollution Prevention and Control: Future perspective (EPPC: FP-2019) held at National Institute of Technology, Karnataka, Surathkal, India. August 2019

Priyanka Bhat, Keyur Raval (Title: Sustainable bioprocess development and optimization for Chitin-deacetylase production) Poster Presentation at 7th Bioprocessing India Conference 2019 held at CSIR-CFTRI, Mysore, Karnataka, India. December 2019

BIO-DATA

ACADEMIC PROFILE

B. Sc. (Biotechnology. Zoology, Botany and Chemistry), **First class**, Dolphin (P.G) institute of Biomedical and Natural Science, **H.N.B Garhwal University, Srinagar Uttrakhand, India.** 2010-2013

M. Sc. (Biotechnology), **First class**, **Central University of Rajasthan, Ajmer (India).** 2013-2015

Ph. D. (Molecular biotechnology), Department of chemical Engineering, **National Institute of Technology, Surathkal, Karnataka (India).** 2016-2021

Thesis Title: Studies on expression of recombinant chimeric Chitin Deacetylase.

Supervisor: **Dr. Keyur Raval** (Associate Professor) Dept. of Chemical Engineering (NITK).

Published Research Articles

Antimicrobial peptide (Cn-AMP2) from liquid endosperm of *Cocos nucifera* forms amyloid-like fibrillar structure. S Gour, V Kaushik, V Kumar, **P Bhat**, SC Yadav, JK Yadav; *Journal of Peptide Science* 22 (4), **(2016)** 201-207

Expression of *Bacillus licheniformis* chitin deacetylase in *E. coli* pLysS: Sustainable production, purification and characterization. **P Bhat**, GM Pawaskar, R Raval, S Cord-Landwehr, B Moerschbacher; *International journal of biological macromolecules* 131, **(2019)** 1008-1013

Conferences and Symposium

Oral presentation at **international Conference on Crystal Ball Vision on Science and Engineering for Societal Upliftment** held at **CSIR-National Institute of Oceanography, Goa, India.**

August 2017

Paper presented (Title: Sustainable bioprocess development and optimization for Chitin-deacetylase production) at **14th International Chitin and Chitosan conference (14th ICC)** and **12th Asia-Pacific chitin and Chitosan Symposium (12th APCCS)** held at **Senriyama campus of Kansai university, Osaka, Japan. (Funded by CSIR travel grant).**

August 2018

Presented Technical paper (Title: Chitosan through Chitin deacetylase: Past, Present and Future) and **won best presentation award** at **National Symposium on Environmental Pollution Prevention and Control: Future perspective (EPPC: FP-2019)** held at **National Institute of Technology, Karnataka, Surathkal, India.**

August 2019

Poster Presented at **7th Bioprocessing India Conference 2019** held at **CSIR-CFTRI, Mysore, Karnataka, India.**

December 2019

